Institut für Pflanzenernährung und Bodenkunde
der Christian-Albrechts-Universität zu Kiel

Microstructural Changes in Soils

Rheological Investigations

In Soil Mechanics

Kumulative Dissertation zur Erlangung des Doktorgrades
der Agrar- und Ernährungswissenschaftlichen Fakultät
der Christian-Albrechts-Universität zu Kiel

vorgelegt von

Dipl. Geogr. Wibke Markgraf

geboren in Langenhagen/Hannover

Kiel, 2006

Dekan: Prof. Dr. J. Krieter
1. Berichterstatter: Prof. Dr. R. Horn
2. Berichterstatter: Prof. Dr. W. Rabbel
Tag der mündlichen Prüfung: 02.11.2006

Gedruckt mit Genehmigung der Agrar- und Ernährungswissenschaftlichen Fakultät der Christian-Albrechts-Universität zu Kiel

Vertrieb:
Institut für Pflanzenernährung und Bodenkunde
Christian-Albrechts-Universität zu Kiel
Olshausenstr. 40
D-24107 Kiel
(e-mail: smevlan@soils.uni-kiel.de)

ISSN 0933-680-X
Preis: 10,- Euro (incl. Versandkosten)

"What we know is a drop.
What we don't know is an ocean."

Isaac Newton (1643-1727)

Contents

Figures

Tables

PART I

Introduction

1. INTRODUCTION AND FUNDAMENTALS

1.1 Introduction

For a basic understanding of soil (micro)mechanical behaviour the particulate nature of soils needs to be recognised: physico-chemical properties, the interaction between single particles, which are defined by their size, shape, mineralogy etc., the interparticle arrangement and interconnected porosity, inherently non-linear non-elastic contact phenomena, and particle forces based on principle laws of Newton (gravity and viscosity), Hooke (elasticity) and Coulomb as introduced in Terzaghi and Jelinek (1954), Kézdi (1974), Fredlund and Rahardjo (1993), Hartge and Horn (1999), or Mitchell and Soga (2005).
The rheological investigation of micromechanical behaviour and microstructural changes in soils needs to be intertwined to such fundamental knowledge of soil mechanics. In a sensitive intergranular system, parameters such as physicochemical properties, single grain characteristics as well as hydraulic properties (water content) are of great importance for shear behaviour and deformation in soils on the microscale. Rheology as soil mechanical topic is limited to phenomenons of yielding or creeping. In early works of Atterberg (1914) definitions of consistence limits and sensitivity (Terzaghi, 1936) of clay rich or pure clay materials are given.
A new aspect of rheometry, either from the classical rheological or soil scientific point of view lies in the linkage of both, soil micromechanical behaviour with respect to soil or single particle properties and rheological characteristics. States of soil cannot be divided strictly into two classes of elastic or plastic (viscous). Moreover, soil obtains several transitional states between elasticity and plasticity, depending on applied stress – steady stress, oscillatory stress - and strain as well as intensity, time and frequency (under oscillatory condition). Small stress-strain considerations are basically focused in rheological measurements.
In this work rheology is introduced as a new methodological approach to soil mechanics with special regard to scale considerations. In order to investigate micromechanical shear behaviour, rheological methods – in this case amplitude sweep tests – are adapted and combined with common methods and fundamental knowledge derived from soil physics, clay mineralogy, and rheology itself. Whenever physicochemical or mechanical interactions at the contact points of single soil particles, aggregates or soil as a whole specimen need to be investigated, diverse measuring methods are applied. Common methods and

characteristics in soil physics as the compression behaviour and derivable parameters of precompression and shear resistance - the angle of inner friction, cohesion, shear stress, deformation and the yield point - are mainly used for process analyses in soils that are defined as three phase system. However, in rheology these parameters are used for the quantification of shear behaviour and deformation of fluids or plastic (viscous) materials. A fundamental introduction to the research area of rheology is described in works of Keedwell (1984), Barnes et al. (1989), Collyer and Clegg (1998), Lagaly et al. (1997), Collyer and Clegg (1998), Schramm (1998), Schulz (1998), and Mezger (2002). Rheology has important applications in engineering, geophysics and physiology. In geotechnical research, where the application of ring shear apparatus'' (Suklje, 1969; Sonderegger, 1985a, 1985b) or simple rigidity tests of rocks are rather common, solid earth materials that exhibit viscous flow over long time scales are known as *rheids*. In engineering, rheology has had its predominant application in the development and use of polymeric materials. Rheological investigations of suspensions, gels and other (in)organic materials on a smaller scale (meso and microscale) are well known in inorganic chemistry, polymer sciences, and applied material sciences (Brandenburg, 1990; Güven and Pollastro, 1992; Cristescu and Gioda, 1994; Kosmulski at al., 1999a, 1999b; Neaman and Singer, 2000; Akroyd and Nguyen, 2003a, 2003b; Tseng 2003). Rheology is principally concerned with extending the disciplines of elasticity and (Newtonian) fluid mechanics to materials, whose mechanical behaviour cannot be described with the classical theories (***Tab. 1-1***). Due to its application predictions for mechanical behaviour (on the continuum mechanical scale) based on the micro- or nanostructure of the material are established. It furthermore unites the seemingly unrelated fields of plasticity and non-Newtonian fluids by recognising that both of these types of materials are unable to support a shear stress in static equilibrium. In this sense, a plastic solid is a fluid and shows a creeping or yielding character. Granular rheology refers to the continuum mechanical description of granular materials.

Tab. 1-1 *Rheology is a discipline of both solid and fluid mechanics, in detail of plasticity and non-Newtonian fluids.*

Continuum mechanics	Solid mechanics or strength of materials	Elasticity	Rheology
		Plasticity	
	Fluid mechanics	**Non-Newtonian fluids**	
		Newtonian fluids	

One of the subjects of rheology is to empirically establish the relationships between deformations and stresses, respectively their derivatives by adequate measurements. These experimental techniques are known as rheometry. Such relationships are then amendable to mathematical treatment by the established methods of continuum mechanics. Microstructural investigations of soils as non-Newtonian, partly linear viscoelastic material are rather uncommon in the wide spectrum of rheology. Linear viscoelasticity had been defined mathematically Dafarmos and Nohel (1980) by the Volterra-equation. Basically rheological methods are related to dimensions, the degree of homogeneity, and viscosity of the investigated substance. Furthermore, accuracy and controllability of the appropriate measuring system are of importance. Rheological tests, which are used for quality control, are based on simple relaxation or rotational test (Mezger, 2002). The application of a parallel plate measuring system, commonly in rotation mode, has been limited to substances as oil (Newtonian fluid), dyes or coatings (Meichsner et al., 2003), ceramics or clay suspensions of low viscosity (Kosmulski at al., 1999a, 1999b; Neaman and Singer, 2000; Tarchitzky and Chen, 2002). An approach to rheological measurements was done by Ghezzehei and Or (2000, 2001), who investigated comparatively steady stress (= internal capillary tensions) and oscillatory stress-strain correlations (= vibration effects, compaction). However, with regard to soil scientific aspects, especially to micromechanical behaviour, this approach seems to be insufficient. Soil substrates, which are completely saturated, are in a state of yielding already; structuring processes, among this aggregation, swelling and shrinkage (Tariq and Durnford, 1993a and 1993b) cannot be proved or quantified rheometrically and directly linked with or transferred to methods as mentioned above. A modified application of a parallel-plate-measuring system, including an appropriate method will be introduced in chapter 2. A new approach of rheometry, which can be adapted to soil micromechanical investigations and be related to common shear tests (oedometer, triaxial test), has had to be developed. Due to this, it has to be proved, whether it is possible to detect micromechanical shear behaviour, with special regard to contact level considerations, of homogenised soil samples (<2mm; specimen volume approximately 4cm³) under saturated or pre-drained conditions. Amplitude sweep tests were conducted with a modular compact rheometer MCR 300 (***Fig. 1-1***); the applied method, investigated substrates and test results will be presented in detail in chapters 2 to 5. Recent collected data show significant differences of resulting parameters, which are correlated to the water content, and other factors that may affect the matric potential: texture, single particle properties, pore size distribution, influence of (cat)ions (osmotic potential), and other physicochemical properties.

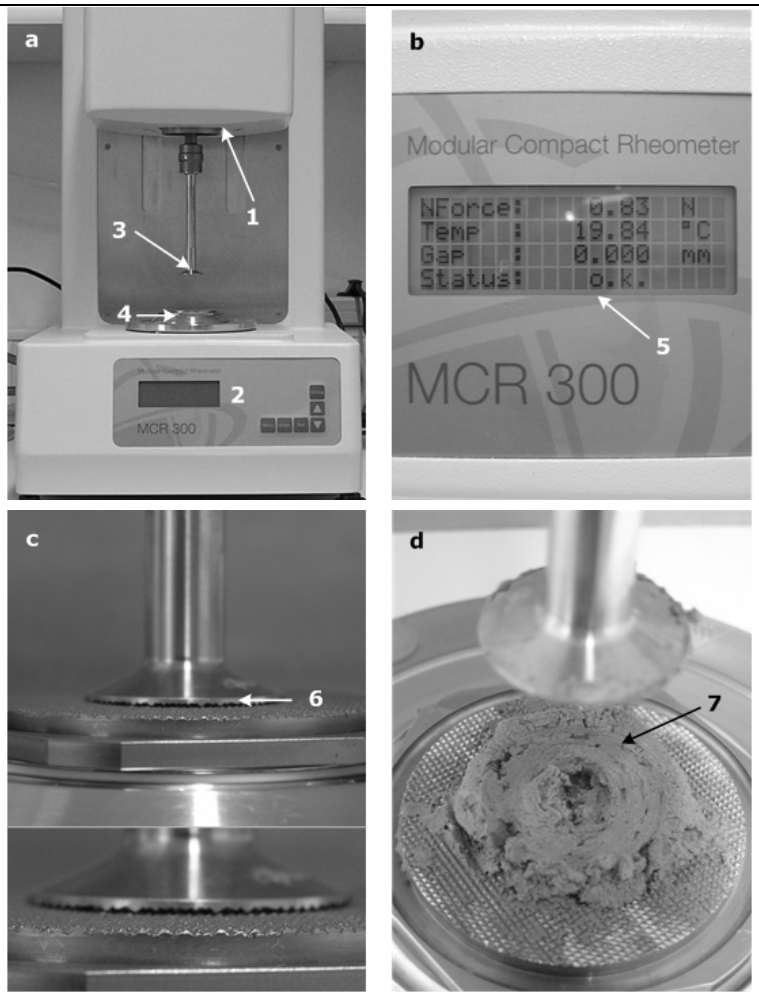

Fig. 1-1a) *modular compact rheometer MCR 300; 1 pneumatic ball bearing, and instrument lift; 2 manual control; 3 rotating bob (25 mm); 4 measuring plate with Peltier unit;* ***b)*** *5 control display;* ***c)*** *6 profiled parallel plate measuring system (25PP MS) in detail (setting of zero-gap);* ***d)*** *7 sheared surface of a sample after an applied amplitude sweep test (AST) under oscillating (OSC) conditions with controlled shear deformation (CSD); duration of one test: 15-18 minutes (f = 0.5 Hz).*

1.2 Fundamentals of soil micromechanics

In the following paragraphs of this chapter, an introduction to general considerations of fundamental soil micromechanics will be given, which are of relevance for a rheological approach to microstructural changes.

1.2.1 Particle associations

Microstructural changes in soils are related to several kinds of particle associations, basically on the association of clay platelets and of single grains. According to van Olphen (1977) clay particles in suspensions can be described as

(1) dispersed with no face-to-face association of particles,
(2) as aggregated in a face-to-face (FF) association with several particles, flocculated in an edge-to-edge (EE) or edge-to-face (EF) state,
(3) and deflocculated under non-associated conditions.

The aggregation of clay particles is correlated to the actual pH value (***Fig. 1-2***) (Jamund and Lagaly, 1993; Chorom et al., 1994; Lagaly et al., 1997; Dörfler, 2002). Cardhouse structures can be formed by edge-to-face and edge-to-edge associations. Under applied stress (compression) these voluminous structures collapse. Higher structural stability is obtained by larger and thicker face-to-face associations (Rosenqvist, 1959, 1962; Kézdi, 1974). As stated by Smith and Reitsma (2002) (see also chapter 2), a different mechanical behaviour is evident, if kaolinite (1:1 layer clay mineral) and montmorillonite (2:1) are compared. In addition, kaolinite is defined as low active clay (LAC, see chapter 5), and montmorillonite as high active clay (HAC) with a high swelling and shrinkage capacity. Montmorillonites have a more distinctive diffuse double. According to the Derjaguin-Landau-Verwey-Overbeek (DLVO) diffuse double layer theory (Derjaguin and Landau, 1941; Verwey and Overbeek, 1948) no physical contact between clay particles necessary for taking up charges or the adsorption of cations. Hence, the osmotic pressure is the actual effective stress between clay platelets in a Na-montmorillonitic soil (compare Ibeco Seal-80, chapter 2). Thus, the residual shear strength of kaolinite remains high (20-25°) even under high stress, in opposite to montmorillonite. Here, the residual shear strength decreases rapidly and remains stable at 5°. This is reflected in sliding shear behaviour versus turbulent shear behaviour in kaolinite or kaolinitic soils.

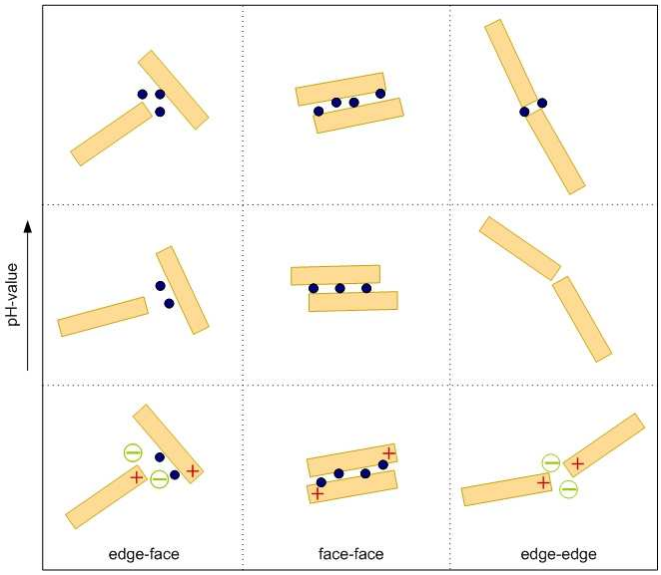

Fig. 1-2 *Aggregation of clay platelets: edge-to-face (EF), face-to-face (FF) and edge-to-edge (EE) in dependency on the pH-value (according to Jasmund and Lagaly, 1993)*

Particle association of compacted clays, single grains in sediments, and finally all soils show a variety of aggregation. In comparison to the particle association in clay suspensions, aggregation is generally related to combinations of the configurations of clay particles, but show differences in water content and density of the soil mass. Three groupings of fabric elements can be identified: elementary particle associations as e.g. individual grains, particle assemblages as organised unit of grains with physical limits and mechanical function, and water or gas filled pores (***Fig. 1-3***). Furthermore the stability of aggregates depends on contents and distribution of texture, organic matter, clay minerals and (hydr)oxides, and water (Emerson, 1967, 1983; Tisdall and Oades, 1982; Oades and Waters, 1991) as well as salt concentrations (Sharpley, 1990; Rengasamy and Olssen, 1991; Shainberg et al., 1981a, 1981b; Shainberg and Levy, 1992; Shani and Dundley, 2001) and other physicochemical properties such as pH, CEC ect. Results of investigated kaolinitic Fe-(hydr)oxide rich Oxisols (Hapludox, USDA 2003) and a smectitic Vertisol (Calciudert, USDA 2003) from Brazil that will be presented in chapter 5 show significant differences in microstructural stability. Theses differences are related to stabilising effects due to variations in clay mineralogy, organic matter content and hematite. Successive leaching of Na-dithionite soluble iron and organic matter by H_2O_2 in combination with visual analyses (scanning electron microscopy and polarised light microscopy) lead to distinctive conclusions.

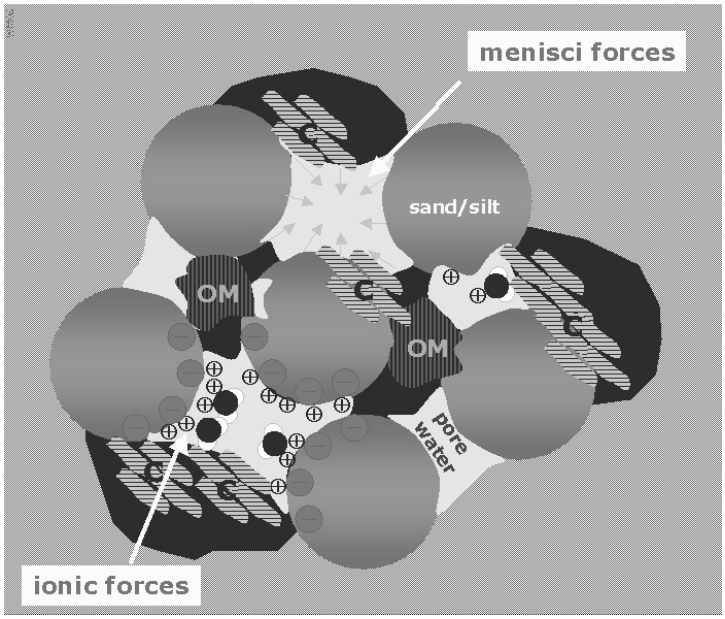

Fig. 1-3 *Sand/silt grains and clay platelets are formed to an aggregate; the three phases of a soil - gaseous, liquid, and solid - are combined by forces as generated due to several bonding mechanisms: ionic (Na^+), covalent (Ca^{2+}, Mg^{2+}), hydration mechanisms, capillary forces (matric potential, influenced by osmotic potential), and associated menisci forces. Other bonds may be built upon organic matter (OM) compounds and are influenced by mineralogical factors as well as parameters, which define pore water characteristics (e.g. salt concentration).*

Similar approaches were made by Bohor and Hughes (1971), Davey (1979), FitzPatrick (1993), Terribile and FitzPatrick (1995), Boivin et al. (2004), and Reed (2005), who applied transmission and scanning electron microscopy for the identification of soil mineralogy and structure using thin sections. Le Bissonnais and Arrouays (1996, 1997) adapted this method to microstructural analyses with focus on soil aggregate stability, which is affected by organic matter compounds. Beside the identification of soil compounds and their association, the quantification of particle forces is of great importance for microstructural analyses, including considerations of interparticle forces and intergranular stresses.

1.2.2 Particle forces

Particle forces at the microscale can be separated into several categories according to Santamarina (2001, 2003), based on earlier works of Ingles (1962) (***Fig. 1-4***):

(1) Forces due to applied boundary stresses: forces are transmitted along granular chains that form within the soil skeleton. Capillary effects at high degree of saturation prior to air entry fall under this category.
(2) Particle-level forces: particle weight, buoyancy and hydrodynamic forces are included. A particle can experience these forces even in the absence of a soil skeleton.
(3) Contact-level forces: capillary forces at a low degree of saturation, electrical forces, and the cementation-reactive force belong to this category. The first two mentioned forces can cause strains in the soil mass even at constant boundary loads. Conversely, the cementation-reactive force opposes skeletal deformation.

The investigation and quantification of particle forces is still on an establishing state. Numerical micromechanics were pioneered by Cundall and Strack (1979), who provided an insight into the distribution and evolution of interparticle skeletal forces in soils. Information about skeletal force distribution was gained from photoelastic studies conducted by Valdes (2002). Micromechanical analyses and mathematical approximations with simulations demonstrate the significance of particle coordination, rotational frustration (after Santamarina 2001) and the buckling of chains on the ability of a soil to mobilise internal strength (Santamarina, 2001). The relevance of rheological methods in micromechanics and their applicability are established and will be introduced in chapter 2.

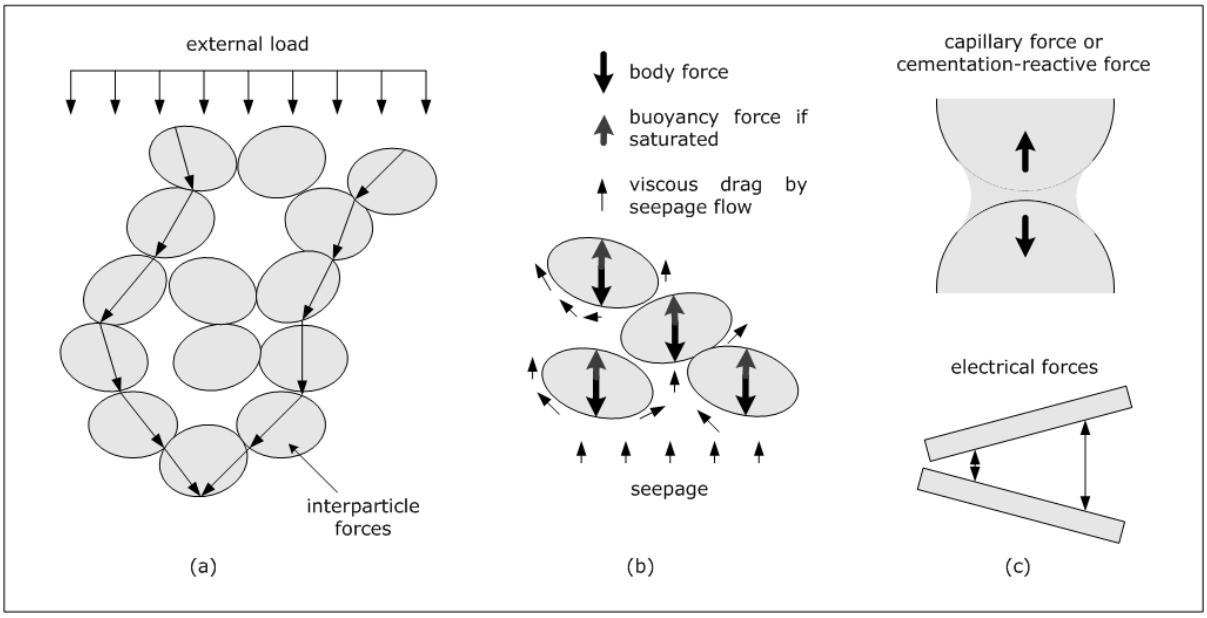

Fig. 1-4 *Interparticle forces at the particle level: (a) skeletal forces by external loading, (b) particle level forces, and (c) contact level forces (after Santamarina, 2003)*

1.2.3 Interparticle forces

Interparticle forces and intergranular stresses occur in association with particle forces or any external applied stress that lead to deformation, viscous or even plastic behaviour. With regard to clay particles, interparticle repulsive forces such as electrostatic forces, surface and ion hydration need to be considered. This mechanism occurs favourable in clay minerals of high swelling potential as i.e. sodium montmorillonites. In this case, hydration beside valency effects predominate soil structural processes. Cations (Na^+, Ca^{2+} or Mg^{2+}) dissolved in e.g. capillary water or under laboratory conditions in form of chlorides in distilled water, and in a certain concentration may either lead to a microstructural stabilisation or destabilization (Emerson and Bakker, 1973). Detailed information is given in following chapters; structural changes in long term fertilised (chapter 3) and natural clay rich substrates (chapter 4) are investigated.

When focused on single grains or microaggregates, several attraction and repulsive forces of both, chemical and physical origin are effective: electrostatic and/or electromagnetic attraction, primary valency bonding, cementation, and capillary stresses (Emerson, 1962a, 1962b; Yimsiri and Soga, 1999, 2000, 2002; Mitchell and Soga, 2005).

Furthermore, soil adhesion can be generally classified into normal adhesion and tangential adhesion. On any scale, the system of soil adhesion consists of soil, solid surface and their interface. Furthermore, the structure of and properties of the interface layer dominate soil adhesion. This aspect can be transferred to the

application of a parallel plate rheometer with a specific surface character, especially with regard to soil-tool interface considerations and micromechanical shear behaviour. In Tong et al. (1994), Santamarina (2001, 2003) and Jia (2004) particle forces at the soil-tool interface are modelled and transferred to practical application. According to Santamarina (2001) the normal adhesion forces (N_A) (***Appendix A, Fig. A-1***) at the interface come from forces caused by intermolecular attraction of bare soil particles (N_{As}), attraction of water meniscus (N_{Am}), attraction of water film due to viscosity (N_{Av}), which is influenced by chemical characteristics of (cat)ions that may change the viscosity and surface tension of a liquid (water), and capillary negative adsorption(N_{ca}). Appropriate illustrations and equations are given in ***Appendix A*** in ***Fig. A-2*** and ***Fig. A-3***.

1.2.4 Effective and intergranular stress

In soil physics mechanical analyses of shear parameters, compression behaviour and resulting hydraulic and mechanical characteristics are conducted on undisturbed structured soil samples and larger single aggregates with respect to further influencing factors. However, soil physical methodology does not include standardised analyses of forces on the scale of contact points (Hartge and Horn, 1999). In general, intergranular stress σ_i' (***Fig. 1-5***) is used synonymously with effective stress. In context of the soil stability discussion and effective tensions the concept of effect stress according to Bishop (1960), and Bishop and Bjerrum (1960) needs to be mentioned. The following equation describes occurring forces between single particles:

$$\sigma' = \sigma - u_a + \chi\,(u_a - u_w) \quad \text{with } \sigma'_i = \sigma' \tag{1.1}$$

σ' = effective stress
σ = total stress
σ'_i = intergranular force
χ = χ-factor in dependency on the degree of saturation of a soil;
χ = 0 (unsaturated) χ = 1 (saturated)
u_a = pore air pressure
u_w = pore water pressure

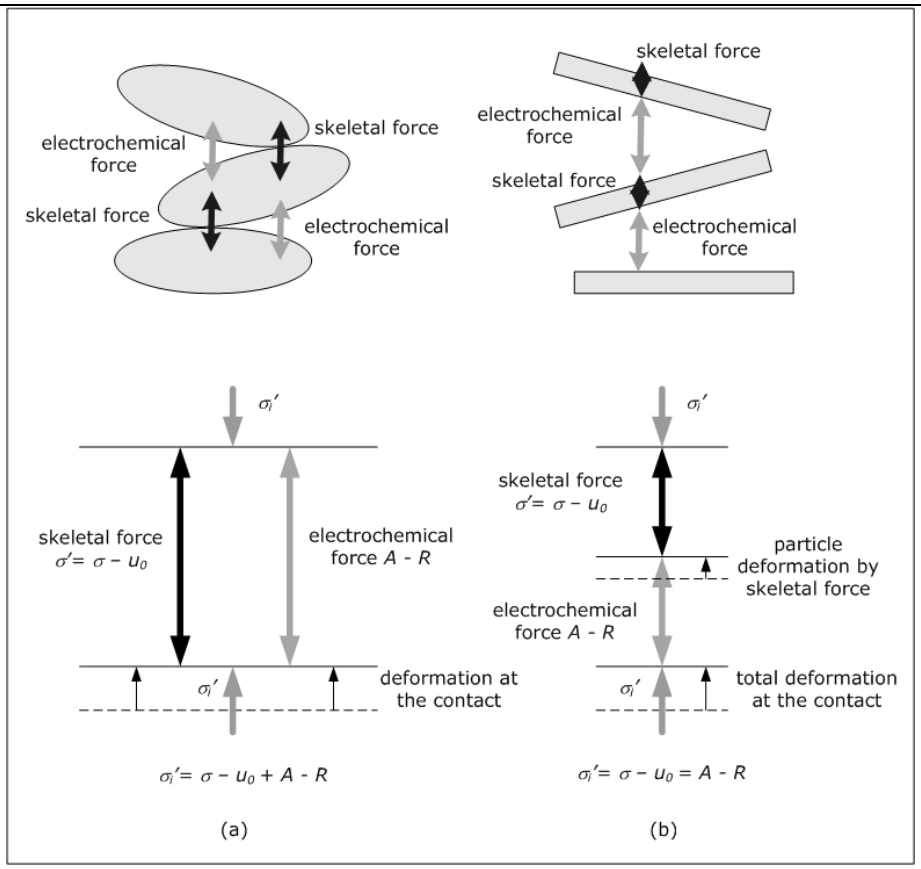

Fig. 1-5 *Contribution of skeletal force ($\sigma - u_o$) and electrochemical forces (A - R) to intergranular force σ_i: (a) parallel model and (b) series model (adapted from Mitchell and Soga, 2005).*

The intergranular stress σ_i' is given by

$$\sigma_i' = \sigma + A - u \qquad (1.2)$$

where u is the hydrostatic pressure between particles or $u = h_m\gamma_w$

$$\sigma_i' = (\sigma - u_0) + (A - R) \qquad (1.3)$$

where $(\sigma - u_0)$ is the skeletal force, and (A – R) electrochemical forces;
A are long range forces and R the long-range pressure,
with
$R = h_s\gamma_w$
where h_s is the osmotic head, and γ_w the unit weight of water.

However, forces between single grains cannot be quantified as well as effects of chemical and physical interaction between particles, aggregates or loose assemblages in natural soils depending on the water content due to a parametrisation of the osmotic potential. The defined χ-factor of this equation has been related to water filled pores and used as parameter for a fundamental understanding of the rigidity of a soil with respect to menisci forces. Terzaghi (1936), Bishop (1960), and Skempton (1960) established and modified this

equation, which has been mentioned in numerous fundamental works of Kézdi, (1974), Drescher et al. (1988), Fredlund and Rahardjo (1993), Horn and Baumgartl (1999), and Mitchell and Soga (2005).
Furthermore, Diamond (1970, 1971), Emerson et al. (1978), Emerson (1983), Fiés and Bruand (1998), Grant et al. (2002), Hartge und Horn (1999, 2002) concluded in their investigations of bonding mechanisms between particles and aggregates that there are different contact points between liquid and solid phase in a soil-tool interface system. Jia (2004) and Shi-qiao et al. (2005) give a mathematical approximation to this research topic (***Appendix A***). In correlation to changes in water tension and water content due to chemical or mechanical influence, shape and size of particles etc. different shear behaviour occurs (Warkentin and Young, 1962; Yong and Warkentin, 1966; Kézdi, 1974; Berilli et al., 2002; Smith and Reitsma, 2002).
As intergranular stress is influenced by electrochemical forces (A - R) cation constituents and their effects on the χ-factor have to be taken into account (***eqn. 1.3***). Bresler et al. (1982) quantify structural stability indirectly due to salt depending changes in hydraulic conductivity, but they do not mention any interaction of particle characteristics and ion concentration. Warkentin and Schofield (1962), Yong and Warkentin (1966), Mitchell and Soga (2005) give a detailed definition of potential interactions with the solid phase, although it is not possible to make any conclusions with regard to soil strength.
Based on rheological investigations of suspensions (water contents >90%) (Jasmund und Lagaly, 1993; Schulz, 1998), thixotropy effects could be proved, which are correlated to clay mineralogy characteristics and (cat)ion properties. In the area of soil micromechanics Ghezzehei and Or (2001), Tuller and Or (2003) showed that osmotic effects are of interest for soil stabilisation in clays, whereas they did not consider other indicators but swelling behaviour, without taking interparticle forces or shear strength into account. Peng et al. (2005) demonstrated structural changes by the influence of salts as they occur in irrigation areas, especially with respect to shrinkage and swelling behaviour on the meso scale.
Homogenised suspensions, pastes as well as natural soil material show on any scale very different hydraulic properties, if compared with undisturbed samples. In this case, additional variations of chemical and physical kind may occur in dependency on the scale (single grain, microaggregate, and undisturbed cylinder sample), changes in texture, bulk density, degree of aggregation, pore tortuosity, water content, salt effects etc. which altogether affect hydraulic parameters. These differences need to be obtained rheologically and measured with appropriate techniques.

1.3 Deformation characteristics

Kézdi (1974), and Mitchell and Soga (2005) give a general introduction to deformation characteristics. They state that strains consist of elastic and plastic parts. Transferred to rheological understanding, combinations of elastic and plastic or plastic and viscous compounds are possible. Soil can be defined as visco-elastic material (see chapter 2). In soil mechanics it is assumed that plastic strains develop only when the stress state satisfies some failure criterion.
According to this fundamental definition, the yield point differentiates the state of soil between elastic and plastic (viscous). From a soil mechanical point of view there is no distinct transition from elastic to plastic behaviour, which is related to cyclic loading. In solid mechanics, the small strain shear modulus G (or Young's modulus E) is defined as

$$G = \tau_c/\gamma_c \tag{1.4}$$

in which τ_c is the applied shear stress and γ_c is the corresponding shear strain.

Under small stresses, strains of solid materials are more or less proportional to the applied stress. The constant of proportionality (elasticity), is given by the inverse of Young's modulus of elasticity, which is a parameter of stiffness. Thus, elasticity is typically modeled by using the linear relationship between stresses and strain. The classic theoretical example of linear elasticity is the perfect spring, whose behaviour is described by Hooke's law. However, linear elasticity is an approximation, whereas natural, real materials exhibit some degree of non-linear behaviour.
Viscoelastic material models are frequently used to describe the behaviour of plastics, polymers or, as presented in this work, of soil. Commonly applied viscoelastic models are the Kelvin-Vogt and the Maxwell model. Each model can be represented by springs and dashpots sets in combinations of series and parallel elements (chapter 2) (Kézdi, 1974; Mezger, 2002).
Fundamental knowledge of soil stiffness in the linear elastic region is important for evaluating soil response under dynamic loadings such as mechanical or vehicle vibrations (Garciano et al., 2001). It also provides indirect information regarding the state and structure of natural soil. Therefore, stiffness values can be used to assess the quality of soil samples. The linear elastic stiffness of soils is evaluated from measurements of elastic wave velocities or use of displacement transducers.

Theoretical analyses of elastic waves are described in detail in Santamarina (2001). For a characterisation of deformation it is useful to differentiate between four zones and three states (***Fig. 1-6***) (Jardine, 1992):

Zone 1: true elastic region
Zone 2: nonlinear elastic region
Zone 3: preyield plastic region
Zone 4: full plastic region

In amplitude sweep tests (oscillatory conditions), a transgression from elastic to plastic (viscous) state is evident. Here, three phases of deformation or, according to Jardine (1992), Jardine et al. (2004), of stiffness degradation can be pointed out (see chapters 4 and 5, ***Fig. 4-1*** and ***5-1***):

Phase 1: an initial state of full elasticity, including a linear viscoelastic deformation range;
Phase 2: a transition state, in which stiffness degradation and plastic (viscous) strain development occur;
Phase 3: a final state of yielding or creeping.

Above a certain stress known as the elastic limit or the yield strength of an elastic material, the relationship between stress and strain breaks down. Beyond this limit, the solid may deform irreversibly, exhibiting plasticity. This phenomenon is often observed using stress-strain curves.
Furthermore, not only solids exhibit elasticity. Some non-Newtonian fluids, such as viscoelastic fluids, will also exhibit elasticity in certain conditions. In response to a small, rapidly applied and removed strain, these fluids may deform and then return to their original shape. Under larger strains, or strains applied for longer periods of time, these fluids may start to flow, exhibiting viscosity.

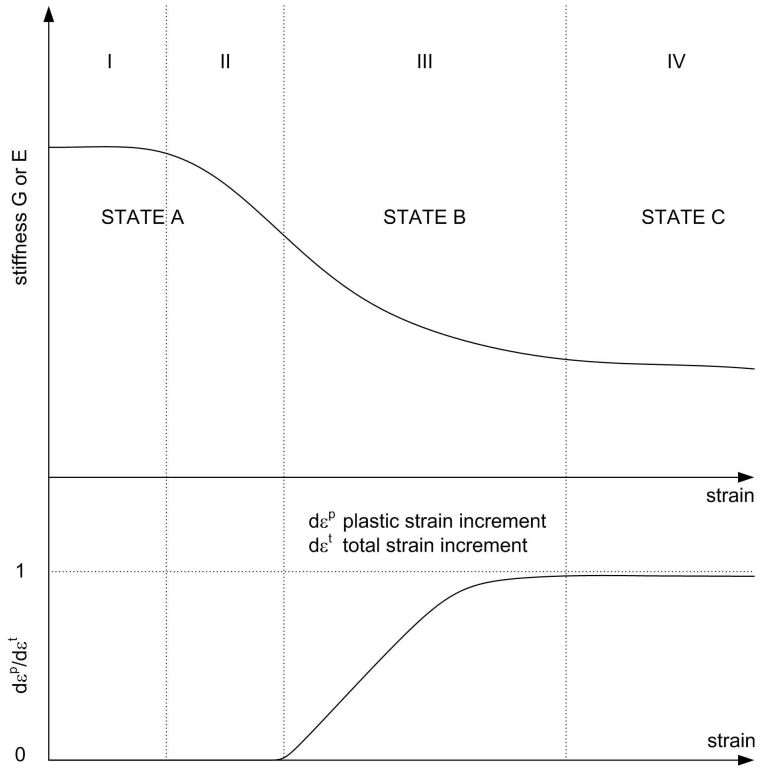

Fig. 1-6 *Four zones of deformation characterisation: stiffness degradation and plastic strain development; an increasing stiffness degradation is associated by an increase of plastic strain. The part of plastic strain ($d\varepsilon^p$) is 0 in state A, the region of true and non-linear elasticity, is approximating in state B, the region of preyielding, and equals total strain ($d\varepsilon^t$) in state C, the full plastic region (after Jardine, 1992).*

1.4 Soil mechanics at the microscale and Rheometry

With respect to mechanical shear behaviour the particle form needs to be taken into account. Interactions of single particles – single grains, tactiles, clay platelets or micro aggregates (<250µm according to Tisdall and Oades, 1982; Oades and Waters, 1991; Sumner and Naidu, 1998) – may occur with great variability, depending on physical properties and on scale considerations. Well known mechanisms like slaking or simple disperging effects have been already described in several works of Emerson (1954, 1983, 1994). Furthermore, in fundamental works of soil mechanics a general introduction to interparticular effects is given (Kèzdi, 1974; Fredlund and Rahardjo, 1993; Mitchell and Soga, 2005) with special regard to capillary forces (menisci forces).
Li (2003) defined a stress-like quantity called the quasi effective stress tensor for unsaturated soils. Suction-induced shear is affected by the pore fluid fabric. He concluded: "as the degree of saturation changes and/or soils deform, this fabric anisotropy could change significantly, […] (and) for any phenomenological relations proposed for unsaturated soils, the impact of this fabric tensor and its

evolution must be carefully considered". Tuller et al. (1999), Tuller and Or (2001a, b; 2002, 2005) describe the influence of particle distribution, resulting flow paths (pore characteristics) and pore water film continuity, which are relevant for mechanical stability. According to Cho et al. (2006) the size and shape of soil particles reflect the formation of a single grain. Chemical processes determine the size and shape of clay and silt particles, whereas mechanical processes are predominantly responsible for surface properties in case of sand and coarser particles. Increasing particle irregularities lead to a decrease in structural stability. An additional loss of elasticity is obtained depending on the state of stress (pressure). This instance can be also transferred to oscillatory shear (***Fig. 1-7***). Based on earlier works of Wadell (1932), Krumbein (1941), Powers (1953), Krumbein and Sloss (1963), Barrett (1980) in Cho et al. (2006) there are three scales in particle shape:

(1) sphericity that is conferred to eccentricity or platiness,
(2) roundness conferred to angularity, and
(3) smoothness, which is conferred to roughness.

Grant et al. (1990) pointed out that the roughness of soil fracture surfaces is an important measure of soil microstructure; thus micromechanical shear behaviour is affected by this parameter. Several particle-level mechanisms that are associated with increasing irregularities, and include a decrease in sphericity and/or roundness, are responsible for a certain macroscale response: hindered rotation, slippage and ability for particle rearrangement, lower interparticle coordination, increased particle level dilatation, lower contact stiffness, and higher proneness to contact deformation (Cho et al., 2006). With respect to adhesion forces, investigations of Tong (1994), Santamarina and Cho (2001, 2004), Jia (2004), Shi-qiao et al. (2005), and Cho et al. (2006) should be taken into account. Thus, relative movement (=shear behaviour) of particles between a parallel-plate measuring system will be of greater significance (***Appendix A, Fig. A-3***).

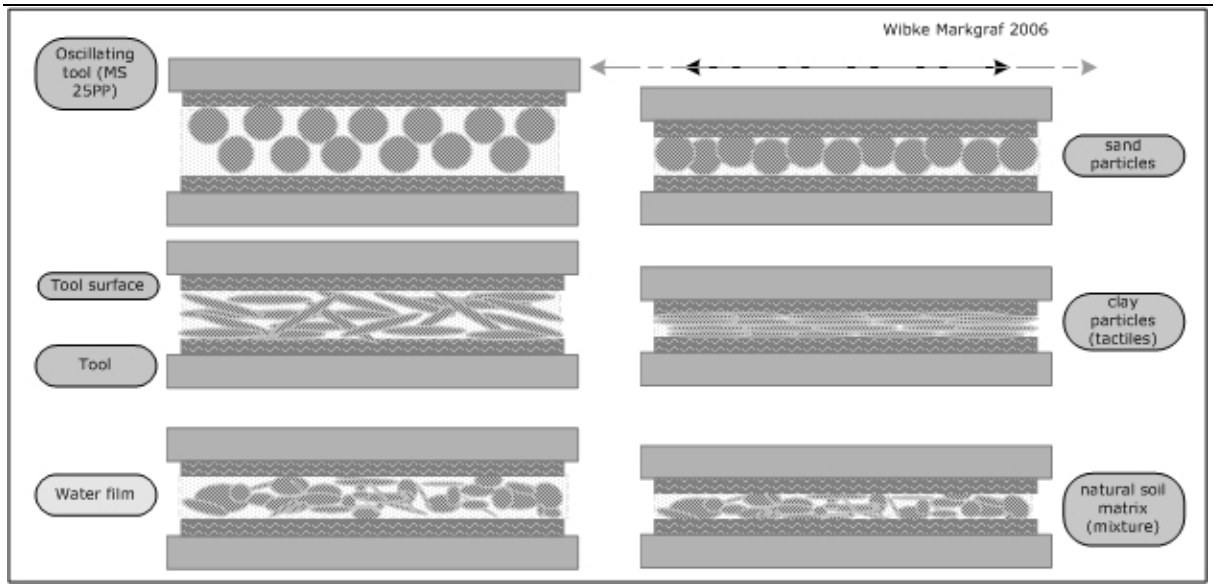

Fig. 1-7 *Rotund, platy and natural soil matrix in contact with an oscillating tool, here, a parallel-plate rheometer MCR 300 with a profiled parallel plate measuring system, 25mm in diameter (MS 25PP). Left side: before oscillatory shear, right side: during/after shearing (amplitude sweep test). Structural changes are induced by mechanical and chemical mechanisms or forces. Oscillatory shear leads to a reorientation, compression, and friction, of soil particles.*

1.5 Objectives

Open questions remain with respect to interparticular processes on the microscale. The following research objectives derive from the general introduction of rheological considerations to soil micromechanics:

(1) Is it possible to apply and modify existing rheological methods to characterise and quantify loss of stiffness on the particle-particle scale? In addition, is it also possible to define micromechanical shear behaviour and to transfer this to the general problem of contact point, soil-tool interface and/or microaggregate-tool interface?

Furthermore:

(2) Which mechanical effects that are correlated to e.g. vibrations (frequency) or stresses can be detected and simulated due to the application of a parallel-plate rheometer in oscillation mode?

In general, the application of amplitude sweep tests with a rotational rheometer MCR 300 for (oscillatory) shear stress investigations in soil mechanics on a particle-particle scale (contact point scale) has to be established and proved.

In this context, relevant parameters in rheology will be introduced in detail that are transferable to soil micromechanical characteristics: shear modulus G, storage and loss moduli G' and G", the linear viscoelastic (LVE) deformation range, and the deformation limit γ. Hooke's law of ideal elastic bodies, Newton's law of ideal fluids (viscosity), viscoelasticity, shear behaviour and micromechanical mechanisms will be defined and brought into context of fundamental soil mechanical considerations. In chapter 2 an approach to rheometry will be made by presenting results of conducted amplitude sweep tests with sodium bentonites, clayey and silty soils.

(3) Can the influence of physicochemical properties on the microstructural stability and hydraulic parameters of soils be quantified, in particular of cations (salts), carbonates and clay mineralogical compounds?

It is unclear, how far the osmotic potential is responsible for the accumulation of fine particles in the contact point region and for the stabilisation of assemblages or particle packages in the three phase system soil. It has to be proved that rheometry is adaptable for the investigation of microstructural changes, which are affected by salts and/or carbonates. Hence, rheological strength analyses of under laboratory conditions treated samples with NaCl and $CaCl_2$-solutions (chapter 2), as well as K^+-treated (fertilised) and of $CaCO_3$-rich soils may show a certain trend of stiffness development (chapter 3).This trend may be confirmed by investigated microstructural changes in a Calcaric Gleysol and a Dystric Planosol (chapter 4). An additional aspect lies in the influence of Fe-(hyrd)oxides and soil organic matter; results from conducted amplitude sweep tests with South-Brazilian soils will lead to interesting findings that will be discussed in chapter 5.

(4) Can particle properties (size, shape, roughness, friction) and their associations be related to shear behaviour and deformation characteristics, which derive from amplitude sweep tests?

Textural effects in correlation to particle properties and water content may be identified by resulting single parameters (e.g. the deformation limit γ_L) of amplitude sweep tests, and curve characteristics of the storage modulus G' and the loss modulus G". Particle associations can be visualised by SEM micrographs; in addition, energy dispersive scan (EDS) analyses support laboratory findings (x-ray diffraction) with regard to microstructural compounds. As shear behaviour

is dependent on particle size, shape and surface roughness, results, which derive from amplitude sweep tests may be explained and supported by such visual findings. Hence, in chapter 5 an interaction between SEM/EDS-analyses and rheological investigations of South-Brazilian soils will be presented to prove that rheometry (amplitude sweep tests) and scanning electron microscopy (SEM) are a reasonable amendment.

PART II

Publications

2. AN APPROACH TO RHEOMETRY IN SOIL MECHANICS: STRUCTURAL CHANGES IN BENTONITE, CLAYEY AND SILTY SOILS

Wibke Markgraf, Rainer Horn, Stephan Peth

Soil Till. Res. (2006)

Abstract

Rheology is regarded as the science of flow behaviour, where, based on isothermic equations, the deformation of fluids and plastic bodies subjected to external stresses may be described. Hooke's law of elasticity, Newton's law for ideal fluids (viscosity), Mohr-Coulomb's equation, and finally, Bingham's yielding are well known relationships and parameters in the field of rheology.
Rheometry is a well established measurement technique to determine the specific rheological properties of fluid and plastic bodies. However, the application of this technique in soil mechanical investigations is yet relatively uncommon. In order to explain point contact processes and strength an extrapolation of such findings to data of triaxial, direct shear or oedometer tests is still missing. Thus, this paper aims to introduce rheometry as a suitable method to determine the mechanical behaviour of soils and mineral suspensions when subjected to external stresses. To do this a Na-bentonite, Ibeco Seal-80 (IS-80) has been used as a testing material, and the suspensions were equilibrated with NaCl solutions in different concentrations in order to determine the ionic strength effects on interparticle strength and changes in mechanical properties. Furthermore a Vertisol, a clayey Oxisol, both from Brazil, and loess material from Israel, saturated with NaCl in several concentrations were analysed.
A parallel-plate-rheometer MCR 300 (Modular Compact Rheometer, Paar Physica, Ostfildern, Germany) has been used to conduct oscillatory tests. From the stress-strain relationship parameters and specific characteristics as thixotropy, storage modulus G' and loss modulus G", viscosity η, yield stress τ_ψ and the linear viscoelastic deformation (LVE) range including a limiting value γ_L were determined and calculated, respectively. With aspect to salt effects, amplitude sweep tests on $CaCO_3$ rich Avdat loess show an increasing stability due to higher NaCl concentrations. In a comparative test of Avdat loess and Ibeco Seal-80, turbulent versus sliding shear behaviour could be illustrated. To demonstrate clay

mineralogy effects or textural effects clay rich substrates from Brazil, a smectitic Vertisol and a kaolinitic Oxisol were compared, showing a higher level of stored elasticity (stability) in case of smectites and a lower value in regard to kaolinites. These preliminary results of amplitude sweep tests show that rheometry is a potential method of investigating microstructural characteristics of mineral suspensions and of clayey or silty soils.

Keywords: Rheology; parallel-plate-rheometer; soil structure; effective stress; osmotic potential

2.1 Introduction

Rheology is a science dealing with the mechanical behaviour of fluids and plastic bodies when subjected to external stresses. However, its technical application has been more conventional in chemical industry e.g. food science, polymer research, but uncommon in soil mechanics, yet.

2.1.1 Research objectives

Generally, soils consist of liquid, solid and gaseous phases (***Fig. 2-1***). Very many experimental papers deal with structured or homogenised systems, mostly ignoring especially the processes at the particle-particle, or particle to liquid scales as the main components of the mechanical strength of grain size, water content, salt concentration, potentials or stresses in connection to rheological methods.

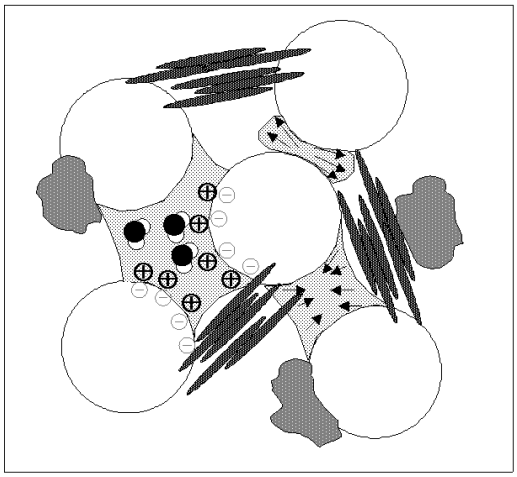

Fig. 2-1 *Soil compounds, aggregation: negatively charged soil particles, rotund sand or silt grains, clay platelets, organic matter, pore water, including nutrients/cations between the particles (different menisci forces) and air filled pores.*

Electrical conductivity (EC) of salt solutions, different textures and pH values, varying water contents of the investigated substrates are partly neglected in the interpretation of mechanical properties (Horn, 1995; Horn et al., 1995), although the effects are not since long well defined like valency and ion concentration effects. A furthermore interesting aspect can be found regarding to scaling. How far can results, calculated or observed during measurements, be transferred from the micro to the macro scale? Which information about effects of agricultural machinery can be deduced by rheological investigations? Do vibrations of farm machines affect soil stability? Oscillatory tests with defined frequency could give concrete hints. Which structural effects can be expected by changing valencies of cations and/or water content? In order to quantify the strengthening effect, the link between Terzaghi's equation for effective stress (Fredlund and Rahardjo, 1993) and the salt concentration (osmotic pressure) has to be established. NaCl has an influence on the net work stability of clay platelets and the menisci forces between single particles (tactiles).

As a comparison between a Na-Ca and a Na-Mg-saturated soil in Sumner and Naidu (1998) already showed, a Na-Mg saturated soil sample is structurally less stable, it has a deleterious effect to the soil structure and its permeability. Magnesium, comparable to sodium, enhances dispersion in montmorillonitic and illitic clays. The reason for that can be found in its different hydrate covering and its diameter. Sodification and salinisation affect mechanical stress, leading to aggregation (salinisation) as well as to slaking and/or dispersion (Yoder 1936, Emerson 1967, Loveday and Pyle 1973, Rengasamy et al. 1984). Additionally to this effect on aggregate size scale, the research work of Tuller and Or (2003) leads to some new considerations regarding the hydraulic functions of swelling soils containing active clays (tactile scale). Different concentrations of cations in a soil water solution are expected to have an influence on the film and corner flow in mesopores, the flow resistance, the clay fabric as well as on the size of flow cross sections. Furthermore, Tuller and Or (2005) postulated an increasing surface tension of 0.17 mN/m in a 1% NaCl solution.

In this context the effective stress σ' (according to Terzaghi 1925, Bishop 1960 in Fredlund and Rahardjo 1993, Horn and Baumgartl 1999, Mitchell and Soga 2005), depends at a given total stress not only on water pressure but should also be affected by potentials in soils with special regard to the osmotic potential Ψ_o. The latter depends on the salt content in the liquid phase and should affect internal strength. It is however unclear, how far Ψ_o must be included in the effective stress equation and to what extent the viscosity and surface tension effects in addition to particle-salt-particle bondings must be considered in order to finally solve this effective stress equation. Furthermore, Kutílek (1973) investigated the influence of clay minerals and exchangeable cations on the soil

moisture potential, including thixotropic behaviour of (Na- and Ca-) montmorillonite as well as of kaolinite. In an earlier work (Kutílek 1964), thixotropy of Na-montmorillonite has been investigated, influenced by interfacial (in solid-liquid phase) forces only, excluding any capillarity effects. Kutílek (1967) postulated that (a) the affinity of water to kaolinites is higher than to montmorillonites, considering that (b) the surface area of montmorillonite is of a higher order of magnitude than that of kaolinite.

To demonstrate mechanical effects on clay minerals or clayey soils, a comparison of micromechanical behaviour between kaolinite (1:1) and montmorillonite (2:1) should be considered. According to Smith and Reitsma (2002), the angle of internal friction remains high in kaolinitic clay soils (20 to 25 degrees) even at high deformation: the residual friction angle equals the critical state friction angle. Platy clay platelets or aligned particles may show a turbulent or a sliding behaviour (***Fig. 2-2***). However, only a low friction angle is always given. However, under steady stress conditions a naturally given structure may show resistance to applied external, vertical stress (①). As soon as external forces are exceeding internal structural strength compaction may be the result, bulk density increases, and the (micro)pore system collapses (②). A sliding shear behaviour can be observed due to a low residual shear strength ϕ_R of 5 to 15 degrees. This state has a more finite, irreversible character in opposite to turbulent shear behaviour, which will be described next. A rotund particle shape is commonly given for sand, silt and kaolinite (e.g. Fe-rich soils), which leads to turbulent shear behaviour and a high residual shear strength ϕ_R of 25 to 30 degrees.

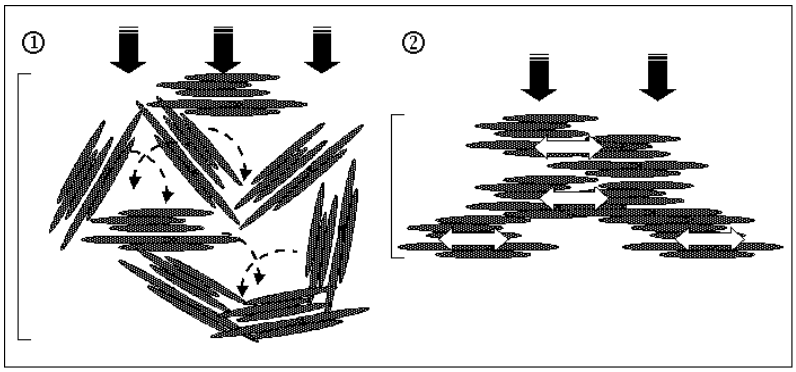

Fig. 2-2 *Mechanical behaviour of clay platelets and aligned soil particles: sliding shear behaviour. ① Platelets/aligned particles in gel state (aggregated), under steady stress condition; ② either under steady or shear stress a sliding shear behaviour is given when external applied stress' prevail internal (structural) forces, the yield stress is exceeded – compaction is the result, bulk density increases, (micro)pore system collapses.*

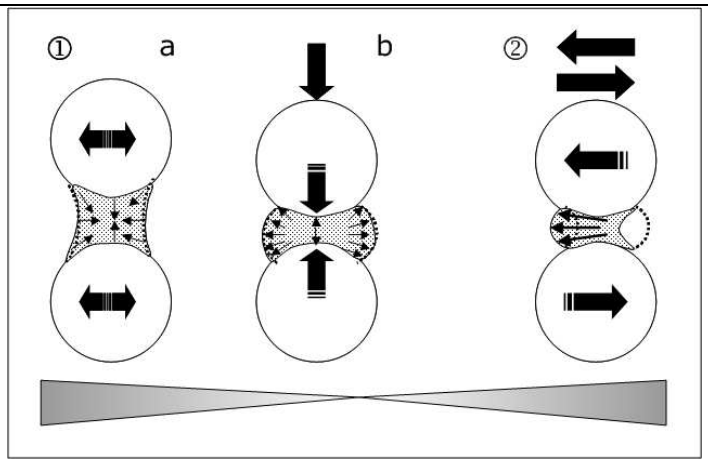

Fig. 2-3 *Mechanical behaviour of sand and silt. ①a-b: vertical stress (compression) applied to two single particles. In ①a water menisci with a concave shape in a resting state, in ①b with a convex form due to the applied vertical stress. ②: shear stress applied to two particles; water menisci show concave and convex shape congruently to the direction of shear. A turbulent shear behaviour is the result of applied stress to rotund particles, either vertical or in shear.*

In a resting state (①a in *Fig.* ***2-3***) a concave menisci shape is given. The angle of internal friction remains high. Under compression (①b) the pore water menisci tend to a convex shape, the angle of internal friction declines: external forces are increasing, whereas internal stress' are decreasing. In practice or in nature not only vertical forces are applied, generally. When shear stress is applied (②) the shear direction affects the menisci shape, as well as the shear strength affects the moment of a structural break down (= breakaway of menisci).

The diffuse double layer theory of Derjaguin-Landau-Verwey-Overbeek (DLVO) according to Derjaguin and Landau (1941), Verwey and Overbeek (1948) in e.g. Jasmund and Lagaly (1993) or Mitchell and Soga (2005) proved, that no physical contact between clay particles is needed to take up charges, but is carried by pore fluid between the plates. Thus, the osmotic pressure Ψ_o between the particles is the actual effective stress σ' in a Na-montmorillonite soil. This effect might be quantifiable due to the relation of salt concentration, respectively salt characters e.g. zeta potential, bonding forces, at corresponding electrical conductivities and defined water content to clay type or, in further investigations, to several soil types with different textures. Finally Ghezzehei and Or (2001) defined effects of water content, clay type and loading frequency on wet soils and clays, but no rheological findings of salt concentration effects (e.g. on the viscosity or thickness of a flow film) in a soil solution were presented. Thus, further research is needed to quantify the effects of salt on several clay types and wet soils. Furthermore, as Ghezzehei and Or (2001) remarked, that "[…] there is a fundamental difference between soil deformation by farm implements (oscillatory stress) and capillary induced strains (steady stress) rooted in the inherent soil properties, manifested in the form of frequency-dependent rheological properties […]" (Ghezzehei and Or 2001, p. 624), we tested a parallel

plate rheometer in soil mechanics for its usefulness to derive strength data, based on defined particle-particle interactions, including ionic compounds. First, we will give a short overview to some fundamentals of Rheology, introducing general parameters and their definitions. Thereafter results of oscillatory tests (amplitude sweep tests), conducted on Na-bentonite, Ibeco Seal-80, a Vertisol, a clayey Oxisol and loess material will be shown and discussed.

2.2 Theoretical remarks on rheometry

There are only few scientific contributions regarding to fundamentals of rheology in soil mechanics. Within the scope of investigations and studies of Keedwell (1984, 1988), Vyalov (1986), Whorlow (1992), Macosko (1994), Collyer and Clegg (1998), Schulz (1998), Ghezzehei and Or (2001), Schramm (2002) and Mezger (2002), basic principles and techniques are described. The following remarks are focused on explanations and definitions of parameters, and their significance in rheology.

2.2.1 Definition of terms

Table 2-1 gives an overview to parameters, that are used in soil mechanics and/or in rheology, whenever shear stress, either under steady state or oscillation is investigated. All parameters will be introduced within the following paragraphs.

Generally, deformation and flow behaviour depend on the type, degree and duration of applied stress, either oscillating or steady stress.
The shear stress (shear strength) τ is defined as

$$\tau = F/A \quad (1)$$

where τ shear strength [Pa], F the force [N], and A is the area [m²].

Tab. 2-1 *Synopsis of parameters of relevance in rheology and soil mechanics, respectively. Further explanations are given in the text.*

Parameter	Soil Mechanics	Rheology	
σ_n		$\sigma_n = F_n/A$	*normal stress,* with F_n the normal force [N] and A the area [mm²]
τ		$\tau = F/A$	*tangential (shear) stress*, with the force F and A the area [mm²]
		$\tau = \tau_B + \eta_B \cdot \dot{\gamma}$	according to Bingham, with the Bingham yield point τ_B [Pa], the Bingham viscosity η_B [Pas], and the shear rate $\dot{\gamma}$ [1/s]
η		$\eta = \tau/\dot{\gamma}$	*viscosity* [Pa·s], with τ the shear stress [Pa] and $\dot{\gamma}$ [1/s]
γ		γ = s/h	*deformation* [%] or [1], with s the deflection [mm] and h the plate distance [mm]
$\dot{\gamma}$		$\dot{\gamma}$ = v/h	*shear rate* [1/s], with v the velocity [m/s] and h the plate distance [mm]
E		$E = \sigma/\varepsilon$	Young's modulus [Pa], where σ is the applied stress [Pa] and ε the elastic strain [%] or [1]
G		$G = \tau/\gamma$	*shear modulus* [Pa], where τ is the shear stress [Pa] and γ the deformation [%] or [1]
G*	-	$G^* = \sigma/\gamma$	*complex shear modulus* [Pa], where σ is the applied stress [Pa] and γ the deformation [%] or [1]
		$\lvert G^*\rvert = \sqrt{(G')^2+(G'')^2}$	*complex shear modulus* [Pa] according to Maxwell
G'	-	$G' = (\tau_A/\gamma_A)\cos\delta$	*storage modulus* [Pa], with τ_A [Pa] and γ_A [%] in an amplitude sweep test, with the phase shift angle δ[°]
G"	-	$G'' = (\tau_A/\gamma_A)\sin\delta$	*loss modulus* [Pa], with τ_A [Pa] and γ_A [%] in an amplitude sweep test, with the phase shift angle [°]
tan δ	-	$\tan\delta = G''/G'$	*loss factor* [1], where δ is the phase shift angle[°] G" the loss modulus [Pa] and G' the storage modulus [Pa]

2.2.1.1 Newton's law of ideal fluids

Another definition of shear stress can be found in the relation of shear viscosity to the shear rate of Newton's law. In 1687 Isaac S. Newton (1643 to 1727) recognizes that the flow resistance of liquids is proportional to the flow velocity. He names the proportionality factor as "lack of slipperiness"- the resistance due to the internal friction of the fluid. Today it is referred to as viscosity. The

mechanical analogue to a perfect dashpot is represented in rheology by an ideal viscous fluid.

$$\tau = \eta \cdot \dot{\gamma} \quad (2.1)$$

where η is the shear viscosity [Pa·s], where η is constant;
the shear rate $\dot{\gamma}$ as

$$\dot{\gamma} = v/h \quad (2.2)$$

$\dot{\gamma}$ is the shear rate [1/s], v is the velocity [m/s], and h the gap height [mm].

To give an insight into dimensions, the average shear rate $\dot{\gamma}$ of sedimentation (according to Stoke's law) e.g. is $\leq 10^{-3}…10^{-2}$ s^{-1}, of mixing or stirring $10…10^{4}$ s^{-1}.

The shear viscosity (plasticity) η is defined as the ratio of shear stress to the shear rate. Typical shear viscosities η are for water 1 (at 20°C), for olive oil 100 and 0.01 to 0.02 mPa·s for gases (Mezger 2002). Newtonian flow is characterized by the resistance of elemental particles to motion and the energy that was invested in deforming viscous material and which is vanishing entirely. Boundary conditions are given by any shear stress > 0, and a constant shearing rate, which is directly proportional to the shear stress.

2.2.1.2 Hooke's law: Elastic flow behaviour and shear modulus G

Newton's law as a definition for viscosity on the one hand and Hooke's law on the other hand for an ideal elastic substance, expressed in the mechanical analogue of a spring (***Fig. 2-4***), are complementing each other as determining factors.
In 1676 Robert Hooke (1635 to 1703) performed tests on wires, springs and beams and recognized that the deformation of solids is proportional to the acting force ("Elasticity Law"). An ideal elastic body is expressed by Hooke's law (eqns (3.1) to (3.3)).

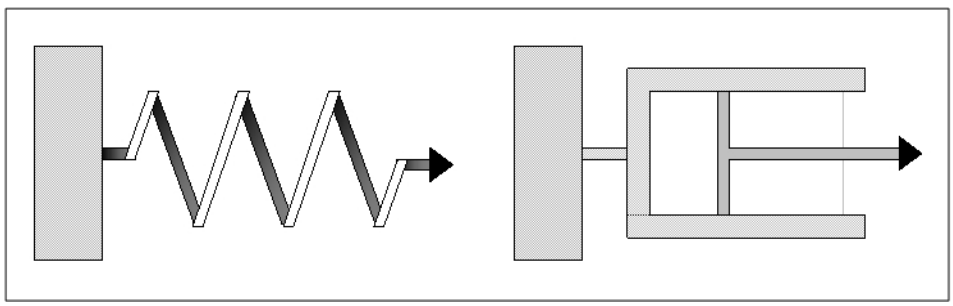

Fig. 2-4 *Spring model according to Hooke's law (ideal elastic) and dashpot model according to Newton's Law (ideal fluid).*

The energy, which was invested in deforming the body is completely stored; as soon as the stress, that caused the deformation, has been removed, the original shape is restored and the energy is recovered.
The linear relation between the extent of elastic strain and the applied stress is, deriving from Young's Modulus E.

$$E = \sigma/\varepsilon \quad (3.1)$$

where σ is the applied stress [Pa], and ε the elastic strain [%] or [1].
According to this, the shear modulus is

$$G = \tau/\gamma \quad (3.2)$$

where G is the shear modulus [Pa], and τ the shear stress [Pa], with the shear deformation γ [%] or [1], which is defined as

$$\gamma = s/h \quad (3.3)$$

and $s/h = \tan\varphi$
where s is the deflection [mm], h represents the distance between the plates [mm] and φ the deflection angle [°]; if s = h or φ = 45°, the deformation is 1, which equals 100 %. The deformation γ [1] or [%] depends on the plate distance h in [mm] and diameter d in [mm]. In ***Fig. 2-5a)*** and ***b)*** a comprising illustration of ideal viscous and elastic bodies in the form of flow curves is shown as well as of ideal fluids and viscoplastic bodies as described in the previous sections.

2.2.1.3 Bingham model: viscoplastic behaviour

Plastic behaviour occurs when substances are not sheared homogeneously. This also happens within the gap of the measuring device. Due to increasing shear stress substances may stay rigid until a material specific yield point is reached.

Above this yield point a transition from plastic to viscous flow behaviour is characteristic. This behaviour is represented by the Bingham model (eqn (4)).

$$\tau = \tau_B + \eta_B \cdot \dot{\gamma} \quad (4)$$

where τ_B is the Bingham yield point [Pa], and η_B the Bingham flow coefficient [Pa·s].

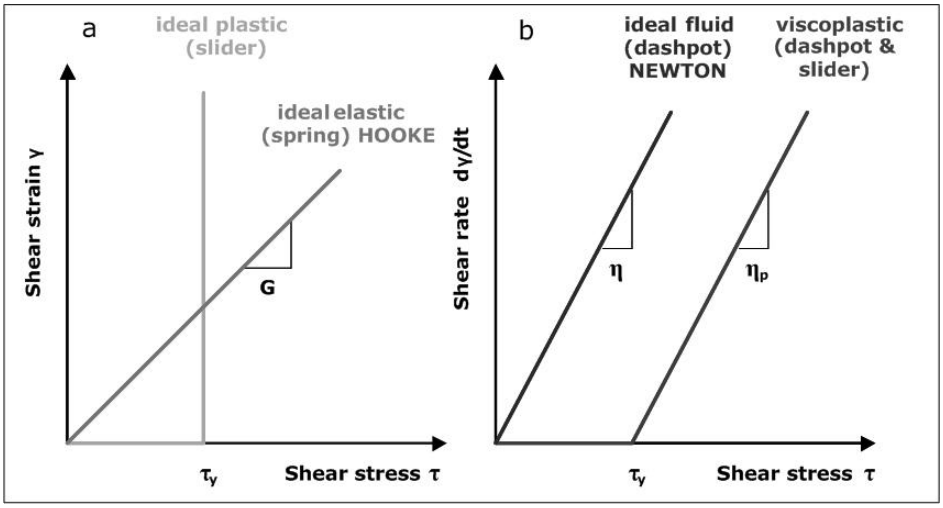

Fig. 2-5a) *Idealised flow curves. Diagram a depicts graphs that represent ideal plastic and ideal elastic materials. According to Hooke's law the value of the shear modulus G – comparable to Young's modulus E – depends on the ratio of shear stress τ to the shear strain (deformation) γ. In case of ideal elastic bodies, the graph starts in the point of origin, increasing constantly. Ideal plastic materials have a certain yield stress τ_y; by reaching this point the graph runs parallel to the y-axis, τ_y = const.*
Fig. 2-5b) *Graphs of an ideal fluid and a viscoplastic body are illustrated. A graph of an ideal fluid runs through the point of origin, the viscosity equals the gradient resulting from the ratio of the shear stress to the shear rate. The graph of a viscoplastic body, according to Bingham, reaches a yield point, τ_y = const. (τ_B) while the shear rate $d\gamma/dt$ increases.*

2.2.2 Viscoelasticity

The term "viscoelastic" stands for a combination of both viscosity and elasticity. Either fluids or solids may show viscoelastic behaviour. To quantify the loss of elasticity, parameters need to be adapted to oscillatory shear: a complex dynamic modulus G*, a storage modulus G' (dynamic rigidity) and an imaginary loss modulus G", deriving from the shear modulus G under steady stress conditions (***Fig. 2-6***).

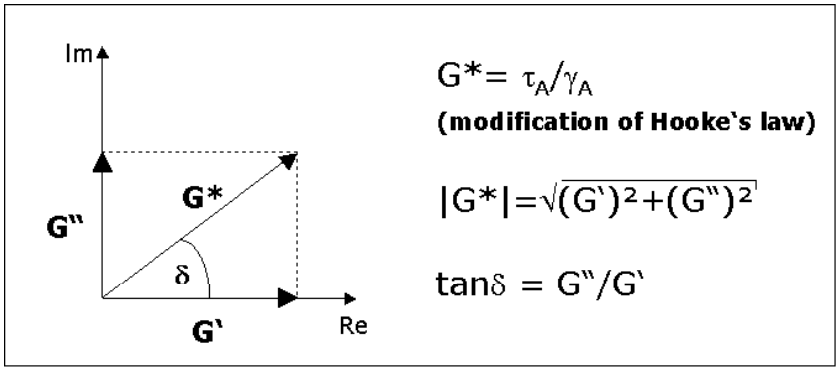

Fig. 2-6 *The complex shear modulus G* as a result from the quotient of the shear stress to the deformation in oscillatory shear (indices $_A$ stand for amplitude), a modification of Hooke's law. The loss modulus tan δ as parameter of elastic, viscoelastic or plastic behaviour: G" divided by G'. tanδ > 1 viscous character; tanδ = 1 viscoelastic; tanδ < 1 elastic behaviour.*

The storage modulus G' [Pa] represents the elastic behaviour of a sample, the loss modulus G" in [Pa] the viscous component.
If G' > G": The elastic component prevails the viscous one, while if
G' < G": a sol-character is given, the viscous component exceeds the elastic; these substances are creeping or running (Mezger 2002).
The LVE (linear viscoelastic) range and the deformation limit γ_L can be calculated by using values from G', the real part of stored elasticity, in opposite to G", as imaginary part of lost elasticity and representing viscosity.

The relation of G" to G' equals tan δ (eqn. (5)):

$$\tan \delta = G''/ G' \qquad (5)$$

If tan δ <1, the elastic component predominates, if tan δ >1 a viscous behaviour is given.

In oscillatory shear the complex shear modulus G* [Pa] is defined by the equation

$$\sigma = G^* \cdot \gamma \qquad \text{where } |G^*| = \sqrt{(G')^2 + (G'')^2} \qquad (6)$$

where σ is the applied stress [Pa], and γ again the deformation [%], according to the Maxwell model (Barnes et al. 1989) of viscoelastic fluids, which will be introduced in the following paragraph comprising to the Kelvin/Voigt model of viscoelastic solids.

2.2.2.1 Oscillatory shear: Maxwell's and Kelvin/Voigt model

The Maxwell model, a combination of a dashpot (plasticity element) and a spring (elasticity element) in a row can be used to illustrate effects of shear stress or strain on viscoelastic fluids occurring in nature, e.g. dispersions. Viscoelastic solids, which show a complete recovery, have an analogous in the Kelvin/Voigt model, a parallel combination of a dashpot and a spring. Gels and soils of certain water contents (pF ≥ 1.5) and texture (clayey, silty) may be an example for this model.
The principle of oscillatory tests is shown in ***Fig. 2-7***. Basically, an idealised illustration of shear strain is given. Due to an applied force F or tangential shear stress on a defined amount of substance, deformation is caused by moving a rectangular or rotund pivotable plate over a face A (stable).
In the case of ideal viscous substances, a delay of the τ(t) curve in relation to the γ(t) curve occurs with a phase shift angle of δ = 90°. As a basic condition, a complete contact between test sample and plates is essential.

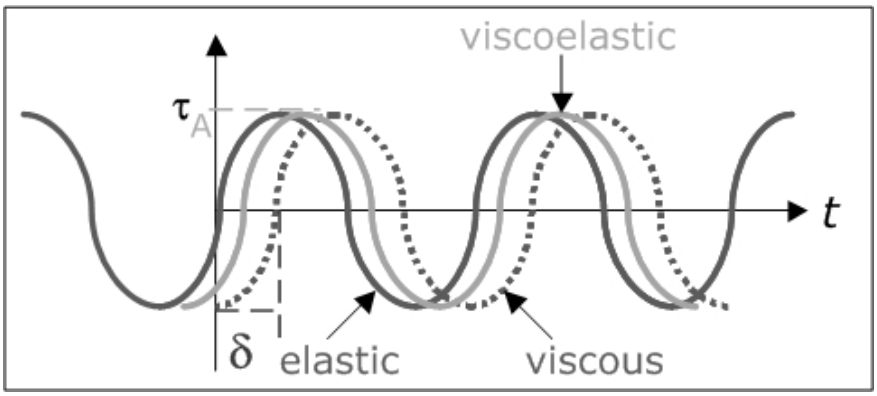

Fig. 2-7 *Principle of an oscillatory shear. Natural substances e.g. soil or clay minerals show a viscoelastic behaviour (dashed line), reacting with a temporal delay, represented by the phase shift angle δ. Drawn through line: elastic substances, dotted line: viscous materials. τ_A shear stress (constant amplitude A) in oscillation, deriving from Hooke's law.*

2.2.2.2 Amplitude sweep test

In order to quantify and investigate structural changes of dispersions and/or soil substrates, oscillatory shear is recommended. Amplitude sweep tests are characterised by a variable amplitude and a constant frequency (***Fig. 2-8***). The term 'sweep' represents a function with a variable parameter. Either the shear stress (CSS) or the shear deformation (CSD) is controlled. Amplitude sweep tests are conducted to achieve informations about the flow behaviour of a substrate and especially its elastic part (stored elasticity), the LVE deformation range, marked as area between the points of the parallel running curves of G' and G" and their transition. The deformation limit γ_L is comparable to the information given by a yield stress; before γ_L is reached, the elastic component prevails the plastic in the case of substrates, which show a gel character in the resting state. When γ_L has been exceeded substances show a plastic (viscous) behaviour.

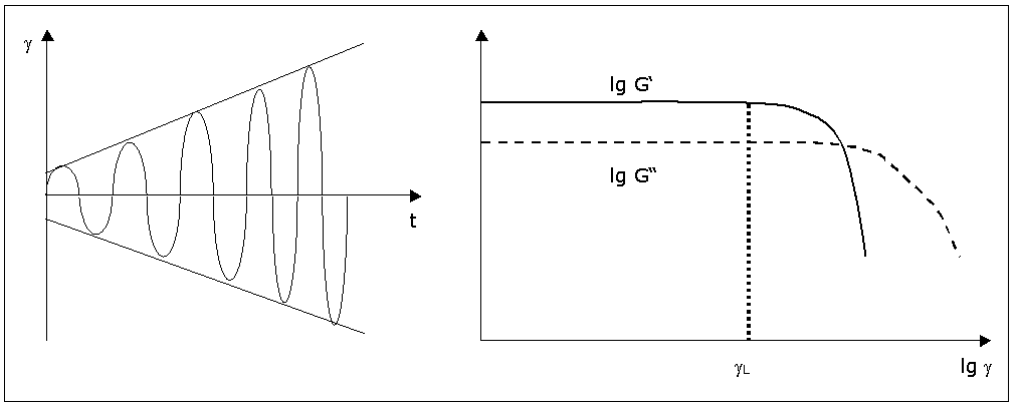

Fig. 2-8 *Amplitude sweep test: a constant frequency and a variable deformation are preset. Result: storage modulus G' (elastic behaviour) and loss modulus G" (viscous behaviour) as well as the limit of the LVE range γ_L. In this case G' prevails G", a gel character is given in the resting state.*

Table 2-2 shows parameters, which were chosen for conducted amplitude sweep tests. The plate distance varies with the texture: for substrates with a grain size ≤ 2µm a gap of 1 to 2mm should be preset, for substrates of coarser fraction (silt, loam, fine sand) a distance of 3 to 4 mm is recommended. A resting period of 30 seconds was inserted to ensure an undisturbed measurement, which might be influenced by the application of the material put on the measuring plate. The deformation is set as logarithmic range from 0.001 or 0.01 to 100% for clayey substrates and 0.0001 to 100% for materials of coarser texture. The frequency was set at a constant value of 0.5 Hz, or π 1/s in SI unit. One run, including 30 measuring points, lasts approximately 15 minutes. It should be considered, that clayey substrates tend to dry out after a short period. Hence, tests should not exceed a duration of 20 minutes.

2.2.3 Measuring device

The plate geometry of the rheometer MCR 300 with parallel-plate measuring system (PP MS) is determined by the plate radius R, according to DIN 53018. The distance H (or d) between the plates has to be H < R. The rotating bob is 25 mm in diameter and has a profiled surface. The distance between the measuring plates is 2-4 mm. During all tests a constant temperature of 20°C is given, regulated by a Peltier unit. The generated normal force averages between 0 to 12 N and should not be exceeded during tests. The high sensitivity of the device is supported by an air bearing. A minimum torsional moment of 0.02µNm and a maximum of 200 can be reached, furthermore minimum frequency of 0.00001 Hz and a maximum of 100 Hz (***Tables 2-2*** and ***2-3***).

Tab. 2-2 *Raw data and metrological specifications in oscillatory shear with controlled shear deformation.*

Oscillation CSD	Metrological specification	Result
Raw data	deflection angle φ(t) [mrad]	torsional moment M(t) [mNm], phase shift angle δ [°]
Rheological measurand	deformation γ(t) [%]	shear stress τ(t) [Pa], phase shift angle δ [°]

The plate distance of the measuring device depends on the texture, including chemical characteristics and specific water content. Hence, an important assumption of any sample should be a fine-grained (<630µm and/or low sand content) and homogeneous consistence (grinded and sieved) to avoid disturbed measurements, caused by any coarse particles. A more extensive description of investigated substrates and their physicochemical properties will be given in the following paragraphs.

Tab. 2-3 *Configuration of conducted amplitude sweep tests with controlled shear deformation (CSD).*

Parameter	
plate distance	d = 2mm (<2µm) d = 4mm (>2µm)
deformation	γ = 0.01 or 0.001… 100% (<2µm) γ = 0.0001… 100% (>2µm)
frequency (angular frequency)	f = 0.5 Hz (SI unit $\omega = \pi$ 1/s)
measuring points	30 pts.
duration	appr. 15 min.

2.3 Material

2.3.1 Substrates

A Na-bentonite, an active clay, two natural clay rich soils from Brazil and loess material from Israel were chosen for these investigations.

2.3.1.1 Ibeco Seal-80

Major constituents of Na-bentonite clays as Ibeco Seal-80 (IS-80) are the minerals montmorillonite and beidellite, which both belong to the mineral group of smectites. Montmorillonite is developed by weathering of mica minerals and as new formations from other weathering products, in particular from volcanic tuffs and ashes. Due to its physical characteristics, montmorillonite is an unusual mineral. Montmorillonite belongs to the group of dioctahedral 2:1-layersilicates. The most conspicuous features of this material are the nearly unrestricted exchangeability of its intermediate layer cations and its excellent swelling capacity in aqueous solutions. The expansion of the interlayers can lead, in extreme cases, to the disintegration of the crystal network. These characteristics make montmorillonite a mineral with broad technical application possibilities. IS-80, a Na-bentonite, can be assigned to the group of activated bentonites. These are bentonites with smectites whose initial composition of alkaline-earth-cations has been replaced with Na^+-ions in a technical process named alkali-activation. In natural Na-bentonites (e.g. Wyoming, Greek or Southern German Bentonites) smectites are predominantly occupied with Na^{2+}-ions in the intermediate layers. In Na-bentonites, Ca^{2+} or Mg^{2+}-ions also occur frequently and in varying concentrations. *Table 4* summarizes some general characteristics of IS-80.

Commonly, IS-80 is applied in construction and civil engineering e.g. as landfill sealing, for Caisson constructions as well as for Geosynthetic Clay Liners (GCL, bentonite mats) and for use in deep-mining.

2.3.1.2 Avdat Loess

In addition a silt rich material was chosen. In opposite to clay rich substrates, in which structural effects are mainly caused due to swelling and shrinking behaviour of the respective clay mineral composition, in loess the given texture and chemical composition are more decisive. Avdat loess, which origins from the Negev Desert in Israel, has a silt content of 64% and a high calcium carbonate content of 52%. Hence, a well developed aggregation can be expected as calcium has a stabilising effect. A x-ray diffractometry result in a high fraction of strongly weathered and swellable smectites and vermiculites. Montmorillonites and magnesium rich forms of smectites beside kaolinite and illite exist in low amounts only.

2.3.1.3 Vertisol and Clayey Oxisol

Vertisols are very clay rich (> 30%) soils. Their genesis is dominated by calcium-silicate and weathered clay rich bedrock (Basalt). In dry periods Vertisols show broad (> 1 cm) cracks due to shrinkage in depth, "slickensides" on aggregate surfaces and a well developed Gilgai-relief (self mulching effect). As clay minerals smectites (montmorillonites) occur predominantly. Hence, a very high calcium content, ranging between 40-70 $cmol_c/kg$ is characteristic. The ratio of calcium and magnesium between the sorbates is close. This region of Rio Grande do Sul, close to the Uruguayan border, is used as pasture land. The pH value is classified as moderately acid, calcium carbonate is present in no noteworthy amounts. The investigated, disturbed material was taken from the vertic Bv horizon (50 cm depth), where a prismatic soil structure is given. The content of organic matter is high within the whole profile, in some cases down to 2m, but rather low when regarded the upper 30 cm (3% C_{org}) only.
An even higher clay content (75%) is given in a clayey Oxisol (WRB: Ferralsol) originating from Santo Angelo, the northwest region of Rio Grande do Sul. This intensively weathered soil type is characteristic for humid regions of the tropics and subtropics, respectively. Desilification shall be mentioned in this context as major process of soil development.

Tab. 2-4 *Physical and chemical properties of Ibeco Seal-80, loess from Avdat/Negev Israel, Vertisol (Bv material), Santana do Livramento/ Escobar and clayey Oxisol, Santo Angelo, Rio Grande do Sul, Brazil.*

substrates	CEC			texture			$CaCO_3$	pH
	Na	Mg	Ca	sand	silt	clay		
	-------- cmolc/kg --------			--------- [%] ---------			[%]	$CaCl_2$
Ibeco Seal-80	44.3 CEC eff.			1.9	29.8	71.6	9.4	n.v.
Avdat loess	1.0	3.5	9.8	17.1	63.9	18.9	52.4	7.6
Vertisol	0.3	15.7	39.6	3.4	31.8	64.9	n.v.	5.5
Oxisol	0.1	2.1	4.3	5.4	19.2	75.4	n.v.	5.0

Apart from ferric oxides the clay fraction is composed of kaolinite; the content of goethite (FeOOH) prevails the hematites' (Fe_2O_3), a brownish colour is preponderant. High Fe and/or Al-content enhance a stable, earthy aggregate structure, well known as pseudosand. Under acidic conditions chemical activity proceeds on a low level.

2.3.2 Preparation of samples

The preparation of the Na-bentonite diverges a little from the natural substrates. This instance derives from the ability of montmorillonites to take up high amounts of water and its textural character as pure clay mineral. For all materials three NaCl salt solutions with concentrations of 0.01, 0.1 and 0.17M (=1%) were produced. Additionally, distilled water was chosen. According to the United States Salinity Laboratory (U.S.S.L. 1954) the osmotic potential Ψ_o [kPa] derives from the EC (electrical conductivity) [dS/m] (eqn (7)), which was measured in all salt solutions:

$$\Psi_o \text{ [kPa]} = -36 \cdot \text{EC [dS/m]} \qquad (7)$$

Hence a concentration of 0.01M equals an EC [dS/m] of 0.1, 0.1M = 1.0 dS/m, and 0.17M = 1.6 dS/m.

2.3.2.1 Preparation of Ibeco Seal-80

250g (250 ml) NaCl salt solution were added to 50g Ibeco Seal-80 (= 5.0kg NaCl salt solution of different concentrations/kg soil) and were manually mixed (10 min.), followed by mechanical stirring (10 min.) with a spatula. The suspensions were stored in beakers with twistable lids over night at room temperature.

2.3.2.2 Preparation of Avdat Loess, Vertisol and Oxisol

For the preparation of the silty and clayey substrates 100 cm³ cylinders were chosen and completely saturated as well as drained at -30 hPa and -60 hPa, respectively. Soil compactness was set at d_B = 1.2 g/cm³ and 1.4 g/cm³

depending on the texture. Depending on the substrate characteristics the saturation of the samples with distilled water covered a period of 24 to 48 hours. In case of salt solutions the period was extended to one week. Thus, an equilibrium state can be assumed.
An appropriate amount of the prepared samples, congruently to a volume of appr. 4 cm³, was taken with a small spatula out of the cylinders, and was carefully placed on the fixed bottom plate. By using the software USD 200 (see 2.2.3), the amplitude sweep test as well as the measuring device, e.g. the lift, are controlled and run automatically, when started.

2.4 Results

2.4.1 Salt effects

Figures 2-9a) and ***b)*** show results from amplitude sweep tests conducted on Avdat Loess with controlled shear deformation (CSD). Generally G' prevails G", a gel character is given at resting state. In ***Fig. 2-9a)*** $G'_{(\text{distilled water})} \leq G'_{(\text{NaCl 0.01 M})} < G'_{(\text{NaCl 0.17 M})}$; the input deformation has a similar effect to the elastic behaviour in silty samples, which are saturated with distilled water or NaCl solutions of low concentrations, here 0.01M. At higher salt concentrations differences in elastic components become apparent, the primary level of G' is $10^{5.5}$ Pa. The response to low deformations is congruent in all cases, the graphs decrease gradually. When γ = 0.01%, which equals a deflection of 0.001 mm, is reached, a transition can be observed. The elastic part decreases more distinctively with increasing deformation, at a constant (angular) frequency.

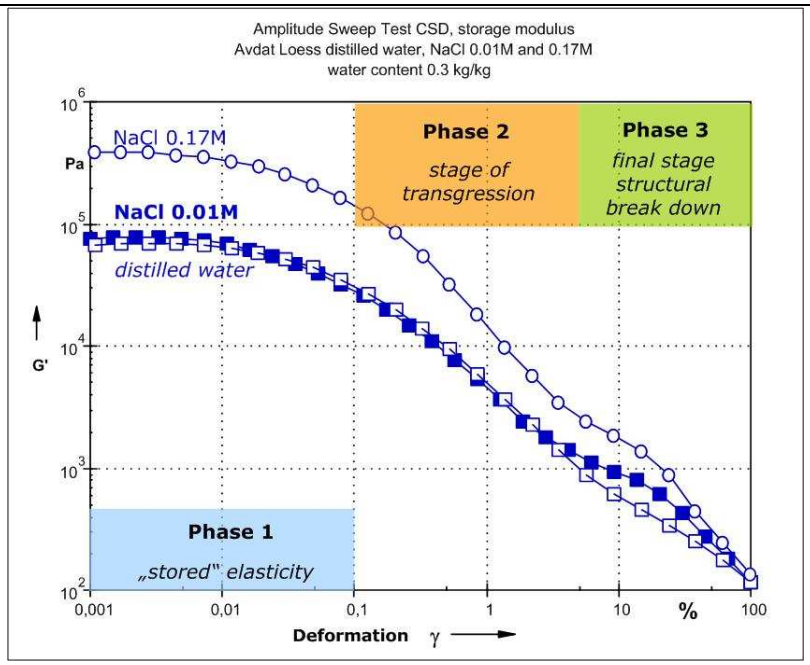

Fig. 2-9a) *Resulting graphs of G'(storage modulus) from a conducted amplitude sweep test with Avdat loess, saturated with distilled water(blank square), NaCl solutions of 0.01M (filled square) and 0.17M (blank circle), respectively. Storage moduli G' are compared. Substrates saturated with distilled water and NaCl solutions of concentrations have similar elastic characteristics; at higher concentrations differences become apparent.*

In ***Fig. 2-9b)*** resulting graphs of loss moduli G" are plotted. An analogical behaviour is given with regard to curve progressions of G': $G''_{(\text{distilled water})} \leq G''_{(\text{NaCl 0.01 M})} < G''_{(\text{NaCl 0.17 M})}$. The significant difference lies within the level of the graphs, which is approximately one order of magnitude smaller than in G'.

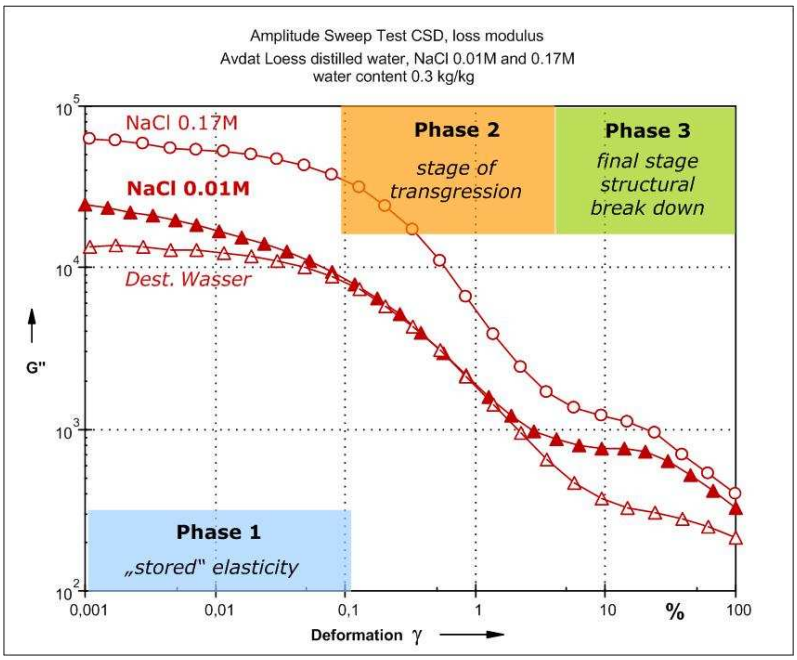

Fig. 2-9b) *Whilst in Fig. 2-9a) storage moduli are compared, loss moduli G" are opposed in this case. The graphs of G" show an analogue developing to G'. Samples saturated with distilled water (blank triangle) and NaCl of 0.01M (filled triangle) have almost the same viscous parts, whereas at a concentration of 0.17M (1%) (blank circle) G" increases, likewise to G'.*

2.4.2 Shear behaviour

In ***Fig. 2-10*** graphs from a conducted amplitude sweep test with Ibeco Seal-80 are illustrated. In comparison to substrates, which are rich in silt, a montmorillonitic substrate, here a Na-bentonite IS-80 has a more distinctive plateau within the LVE range and a well defined, clear deformation limit γ_L. When γ_L IS-80 is exceeded, G" is increasing until a deformation of about 12% is reached. The state of elastic behaviour passes into viscous behaviour, the yield point has been exceeded.

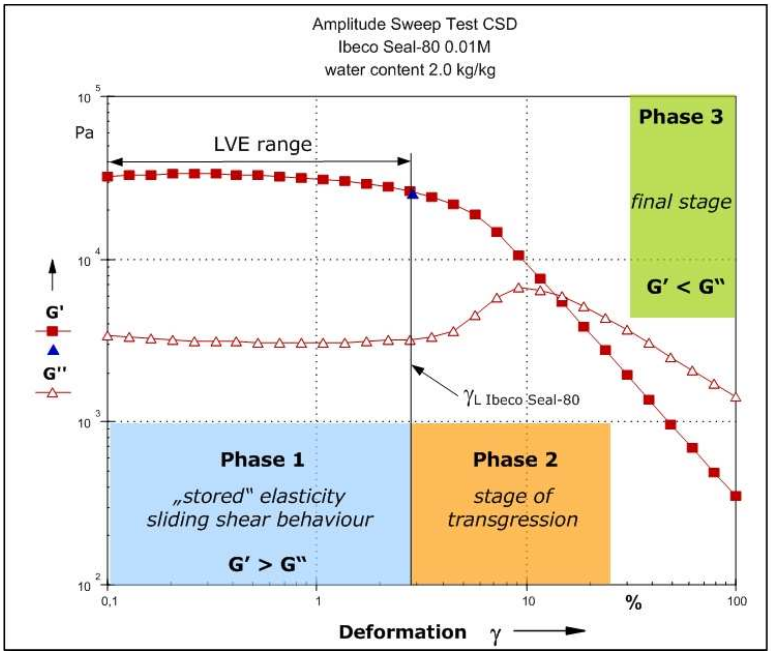

Fig. 2-10 *Result from a conducted amplitude sweep test with Ibeco Seal-80, saturated with NaCl salt solution 0.01M. Basically, clay minerals are appropriate to show a distinctive LVE range including the limit of deformation γ_L and a well defined crossover of G' and G", the transgression of the yield point.*

2.4.3 Clay mineralogical effects

A comparison of the Brazilian substrates, a clay rich Oxisol and a Vertisol is shown in ***Fig. 2-11***. A crossover of G' and G" occurs earlier regarding to Vertisol and is better defined. Even at lower deformation (not illustrated) a plateau does not exist, G' and G" are decreasing constantly. This behaviour is even more distinctive in case of the clayey Oxisol. A crossover happens to be slightly. It comprises more than a single point and has a transgression character.

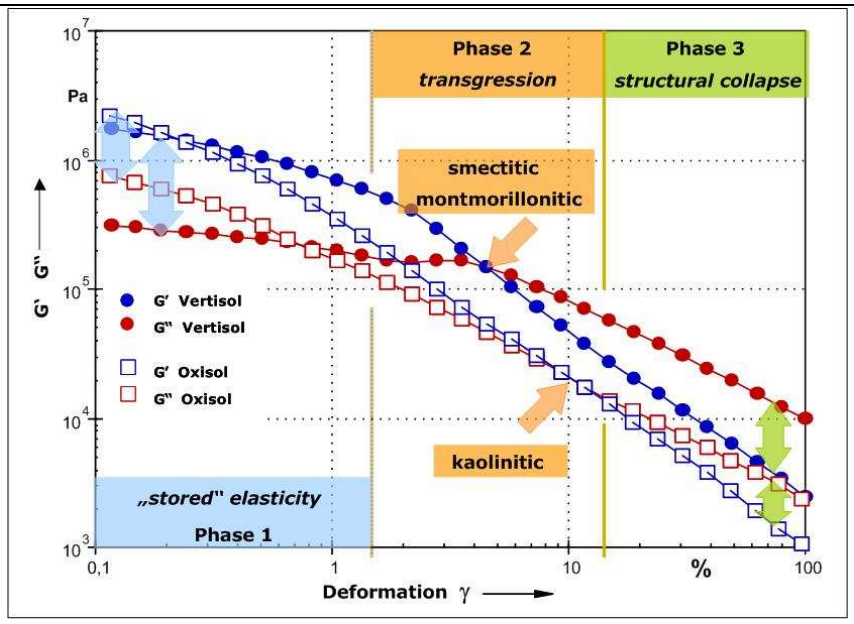

Fig. 2-11 *Resulting graphs of G' and G" from conducted amplitude sweep tests. The clayey Oxisol and Vertisol, both saturated with distilled water are compared. According to their natural conditions (e.g. texture, mineralogy) differences in elastic and plastic parts can be derived from the plots. G' Vertisol > G' clayey Oxisol in phase 1; although the intersection of G' and G" of the Vertisol in phase 2 is reached earlier, the level of G' and G" remains high compared to the kaolinitic Oxisol. The Vertisol shows a more distinctive part of "stored elasticity" than the clayey Oxisol.*

The primary levels of G' are very similar, but deviating when G" is considered. The difference between G' and G" of the Vertisol is about one order of magnitude.
The storage and loss moduli of the clayey Oxisol converge and diverge in same dimensions, having almost a linear decreasing character.

2.5 Discussion

Amplitude sweep tests were chosen to investigate structural effects under oscillatory shear, simulating conditions, which might be given in nature or in practice (e.g. aligned particles due to trafficking). Textural effects and those deriving from different water contents have already been mentioned in Ghezzehei and Or (2001), but are based on rotational and frequency sweep tests, with configured varying frequencies during a test versus a constant frequency in an amplitude sweep test. Basically, conducted rotational tests may give a certain insight into yield stress considerations, but are limited in significant data. Frequency tests are usually applied, when substrates with a more viscous character, initially, need to be investigated at a very low viscosity range, where differences close to the resting state become significant (e.g. paint). In opposite to this, amplitude sweep tests as applied in these investigations include more information about possible textural effects,

influenced by certain salt concentrations, clay mineralogy and water content, apart from flow behaviour in viscoelastic material. Different shear behaviour due to textural effects becomes obvious when primary levels of G' of the loess material, IS-80 and both Brazilian soils are compared. Generally, three sections are characteristic, as presented above:

Phase 1: a stage at low shear deformation, where the resting state (G'>G") and the LVE range can be defined, including the deformation limit $\gamma_{L,}$
Phase 2: a transgression stage with the intersection of G' and G",
Phase 3: viscoelastic, solid materials are creeping or running, G'<G".

At each stage specific attributes influence the curve progression, e.g. texture and physicochemical properties: the level of G' and G", the point of intersection and the slope of the curves. In case of silty substrates, e.g. loess material the primary level of G' is at 10^5 of G" at 10^4 Pa, for clay rich soil applies G' at 10^6 and G" at 10^5 Pa. Hence, the level of G' and G" is higher in case of clay rich substrates, which still might include also coarser particles, which need to be aligned first. A higher input of deformation can be observed here. Conducted amplitude sweep tests on the $CaCO_3$ rich, silty Avdat Loess showed a higher structural stability due to increasing NaCl concentrations, which might be explained by the reaction of $2NaCl+CaCO_3 \rightarrow Na_2CO_3+CaCl_2$. The dispersive effect of Na would be substituted by the stabilising effect of $CaCl_2$. Here, mechanisms of hydration as well as of selectivity according to the Gapon equation become obvious. Na (ionic bonds) tend to have an extensive hydration character in opposite to Ca, which forms covalent bonds, that lead to a limited hydration (e.g. Rengasamy and Olssen 1991, Mitchell and Soga 2005, Peng et al. 2005). Differences of clay mineralogical effects in the tested clay rich, kaolinitic Oxisol and the smectitic Vertisol could be demonstrated and quantified. Both turbulent and sliding shear behaviour as differentiated and elaborated in Smith and Reitsma (2002) were shown. The significance of the storage modulus as parameter of "stored elasticity" and the loss modulus, representing the loss of elasticity and increase of plasticity has been demonstrated. Physical and chemical properties of substrates, namely water content, texture, salt concentrations etc. influence the level and progression of the graphs as well as the duration and character of each phase. In tests with Ibeco Seal-80 a sliding shear behaviour could be proved nicely considering the wide LVE range and parallel progression of both, G' and G" in the first phase. The significance of the second stage could be demonstrated in case of the clay mineralogical comparison (textural effects) between the clayey Oxisol and the Vertisol.

Here, the moment and significance of intersection of G' and G" are decisive factors: although smectitic, montmorillonitic substrates (Vertisol) occur to reach an earlier point of intersection than kaolinitic (Oxisol), the level of G' and G" as already shown in ***Fig. 2-11*** remains high after intersection in case of the Vertisol and is well defined. Phyllosilicates with a high swelling potential show a trend of stabilisation. The layer structure seems to compensate a higher deformation energy input. This effect is intensified when Ibeco Seal-80, a typical Na-bentonite with stronger montmorillonitic character is considered: the absorbed water, including cations in solution and/or on the inner and/or outer surface has an additional elastic influence. Not until a high deformation is reached, the water between the layers is squeezed out, transgressing into a sliding shear behaviour, compression, and final structural break down. In any case of viscoelastic substrates, namely soils or clay minerals, a flow or creeping character occurs in the third phase, G" prevails G', the elasticity is lost, finally.
All conducted amplitude sweep tests showed, that a rheometer can be applied, whenever salt or textural effects and shear behaviour have to be quantified and demonstrated on a particle-particle-scale regarding clay-rich and silty substrates. In forthcoming investigations, vibration effects of farm implements can be simulated by varying constant frequencies in amplitude sweep tests, based upon values of e.g. Garciano et al. (2001). Furthermore, Kutílek and Nielsen (1994) mentioned, that shear strength and the soil water ratio of soils are small after any mechanical disturbance (deformation) and increases with time. Not only swelling but also thixotropic behaviour of the soil water ratio and the volumetric soil water content is time dependent and strongly reduced in the subsoil due to overburden pressure in the topsoil. With respect to this, the significance of rheometry in soil hydrology on a pore scale should be corroborated. Findings regarding valency effects, mechanisms of hydration and other physico-chemical variations need to be extended, additionally.

2.6 Conclusions

Due to higher NaCl concentrations the microstructural stability is increased, especially when regarded to $CaCO_3$ rich substrates. Clay mineralogical effects could be presented in case of natural, clay rich substrates as well as of an industrial produced Na-bentonite. Generally, high clay contents lead to a sliding shear behaviour in opposite to silty material, which shows a more turbulent shear behaviour. Considering the first case, swellable smectitic, montmorillonitic substrates tend to have a more distinctive sliding character than non-expandable kaolinites. Hence, a rheometer with a parallel plate measuring device is applicable for the detection of small scale interactions.

2.7 Acknowledgment

The first author thanks Mr. Stefan Büchner, Anton Paar, for his professional advice, Dr. Niall Young and the NRS, for their support and inspiration, Dr. Jan Gustafsson for his advice, and Dr. Heiko Frahm, Institute for Inorganic Chemistry CAU Kiel, for giving a first insight into rheology.

2.8 References

Barnes, H.A., Hutton, J.F., Walters, K., 1989. An Introduction to Rheology. Rheology Series 3. Elsevier. Amsterdam, Oxford, New York, Tokyo. 199 pp. ISBN 0-444-87469-0

Bishop, A.W., 1960. The principle of effective stress. Publikasjon Norges Geotekniske Institutt 23:1-5. ISSN 0078-1193

Collyer, A.A., Clegg, D.W. (eds.), 1998. Rheological Measurement. 2nd edition. Chapman & Hall. London. 779 pp. ISBN 0-412-72030-2

Derjaguin, B.V., Landau, L., 1941. Theory of the Stability of Strongly Charged Lyophobic Sols and of the Adhesion of Strongly Charged Particles in Solutions of Electrolytes. Acta Physicochim. (URSS) 14: 633–662.

DIN 53018, 1976. Measurements of the dynamic viscosity of Newtonian fluids using rotational viscometers.

Emerson, W.W., 1967. A Classification of Soil Aggregates based on their Coherence in Water. Austr. J. Soil Res. 5: 47-57. ISSN 0004-9573

Fredlund, D.G., Rahardjo, H., 1993. Soil Mechanics for Unsaturated Soils John Wiley & Sons Inc., New York. 517 pp. ISBN 0-471-85008-X

Garciano, L., Torisu, R., Takeda, J., Yoshida, J., 2001. Resonance Identification and Mode Shape Analysis of Tractor Vibrations. J. JSAM 63 (6):45-50. ISSN 0285-2543

Ghezzehei, T.A., Or, D., 2001. Rheological Properties of Wet Soils and Clays under Steady and Oscillatory Stresses. Soil Sci. Amer. J. 65: 624-637. ISSN 0361-5995

Horn, R., 1995. Aggregate strength of differently structured soil and its alteration with external stress application, p. 177-182, In B. H. So, Smith, G.D., Raine, S.R., Schafer, B.M. and Loch, R.J. (eds.). Sealing, Crusting and Hardsetting Soils: Productivity and Conservation. Proceedings of the 2nd International Symposium. Australian Society of Soil Science, Inc. - Queensland Branch, University of Queensland, Brisbane, Australia, 7-11 Feb. 1994.

Horn, R., Baumgartl, T., Gräsle, W., Richards, B.G., 1995. Stress induced changes of hydraulic properties in soils. pp. 123-128. *In* Alonso, E.E., Delage, P. (eds.). Unsaturated Soils. Balkema Verlag, Rotterdam, Berlin. ISBN 9-0541-0583-6

Horn, R., Baumgartl, T., 1999. Dynamic properties of soils. pp. A19-A51. In: Sumner, M.E. (ed.), 1999. Handbook of Soil Science. CRC Press. Boca Raton, Florida. appr. 1100 pp. ISBN 0-8493-3136-6

Jasmund, K., Lagaly, G. (eds.), 1993. Tonminerale und Tone: Struktur, Eigenschaften, Anwendungen und Einsatz in Industrie und Umwelt. Steinkopff-Verlag. Darmstadt. 490 pp. ISBN 3-7985-0923-9

Keedwell, M.J., 1984. Rheology and Soil Mechanics. MacMillan. London and New York. 323 pp. ISBN 0-8533-4285-7

Keedwell, M.J. (ed.), 1988. International Conference on Rheology and Soil Mechanics. Elsevier Applied Science. London and New York. 371 pp. ISBN 1-85166-273-1

Kutílek, M., 1964. the influence of soil colloids upon the values of some hydrolimits. Rostlinná výroba 10:605-623. ISSN 0370-663X

Kutílek, M., 1967. The affinity of water to kaolinites and montmorillonites. Proc. Int. Soil Water Symp., Prague I: 73-82.

Kutílek, M., 1973. The influence of clay minerals and exchangeable cations on soil moisture potential. pp. 153-160. In: Hadas, A., Swartzendruber, D., Rijtema, P.E., Fuchs, M., Yaron, B: Physical Aspects of Soil Water and Salts in Ecosystems. Ecological Studies 4. Springer-Verlag. Berlin. ISBN 3-540-06109-6

Kutílek, M, Nielsen, D.R., 1994. Soil Hydrology. GeoEcology textbook. Catena. Cremlingen. ISBN 3-923381-26-3

Loveday, J., Pyle, J., 1973. The Emerson Dispersion Test and Its Relationship to Hydraulic Conductivity. CSIRO Australian Division of Soils, Technical Paper No. 15: 1-7.

Macosko, C.W., 1994. Rheology – Principles, Measurements, and Applications. VCH Publishers. New York. 550 pp. ISBN 1-56081-579-5

Mezger, T., 2002. The Rheology-Handbook – For users of rotational and oscillatory rheometers. Vincentz Verlag. Hannover. 252 pp. ISBN 3-87870-745-2

Mitchell, J.K., Soga, K., 2005. Fundamentals of soil behavior, 3rd edition. John Wiley & Sons, Hoboken, NJ. 577 pp. ISBN 0-471-46302-7

Peng, X., Horn, R., Deery, D., Kirkham, M.B., Blackwell, J., 2005. Influence of soil structure on the shrinkage behaviour of a soil irrigated with saline-sodic water. Austr. J. Soil Res. 43:555-563. ISSN 0004-9573

Rengasamy, P., Greene, R.S.B., Ford, G.W., Mehanni, A.H., 1984. Identification of Dispersive Behaviour and the Management of Red-brown Earth. Austr. J. Soil Res. 22:413-431. ISSN 0004-9573

Rengasamy, P., Olssen, K.A., 1991. Sodicity and soil structure. Austr. J. Soil Res. 29: 935-952. ISSN 0004-9573

Schramm, G., 2002. Einführung in Rheologie und Rheometrie. 2. Auflage. Haake GmbH, Karlsruhe. 360 pp. (no ISBN)

Schulz, O., 1998. Berichte aus der Chemie: Strukturell - rheologische Eigenschaften kolloidaler Tonmineraldispersionen. Dissertation zur Erlangung des Doktorgrades. Institut für anorganische Chemie Christian-Albrechts-Universität zu Kiel. Shaker Verlag. Aachen. 501 S. ISBN 3-8265-4439-0

Smith, D.W., Reitsma, M.G., 2002. Towards an explanation for the residual friction angle in montmorillonite clay soil. pp. 27-44. In: Vulliet, L., Laloui, L., Schrefler, B. (eds.), 2002. Environmental Geomechanics – Monte Verità 2002. EPFL Press. Monte Verità. 423 pp. ISBN 2-8807-4512-2

Sumner, M.E., Naidu, R., (eds.), 1998. Sodic Soils: distribution, properties, management and environmental consequences. Oxford University Press, New York. 207 pp. ISBN 0-19-509655-X

Terzaghi, K., 1925. Erdbaumechanik auf bodenphysikalischer Grundlage. Deuticke, Leipzig. 399 pp. (no ISBN)

Tuller, M., Or, D., 2003. Hydraulic functions for swelling soils: pore scale considerations. J. Hydrol. 272:50-71. ISSN 0022-1694

Tuller, M., Or, D., 2005. Water films and scaling of soil characteristic curves at low water contents. Water Resour. Res. 41:W09403 (1-6 pp.). ISSN 0043-1397

U.S.S.L. 1954. Diagnosis and Improvement of Saline and Alkaline Soils. USDA Handbook No. 60. GPO, Washington D.C.

Verwey, E.J.W., Overbeek, J.T.G., 1948. Theory of the Stability of Lyophobic Colloids: the Interaction of Soil Particles having an Electric Double Layer. Elsevier. New York. 205 pp. (no ISBN)

Vyalov, S. S., 1986. Rheological fundamentals of soil mechanics. Elsevier, Amsterdam. 564 pp. ISBN 0-444-42223-4

Whorlow, R.W., 1992. Rheological Techniques. 2nd edition. Ellis Horwood Ltd. Chichester. 460 pp. ISBN 0-13-775370-5

Yoder, R.E., 1936. A direct method of aggregate analysis of soils and a study of the physical nature of erosion losses. J. Amer. Soc. Agronomy 28:337-351. ISSN 1435-0

3. Rheological Strength Analysis of K^+-treated and of $CaCO_3$-rich soils

Wibke Markgraf, Rainer Horn

J. Plant Nutr. Soil Sci. 169, 3, pp.411-419 (2006)

Abstract

Rheological methods are applied whenever flow behaviour of substances needs to be investigated on a particle to particle scale executed by a parallel plate rheometer. Under oscillation mechanical effects due to trafficking or vibrations caused by agricultural and forest machinery can be simulated by conducting amplitude sweep tests.

Hooke's law of elasticity, Newton's law for ideal fluids (viscosity), Mohr-Coulomb's equation, and finally, Bingham's yielding are well known relationships and parameters in the field of rheology. This paper aims to introduce rheometry as a suitable method to determine the mechanical behaviour of salt affected soils when subjected to external stresses. K^+ treated loamy sand from the Halle (Saale) region and loamy silt from Kassel, Germany, as well as Loess from Israel, saturated with NaCl solutions in several concentrations were analysed. From the stress-strain relationship parameters like the storage modulus G' and loss modulus G", yield stress τ_y and the linear viscoelastic (LVE) deformation range including the deformation limit γ_L i.e. the transition from an elastic to a viscous state were determined and calculated, respectively.

With respect to salt effects, amplitude sweep tests on originally $CaCO_3$ rich Avdat Loess show an increasing stability if saturated with higher NaCl concentrations. Comparable tests with K^+ rich substrates from Halle and Kassel evinced similar tendencies including the phenomenon of a critical K^+ content, which becomes more obvious in case of the drained (-60hPa) loamy silt samples from Kassel. Nevertheless, a higher microstructural stability is given in both substrates from Halle *and* Kassel, affected by different water contents, in general, which influence the exchange and availability of cations.

The results verify that oscillatory tests are applicable for retracing salt induced effects, beside those ones, which are influenced by texture, actual water content and/or further chemical parameters.

Keywords: amplitude sweep test/ mechanical behaviour of single particles/ structural changes/ salt effects

3.1 Research objectives

Rheological techniques are adaptable not only in polymer science, but also in the quality control in food industries or in clay mineralogy. Markgraf et al. (2006) analysed the effect of texture on inter-particle forces as micromechanical aspects in soil mechanics for Na-bentonite (Ibeco Seal-80), clay rich soils from Brazil and Avdat loess at a saturated stage and concluded that there are differences either in shear behaviour as well as in microstructural stability. However, the interaction between chemical and textural properties on strength are still not understood as will be shown in the following and are the basis for the own research approach.

It is well defined that salinisation and sodification due to irrigation are well known environmental problems especially in semi-arid areas, leading to soil crusting and sealing including strengthening on the surface or in the pan layer. Transferred to central European temperate climate conditions, fertilisers especially when applied under irrigation are the major source of salts applied to arable land or in glasshouse horticulture. Natural salty properties are to be found e.g. in coastal areas, and marsh regions.

In agriculture, knowledge about the effect of ionic strength on soil aggregation is often related to Ca^{2+} concentration but seldom to K^+ (which is mostly applied as K_2O), while Mg^{2+} saturated soils derived from Amaltheen-clay will have a weak structure, a high sensitivity for creeping and are therefore also classified as not very productive sites. With increasing valency stronger binding mechanisms should occur.

Young and Warkentin (1966), Mitchell (1993) have described the strengthening effect based on the hydration energy and ion radius, but the actual inter-particle forces as well as the main friction related processes were not quantified. Mechanical disturbances, which are induced by tillage compaction, enhance due to an increased accessibility of the exchange places the transfer of nutrients but result at the same time also in an increased pore tortuosity, a reduction in coarse pores and a weakening of the total pore system. Thus, it also results in different mechanical behaviour between aggregates and single particles (Horn et al., 1995; Peng et al., 2005). Based on the Gapon equation, accumulation of potassium inhibits an uptake of magnesium. Thus, until a critical concentration of potassium is reached, we can also expect that aggregation and structure stabilisation may be effected. In $CaCO_3$ rich soils, an addition of NaCl may also have a stabilising effect, as calcium chloride, deriving from the reaction $2NaCl + CaCO_3 \rightarrow Na_2CO_3 + CaCl_2$, has a strengthening character if applied in higher

concentrations due to the above mentioned concentration effect rather than through the valency interactions. It can be therefore also postulated that the micromechanical behaviour is influenced by ionic concentration in the soil solution and/or adsorbed at the exchange places or as chemical precipitation depending on the properties of the chemical elements (valencies, degree of hydration) and boundary forces. As described in the DLVO theory according to Derjaguin and Landau (1941), Verwey and Overbeek (1948), and Osipov (1975) the interaction between the liquid and solid phase, especially when regarded to colloidal solutions, represents an important factor within these considerations. According to Mitchell (1993) ionic forces (Na^+) and Van der Waals bonds (Ca^{2+}, Mg^{2+}) are the major binding mechanisms (Peng et al., 2005). Further considerations have to be made regarding a link between Terzaghi's equation for effective stress (Fredlund and Rahardjo, 1993) and the salt concentration, or rather the osmotic potential Ψ_o.

In this context, the effective stress σ' (according to Terzaghi 1923, Bishop (1960) in Mitchell 1993, Fredlund and Rahardjo 1993, Horn and Baumgartl 1999), depends at a given total stress not only on water pressure but should also be affected by potentials in soils with special regard to the osmotic potential. The latter depends on the salt content in the liquid phase and should affect internal strength.

Smith and Reitsma (2002) in Vulliet et al. (2002) described the textural effects on strength and their changes with stress and strain if we also the kind of minerals as well as their sizes are considered. It can be concluded that the friction of internal strength remains high in kaolinitic clay soils (20 to 25 degrees) even at high deformation: the residual friction angle equals the critical state friction angle. In comparison to this fact, the residual friction angle decreases in e.g. montmorillonitic clay soils with increasing deformation and results in a sliding shear behaviour with small values for the friction angle Such behaviour can be attributed especially to platy clay platelets or aligned particles (***Fig. 3-1***). Such behaviour also requires generally homogenous conditions. If however, steady stress conditions are applied for a naturally given structure it shows a higher resistance to the applied external, vertical stress even if in case of exceeding the internal structural strength by the external forces compaction, bulk density increases, and the (micro)pore system collapse can be determined

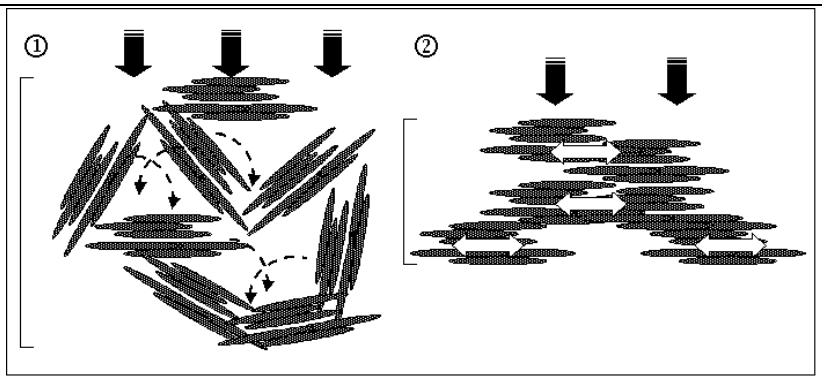

Fig. 3-1 *Mechanical behaviour of clay platelets and aligned soil particles: sliding shear behaviour.* ***①*** *Platelets/aligned particles in gel state (aggregated), under steady stress condition;* ***②*** *either under steady or shear stress a sliding shear behaviour is given, when external applied stress' prevail internal (structural) forces, the yield stress is exceeded – compaction is the result, bulk density increases, (micro)pore system collapses.*

(succession from ① to ②). Such changes will be more pronounced if sliding shear behaviour occurs and results in a lower residual shear strength ϕ_R as was already described by Horn (1976). This state has a more finite, irreversible character in contrast to turbulent shear behaviour. A rotund particle shape as commonly given for silt, sand, and especially in case of Fe-rich soils, for kaolinite, leads to turbulent shear behaviour and a high residual shear strength ϕ_R of 25 to 30 degrees. In a resting state (①a in ***Fig. 3-2***) a concave menisci shape is given. The angle of inner friction remains high. Under compression (①b) the pore water pressure results in positive values and the menisci shape becomes convex resulting in declining values for the angle of inner friction if external forces increase. Because under in situ conditions, not only vertical forces are applied, but also shear stress application must be considered, we have also to regard a shear directed change in the menisci shape, as well as the shear strength affects the moment of a structural break down (= breakaway of menisci).

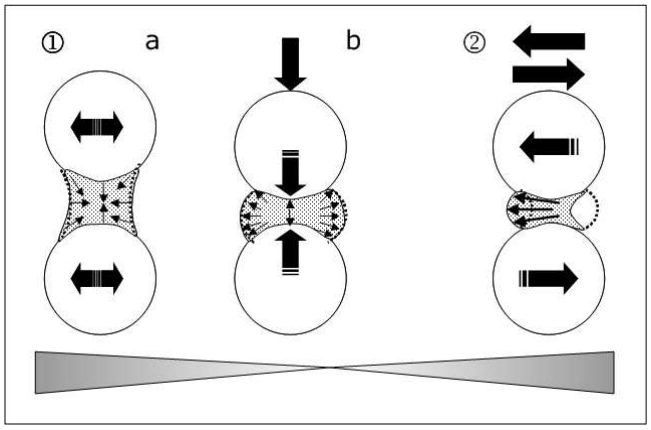

Fig. 3-2 *Mechanical behaviour of rotund particles.* ***①****a-b: vertical stress (compression) applied to two single particles. In* ***①****a water menisci with a concave shape in a resting state, in* ***①****b with a convex form due to the applied vertical stress.* ***②****: shear stress applied to two particles; water menisci show concave and convex shape congruently to the direction of shear. A turbulent shear behaviour is the result of applied stress to rotund particles, either vertical or in shear.*

With respect to the mechanical strength parameters, the applied mechanical tests or the effect of applied hydraulic stresses on internal strength have to be differentiated as also Ghezzehei and Or (2001, p. 624) stated, that "[…] there is a fundamental difference between soil deformation by farm implements (oscillatory stress) and capillary induced strains (steady stress) rooted in the inherent soil properties, manifested in the form of frequency-dependent rheological properties […]".
Thus the following open questions can be defined which will be dealt with in the following: Is rheometry an appropriate method when salt effects have to be investigated on a microscale? Which effects occur due to changes in physical and chemical preconditions? Additionally, is it possible to investigate mechanical behaviour of single particles, sand, silt or clay (minerals), and which differences can be elaborated?

3.2 Some remarks about the rheological method

An approach of rheometry in soil mechanics has already been introduced by Markgraf et al. (submitted 2005), based on works of Keedwell (1984), Whorlow (1992), Macosko (1994), Collyer and Clegg (1998), Schulz (1998), Ghezzehei and Or (2001), Schramm (2002) and Mezger (2002). Natural substances i.e. soils consist of elastic and viscous compounds. The proportion of those depend on physical and chemical properties, i.e. texture, porosity, water content, and ionic composition of the liquid phase. Elasticity and viscosity of substrates and liquids can be described mathematically by the fundamental laws of Hooke and Newton. Generally, deformation and flow behaviour depend on the type, degree and duration of applied stress, either oscillating or steady stress. The shear stress (shear strength) τ is defined as

$$\tau = F/A \qquad [1]$$

τ = shear strength [Pa]
F = force [N]
A = area [m²]

3.2.1 Hooke's law: Elastic flow behaviour and shear modulus G

Hooke's law defines an ideal elastic substance, which can be expressed in the mechanical analogue of a spring (eqns [2.2] and [2.3]).

The energy, which was invested in deforming the body is completely stored; as soon as the stress, that caused the deformation, has been removed, the original shape is restored and the energy is recovered. The linear relation between the extent of elastic strain and the applied stress is:

Derived from the Young's Modulus E [Pa]

$E = \sigma/\varepsilon$ where σ = tensile stress [Pa] [2.1]
ε = tensile strain [ ] or [%]

the shear modulus is

$G = \tau/\gamma$ where G = shear modulus [Pa] [2.2]
τ = shear stress [Pa]
γ = shear deformation [ ] or [%]

with the shear deformation γ

$\gamma = s/h$ s = deflection [mm] [2.3]
$s/h = \tan \varphi$ h = distance between the plates [mm]
φ = deflection angle [°]

if s = h or φ = 45°, then γ = 1 = 100 %.

The shear deformation γ [ ] or [%] depends on the plate distance h [mm] and diameter d [mm].

3.2.2 Newton's law of ideal fluids

The relation of shear viscosity to the shear rate of Newton's law ("lack of slipperiness"), can be defined as the shear stress and can be explained by the resistance due to the internal friction of the fluid. The mechanical analogue to an ideal viscous fluid is represented in rheology by a dashpot.

$\tau = \eta \cdot \dot{\gamma}$ η = shear viscosity [Pa·s] [3.1]
η = const.

the shear rate $\dot{\gamma}$ as

$\dot{\gamma} = v/h$ $\dot{\gamma}$ = shear rate [1/s] [3.2]
v = velocity [m/s]
h = gap h [m].

Newtonian flow is characterized by the resistance of elemental particles to motion and the energy that was invested in deforming viscous material and which is vanishing entirely. Boundary conditions are given by any shear stress > 0, and a constant shearing rate, which is directly proportional to the shear stress.

3.2.3 Viscoelasticity

A combination of both viscosity and elasticity is expressed by the term "viscoelastic". Either fluids or solids may show viscoelastic behaviour. To quantify the loss of elasticity, shear parameters need to be adapted to oscillatory tests: a complex dynamic modulus G*, a storage modulus G' (the so called dynamic rigidity) and an imaginary loss modulus G", deriving from the shear modulus G under steady stress conditions. The storage modulus G' [Pa] represents the elastic behaviour (Hooke's law) of a sample, the loss modulus G" [Pa] the viscous component (Newton's law). The LVE (linear viscoelastic) range and the deformation limit γ_L can be calculated by using values from G', the real part of stored elasticity, in opposite to G", as the imaginary part of lost elasticity and representing viscosity (Markgraf and Horn, 2005, Markgraf et al., 2006).
In oscillatory shear the complex shear modulus G* is defined by the equation

$$G^* = \sigma/\gamma \qquad \text{where } |G^*| = \sqrt{(G')^2 + (G'')^2} \qquad [4]$$

which is a modification of Hooke's law, a parallel combination of a dashpot and a spring, namely the Kelvin/Voigt model of viscoelastic solids.

3.2.4 Amplitude sweep test

Viscoelastic solids, e.g. gels but also soils of certain water contents (pF ≥ 1.8) and texture (clayey, silty), which show a complete or partial recovery from applied stress are defined by the Kelvin/Voigt model. Natural viscoelastic substances react with a temporal delay. This is represented by the phase shift angle δ, whereas tan δ equals the relation of G" to G' (eqn. [5]). The latter defines the relation of lost and stored elasticity:

$$\tan \delta = G''/G' \qquad [5]$$

In order to quantify and to investigate structural changes of dispersions and/or soil substrates with a parallel plate rheometer (MCR 300, Paar Physica),

oscillatory tests, amplitude tests, and a constant frequency are recommended. The term 'sweep' represents a function with a variable parameter. Either the shear stress (CSS) or the shear deformation (CSD) is controlled. Amplitude sweep tests are conducted to achieve informations about the flow behaviour of a substrate and especially its elastic part (stored elasticity), the LVE deformation range, marked as area between the points of the parallel running curves of G' and G" and their transition.

In ***Fig. 3-3*** G' and G" are illustrated comparatively. In an *initial or plateau phase*, an almost constant level is given. At this stage the elastic component prevails the plastic in case of substrates, which show a gel character in the resting state: G'>G". The LVE range is limited by a certain deformation value, namely γ_L or deformation limit [%]. This value is defined by material properties, especially elastic compounds. The deformation limit may be used synonymously to the term yield stress τ_y, considering that the shear stress τ [Pa] would be controlled (CSS) in this case, not the deformation (CSD). In the second stage, a phase of *transgression*, values of G' decrease, substances are in a state between elastic and viscous flow behaviour. Here, the slope of decline is significant. In phase 3, the *final stage*, a viscous character is given, γ_L has been exceeded: G'<G", substances are creeping, a structural break down has been induced (***Fig. 3-3***).

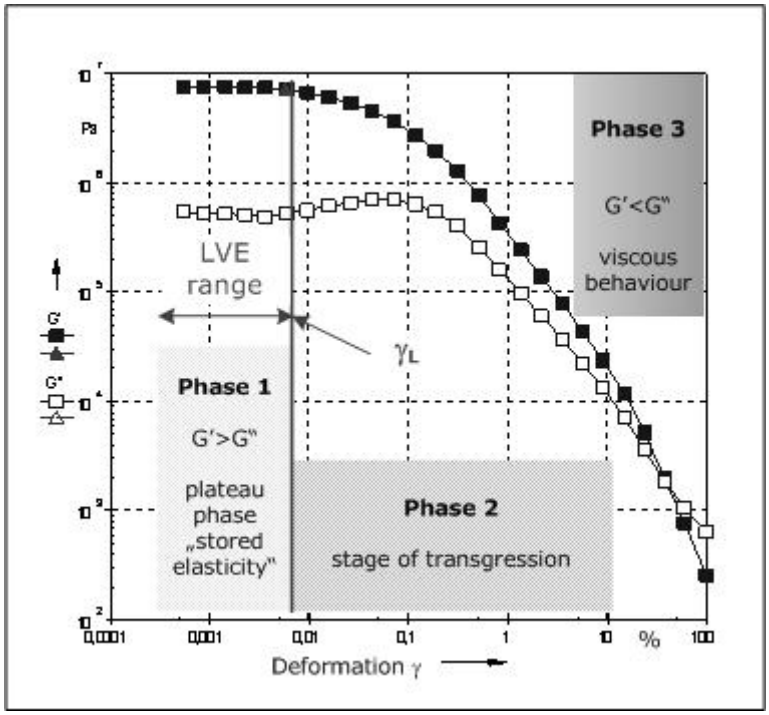

Fig. 3-3 *Representative illustration of resulting graphs deriving from conducted amplitude sweep tests with controlled shear deformation (CSD) [%]. Curves of G' (storage modulus) and G" (loss modulus) [Pa] are shown, which are characterised by three stages: an initial or plateau phase (1) including the linear viscoelastic range (LVE range), that is defined by a deformation limit γ_L, a stage of transgression (2) and a final phase (3) of structural collapse.*

3.2.4.1 Test Configuration

Table 3-1 informs about parameters, which were chosen for the amplitude sweep tests. The plate distance varies with the texture: basically, for substrates with a grain size ≤ 2 µm a gap of 1 to 2 mm should be preset, for substrates of coarser fraction (e.g. silt, loam, fine sand) a distance of 4 mm is recommended. The plate geometry of the rheometer with a parallel plate measuring system (PP MS) is determined by the plate radius R, according to DIN 53018. The rotating bob is 25mm in diameter and has a profiled surface. During all tests a constant temperature of 20°C is given, regulated by a Peltier unit. The generated normal force averages between 0 to 12 N and should not be exceeded during tests. A resting period of 30 seconds in the beginning was inserted in the test software (USD 200) to ensure a reorientation of the particles and an undisturbed measurement. Both cases might be induced by the application of the material on the measuring plate. The deformation γ is preset as logarithmic range from 0.0001 to 100%, the frequency at a constant value of 0.5 Hz, or π 1/s in SI unit. One run, including 30 measuring points, lasts approximately 15 minutes. The correlation between frequency and duration is inversely proportional, e.g. 1 Hz leads to test duration of 7 minutes.

Tab. 3-1 *Configuration of conducted amplitude sweep tests with controlled shear deformation (CSD).*

Parameter	
plate distance	d = 4 mm (>2 µm)
plate radius	R = 25 mm (profiled)
shear deformation	γ = 0.0001… 100% (>2 µm)
angular frequency (frequency)	$\omega = \pi$ 1/s (f = 0.5 Hz)
measuring points	30 pts.
duration	appr. 15 min.

3.3 Material

Homogenised (grinded and sieved < 2 mm) soil material has been prepared of several silt rich substrates originating from Halle and Kassel (Germany) and Avdat Desert (Israel).

3.3.1 Substrates

A range of silt rich substrates, treated with K^+ fertiliser as well as naturally enriched with $CaCO_3$, was chosen. Disturbed samples of a loamy sand from Halle/ Saale (Haplic Chernozem) and a loamy silt from Kassel (Luvisol), Germany, were taken from three (H1, H7, H15) and four depths (KA2, KA5, KA8, KA15), respectively, considering different K^+ (K_2O) concentrations. In Halle, the region of "Eternal Rye Growing" (est. in 1878), with long-term fertilisation experiments were chosen, which were established in 1949. Similar investigations have taken place in Kassel, Niestetal since 1978, where the effects of a reduced application of potassium fertilizers have been within the scope of research. Generally, with increasing depth, K^+ contents incline; as an indicator for an inhibited nutrient uptake due to a K^+ treatment, Mg^{2+} contents rise at the same time. The samples from Kassel are characterised by greater Mg^{2+} accumulations. Measured pH values are to be classified as weakly acid (Halle) to basic (Kassel) (data MLU Halle, 2005). Avdat Loess, which origins from the Negev Desert in Israel, has a silt content of 64% and a natural high calcium carbonate content of 52%. A x-ray diffractometry result in a high fraction of strongly weathered and swellable smectites and vermiculites. Montmorillonites and magnesium rich forms of smectites beside kaolinite and illite exist in low amounts only.
Exchangeable cations were extracted by 1M ammonium acetate. According to standardised methods, K^+ and Na^+ were measured by flame emission; concentrations of Mg^{2+} and Ca^{2+} were detected by atomic absorption spectrophotometer. Water contents of the soil samples range from 30% (w/w) in case of saturated samples from Halle, 45% (w/w) for Kassel, to 20% (w/w) regarding drained loamy sand material (-60hPa) as well as 30% in the latter case of loamy silt substrate. The saturated Avdat loess has a water content of approximately 33% (w/w). ***Table 3-2*** summarises physical and chemical properties of the tested material.

Tab. 3-2 *Physical and chemical properties of disturbed soil material from Halle (Haplic Chernozem) with the labels H1, H7, H15 from 1, 7, and 15 cm depth, and Kassel (Luvisol on Loess) with KA2, KA5, KA8, KA15, from 2, 5, 8, and 15 cm depth, Germany, and Loess from Avdat/Negev, Israel.*

Substrates	**CEC**				**Texture**			**$CaCO_3$**	**pH**	**EC**
	K	Na	Mg	Ca	sand	silt	clay			
		$cmol_c/kg$				[%]		[%]	$CaCl_2$	µS/cm
Halle										
H1	2.6	n.d.	3.4	0				0	5.8	64.1
H7	8.0	n.d.	3.9	0	56	32	12	0	5.7	72.8
H15	13.1	n.d.	4.5	0				0	5.7	166.1
Kassel										
KA2	4.1	n.d.	11.3	0				0	6.6	98.6
KA5	8.6	n.d.	12.6	0	9	79	12	0	6.6	113.7
KA8	11.0	n.d.	12.2	0				0	6.7	104.9
KA15	14.1	n.d.	16.0	0				0	6.3	132.4
Avdat Loess	0.8	1.0	3.5	9.8	17	64	19	52.4	7.6	474.0

n.d. = no data

3.3.2 Preparation of samples

Samples from Halle and Kassel were repacked in 100 cm³ cylinders at a bulk density d_B of 1.4 g/cm³ and saturated with distilled water. Half of the prepared samples were drained at -60 hPa (pF 1.8), three replicates of each were produced. Additionally, three NaCl salt solutions with concentrations of 0.01, 0.1 and 0.17M (=1%) were prepared for the pre-treatment of the $CaCO_3$ rich Avdat Loess. According to the United States Salinity Laboratory (U.S.S.L.,1954) the osmotic potential Ψ_o [kPa] derives from the EC (electrical conductivity) (eqn [6]), which was measured in all NaCl salt solutions:

$$\Psi_o\,[\text{kPa}] = -36 \cdot \text{EC}\,[\text{dS/m}] \qquad [6]$$

Hence a concentration of 0.01M equals an EC [dS/m] of 0.1, 0.1M = 1.0 dS/m, and 0.17M = 1.6 dS/m. Additionally, the EC (at 25°C) was measured in 1:5 soil:water extracts of all samples (***Tab. 3-2***); the KCl reference solution has an EC 1,430 µS/cm.

3.4 Results

It can be assumed, that based on the tested soil texture, a turbulent shear behaviour occurs. By executing oscillatory tests, information about shear behaviour can be derived from collected data regarding internal strength ("stored elasticity"). Curve characteristics as i.e. the level and progression of graphs may lead to conclusions about turbulent or sliding shear behaviour due to textural effects.
With the intention to demonstrate structural changes in K^+ treated and naturally $CaCO_3$ enriched soils, the following results are plotted as flow curves of the storage modulus G', showing changes in elasticity in three stages. Furthermore, in one representative example, as graphs of both, storage G' and loss modulus G" differentiate textural effects, Generally, phase 1 is characterised by the LVE range, the linear viscoelastic range, in which the "stored" elasticity (G') is defined as representatively shown in ***Fig. 3-4*** through ***3-7***. The level and progression of the curve are decisive.

3.4.1 Effects of water content, K^+ and NaCl

Figures 3-4 and ***3-5*** show results for storage modulus' G' of amplitude sweep tests, which were conducted on/with K^+ treated samples from Halle and Kassel, saturated with distilled water (filled symbols) and drained at -60hPa (blank symbols). Although the curve progression has a parallel character, the higher level of drained samples is obvious. Higher values of G' are an indicator for a higher structural stability (rigidity). Differences in stored elasticity are affected by the water *and* the K^+ content (e.g. ***Fig. 3-5***, KA15 drained). Samples from Halle, loamy sand, show a higher rigidity in a saturated state than the loamy silt from Kassel. A comparable level of G' is reached in both cases of drained substrates: $G' \approx 10^7$ Pa. In the stage of transgression, at a deformation input of approximately 0.1…10%, a steeper slope becomes distinctive regarding the loamy sand. A structural break down is initiated in the final phase, which occurs relatively late in both cases, lasting three to four measuring points only (at f=0.5Hz, ca. 20 seconds).

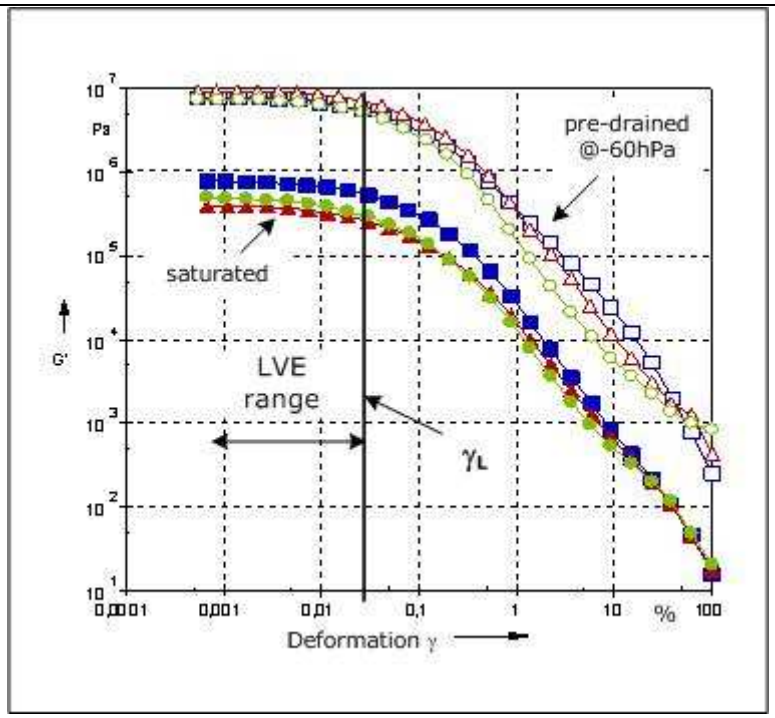

Fig. 3-4 *Storage modulus G' of Halle samples H1 (filled rectangle) saturated with distilled water, filled triangle: H7, filled circle: H15; blank symbols represent values of the storage modulus, congruently to G' of the filled symbols, deriving from measurements conducted on soil samples which are drained at –60hPa. Additionally illustrated: linear viscoelastic range (LVE range), that is defined by a deformation limit γ_L. (H1, 7, 15 = Halle, 1, 7, and 15 cm depth)*

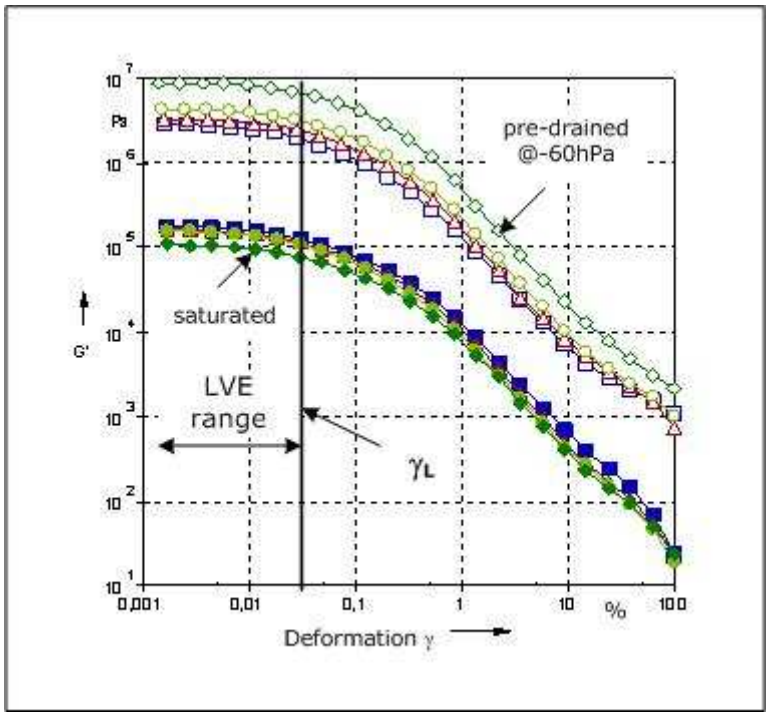

Fig. 3-5 *Storage modulus G' of Kassel samples KA2 (filled rectangle) saturated with distilled water, filled triangle: KA5, filled circle: KA8, filled rhombus: KA15; blank symbols represent values of the storage modulus, congruently to G' of the filled symbols, deriving from measurements conducted on soil samples which are drained at -60hPa. The linear viscoelastic range (LVE range) as well as the deformation limit γ_L are given. (KA2, 5, 8, 15 = Kassel, 2, 5, 8, and 15 cm depth)*

In comparison to these results deriving from effects of water and K^+ content, the following shall show structural effects due to NaCl salt solutions of different concentrations in a $CaCO_3$ rich system, Avdat loess, respectively. Basically, a characteristic progression is given: an initial or plateau phase, limited by γ_L, a transgression phase and a final stage of structural break down. However, only small differences can be detected. Whilst in phase 1 of both, the loamy sand and the loamy silt, curves are declining (***Fig. 3-4*** and ***3-5***), values of G' tend to incline before they decrease (***Fig. 3-6***) at a generally lower level of G'≈10^5. The transgression stage shows a similar curve progression as well as the final phase; minor deviations are distinctive regarding the duration.

The analysis of the significant influences of water content and/or salts on the structure has to be limited to G', in order to also ensure a direct comparison between the different substrates. With respect to textural effects, more information is needed, hence, G" has to be considered furthermore.

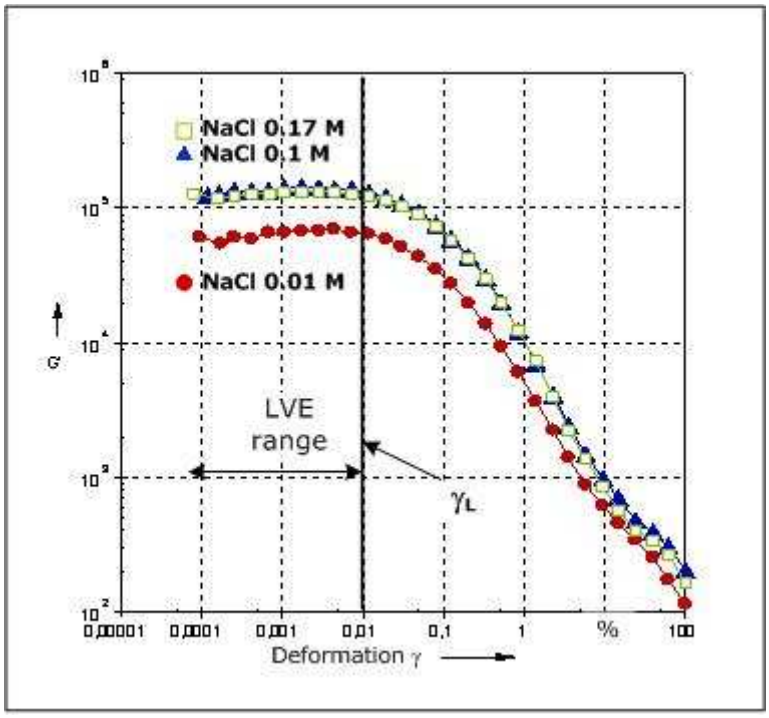

Fig. 3-6 *Results of conducted amplitude sweep tests on Avdat Loess, saturated with three NaCl salt solutions. Filled circle: 0.01M; filled triangle: 0.1M; blank rectangle: 0.17M. In comparison to the samples originating from Halle and Kassel, differences in the level of the graphs become obvious, which derive from the influence of NaCl.*

3.4.2 Textural effects

The presented data furthermore depend on textural effects (***Fig. 3-7***). The loss modulus G" has been included as secondary information to demonstrate both, difference in shear behaviour as well as in the texture for loamy sand versus loamy silt. With respect to G', filled symbols, the already mentioned higher level of the loamy sand samples from Halle are obvious, but a nearly congruent progression is given in both cases. When G" is regarded, an increase of "lost" elasticity due to a higher deformation input is defined for loamy sand. The moment of intersection of G' and G" is reached earlier, in contrast to the loamy silt. In the latter case, phase 3 comprises only, two to three points and the stage of structural break down can hardly be defined. Generally, levels of G' and G" are higher regarding the loamy sand, the curve progression has a more diverging and better defined character in phase three, also with respect to the point of intersection.

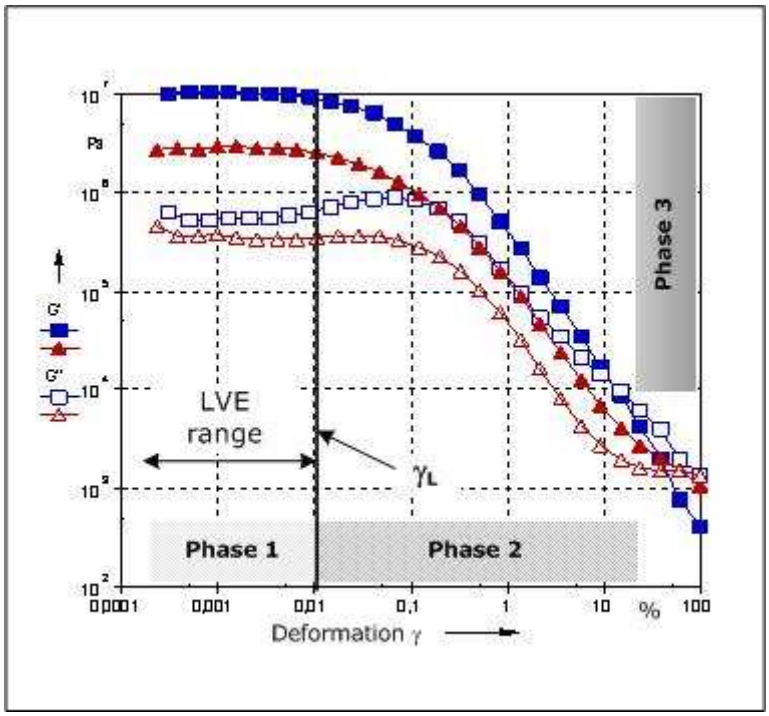

Fig. 3-7 *Storage modulus G' and loss modulus G" are depicted, as results of two executed amplitude sweep tests with the K^+ treated samples from Halle and Kassel (drained at -60hPa). Filled rectangle: G' Halle H1; blank rectangle: G" Halle H1; filled triangle: G' Kassel KA2; blank triangle: G" Kassel KA2. Decisive factors are the duration of the three stages, the level of the graphs, and, as an additional criteria, the intersection of G' and G".*

3.5 Discussion

Rheology has been within the scope of investigations regarding to polymer science (Heller and Keren, 2002) or to clay minerals in form of clay (mineral) dispersions in i.e. Neaman and Singer (2000), Bekkour et al. (2001), Tarchitzky and Chen (2002) as related links to soil science in the broadest sense. While in soil mechanics triaxial and direct shear tests are common, and samples with volumes greater than 200 cm³ and with a diameter to width ratio of >3 are used, the volume is about 4 cm³ only, depending on the texture in Rheometry. Due to this latter precondition, it is possible to achieve information about mechanical behaviour of single particles, either single grains, platelets or aligned particles. Especially in the first phase of amplitude sweep tests, within the LVE range, sliding or turbulent shear behaviour (Smith and Reitsma, 2002) can be defined. Beside effects of the water content, as already described in Ghezzehei and Or (2001), the influence of salt and/or in combination with their effects on water menisci forces were proved by differences between K^+ and NaCl induced effects. Regarding K^+, strengthening effects could be demonstrated with increasing concentrations and depths as well as lower water contents. The latter aspect is obvious, as under saturated conditions menisci forces and salt effects can be neglected, but are needed as initial conditions. Furthermore, drained samples from Kassel show a slow increase of stability with ascending K^+ contents while only in KA15, in which K^+ is 14.1 $cmol_c$/kg at a high Mg^{2+} content was detected the most stable state. In comparison, H15, in which K^+ is 13.1 $cmol_c$/kg at a relatively low Mg^{2+} content, strengthening effects seem to be rather induced by differences in water contents, and the loam-sandy texture, than by K^+ concentration. Sharpley (1990) investigated reactions of fertilizer potassium in soils with special regard to clay mineralogy including the problem of K^+ fixation and deduced recommendations for its application considering taxonomic and mineralogical properties. The mechanical and physical behaviour of natural Ca-clay and K-clay soils had been within the scope of a research study done by Ravina (1973). General remarks on effects of potassium fertilizers considering i.e. K^+ uptake and release against water content were made by Throe and Thompson (1993). Furthermore, Ghezzehei and Or (2000, 2001) described an increase of the yield stress (according to Bingham) at descending gravimetric water contents (33 to 25%) by executing shear stress controlled rotational tests with Millville silt loam. In case of Halle and Kassel it can be assumed, that if the saturated and the drained case are considered separately, and differences in the level of G' and/or G" become clear within each, then this behaviour is primarily caused by (higher) K^+ concentrations and might be influenced by the level of

Mg^{2+}, additionally (Peng et al., 2005). Hence, data about microstructural stability induced by salt effects become more obvious and are in agreement with those data published by e.g. Emerson (1954, 1967), Emerson et al. (1978), Ravina (1973), Rengasamy and Olssen (1991), Sumner and Naidu (1998). However, these interactions are furthermore altered by textural effects. The coarser loamy sand, which originates from Halle, shows a higher initial resistance against deformation than the loamy silt from Kassel. But, in the state of transgression to the final state, values of G' and G" of the loamy silt are decreasing constantly, the point of intersection is reached later than for the loamy sand. Hence, considering this parameter, the structural stability as a whole or the rigidity of the loamy silt is higher than in loamy sand, as the slow decline and the delayed moment of intersection indicate. When the NaCl treated, originally $CaCO_3$ rich loess samples are compared to these findings, a specific soil chemical aspect should be taken into account. Parts of elasticity (= initial level of G') in saturated loamy silt from Kassel and saturated loess from Avdat are almost identical. Nevertheless, a structural stabilisation has been caused, if the salt concentrations exceeded 0.1M. In general, critical concentrations of both, either K^+ or NaCl, may lead to a stable state of structural forming, depending on additional factors e.g. water content, chemical reactions, bonding forces. Complementarily to findings, which were made by e.g. Fredlund and Rahardjo (1993), Myers (1999), Peng et al. (2005), effects of ionic or Van der Waals bonds can be differentiated on a micro-scale due to the interpretation of data deriving from oscillatory tests. Hence, Van der Waals bonds should be reflected in a higher level of G' in comparison to ionic forces, depending on the water content.

3.6 Conclusions

Presented data show, that a parallel plate rheometer is applicable for investigations regarding to microstructural changes in soil samples, which may have a grain size of ≤ 630 µm i.e. loamy sand, loamy silt or loess material; measurements can be conducted either with saturated or drained (-60hPa) samples. Critical values of K^+ and $CaCl_2$, deriving from the presented chemical reaction, are responsible for different structural effects on the particle-particle scale. Results of conducted amplitude sweep tests showed, that strengthening effects, induced by ionic forces have a smaller influence than Van der Waals bonds. In addition, textural effects could be pointed out. Although sand or silt rich materials show a similar mechanical behaviour, structural strength in loamy silt prevails that one in loamy sand.

Based on these findings as well as on those submitted in a previous paper (Markgraf et al., 2006), further investigations have to be carried out on substrates of different physical and chemical properties. Consequently it can be expected that new findings regarding salt effects e.g. valency effects, other textural effects, which also might be influenced by clay mineralogical compounds, and effects of water content may confirm the applicability of a rheometer, by executing oscillatory tests, in soil mechanics, furthermore.

3.7 Acknowledgments

The first author thanks S. Büchner (Paar Physica) for his technical support. Thanks also due to Prof. Dr. O. Christen and Dr. O. Hofmann (MLU Halle) for their interest in rheology and their cooperation. Geochemical analysis was gratefully supported by P. Fiedler, Institute of Geosciences (CAU Kiel).

3.8 References

Bekkour, K., Ern, H., Scrivener, O. (2001): Rheological Characterization of Bentonite Suspensions and Oil-In-Water Emulsions Loaded with Bentonite. Appl. Rheol. 11:178-187. ISSN 1430-6395

Collyer, A.A., Clegg, D.W. (eds.) (1998): Rheological Measurement. Chapman & Hall, London. ISBN 0-412-72030-2

Emerson, W.W. (1954): The determination of the stability of soil crumbs. J. Soil. Sci. 5:235-250. ISSN 0022-4588

Emerson, W.W. (1967): A classification of soil aggregates based on their coherence in water. Austr. J. Soil Res. 5:47-57. ISSN 0004-9573

Emerson, W.W., Bond, R.D., Dexter, A.R. (eds.) (1978): Modification of Soil Structure. John Wiley & Sons, Chichester, New York, Brisbane, Toronto. ISBN 0-471-99530-4

Fredlund, D.G., Rahardjo, H. (1993): Soil Mechanics for Unsaturated Soils. John Wiley & Sons Inc., New York. ISBN 0-471-85008-X

Garz, J., Scharf, H., Stumpe, H., Scherer, H.W., Schliephake, W. (1993): Effect of potassium fertilization on some chemical properties in a long-term trial on sandy loess. Potash Review 3:1-12. ISSN 0032-5546

Ghezzehei, T., Or, D. (2000): Dynamics of soil aggregate coalescence governed by capillary and rheological processes. Water Resour. Res. 36:367-379. ISSN 0148-0227

Ghezzehei, T., Or, D. (2001): Rheological Properties of Wet Soils and Clays under Steady and Oscillatory Stresses. Soil Sci. Amer. J. 65:624-637. ISSN 1435-0661

Heller, H., Keren, R. (2002): Anionic Polyacrylamide Polymers Effect on Rheological Behavior of Sodium-Montmorillonite Suspensions. Soil Sci. Amer. J. 66:19-25. ISSN 1435-0661

Horn, R. (1976): Festigkeitsänderungen infolge von Aggregierungsprozessen eines mesozoischen Tones. Ph.D. Thesis, Technical University, Hannover.

Horn, R., Baumgartl, T., Gräsle, W., Richards, B.G. (1995): Stress induced changes of hydraulic properties in soils., pp. 123-128. In Alonso, E.E., Delage, P. (eds.): Unsaturated Soils, Vol. 1. Balkema Verlag, Rotterdam, Berlin. ISBN 9-0541-0583-6

Keedwell, M.J. (1984): Rheology and Soil Mechanics. MacMillan, London, New York. ISBN 0-8533-4285-7

Macosko, C.W. (1994): Rheology - Principles, Measurements, and applications. VCH Publishers, New York. ISBN 1-56081-579-5

Markgraf, W., Horn, R. (2005): Rheology in soil mechanics - structural changes in soils depending on salt and water content, pp. 149-154, In S. L. Mason, ed. Papers presented at the Nordic Rheology Conference, Tampere, Finland, June 1-3, 2005, Vol. 13, 1st ed. IKON, Vallensbaek. ISBN 87-988486-5-8

Markgraf, W., Horn, R., Peth, S. (2006): An Approach to Rheometry in Soil Mechanics. Soil Till. Res.: *doi 10.1016/j.still.2006.01.007* (in print) ISSN 0167-1987

Mezger, T. (2002): The Rheology-Handbook - For users of rotational and oscillatory rheometers. Vincentz Verlag, Hannover. ISBN 3-87870-745-2

Myers, D. (1999): Surfaces, Interfaces, and Colloids: Principles and Applications. 2nd ed. Wiley-VCH, New York. ISBN 0-471-33060-4

Neaman, A., Singer, A. (2000): Rheological Properties of Aqueous Suspensions of Palygorskite. Soil Sci. Amer. J. 64:427-436. ISSN 1435-0661

Osipov, V.I. (1975): Structural Bonds and the Properties of Clay. Bull. Intern. Assoc. Eng. Geol. 12:13-20. ISSN 0074-1612

Peng, X., Horn, R., Deery, D., Kirkham, M.B., Blackwell, J. (2005): Influence of soil structure on the shrinkage behaviour of a soil irrigated with saline-sodic water. Austr. J. Soil Res. 43 (4):555-563. ISSN 0004-9573

Ravina, I. (1973): the Mechanical and Physical Behavior of Ca-Clay Soil and K-Clay Soil. pp. 131-140. In Hadas, A., Swartzendruber, D., Rijtema, P.E., Fuchs, M., and B. Yaron, (eds.): Physical Aspects of Soil Water and Salts in Ecosystems, Vol. 4. Springer Verlag, Berlin.

Rengasamy, P., Olssen, K.A. (1991): Sodicity and soil structure. Austr. J. Soil Res. 29:935-952. ISSN 0004-9573

Schramm, R. (2002): Einführung in Rheologie und Rheometrie. 2nd ed. Haake GmbH, Karlsruhe. (no ISBN)

Schulz, O. (1998): Strukturell-rheologische Eigenschaften kolloidaler Tonmineral-dispersionen. Berichte aus der Chemie. Ph.D. Thesis, Christian-Albrechts-University of Kiel, Shaker Verlag, Aachen. ISBN 3-8265-4439-0

Sharpley, A.N. (1990): Reaction of Fertilizer Potassium in Soils of Differing Mineralogy. J. Soil Sci. 149 (1): 44-51. ISSN 0022-4588

Smith, D.W., Reitsma, M.G. (2002): Towards an explanation for the residual friction angle in montmorillonite clay soil., p. 27-44, In Vulliet, L., Laloui, L., Schrefler, B.

(eds.): Environmental Geomechanics - Monte Veritá 2002. EPFL Press, Monte Veritá. ISBN 2-8807-4512-2

Tarchitzky, J., Chen, Y. (2002): Rheology of Sodium-montmorillonite suspensions: Effect of humic substances and pH. Soil Sci. Amer. J. 66:406-412. ISSN 1435-0661

Throe, F.R., Thompson, L.M. (1993): Soil and Soil Fertility. 5th edition. Oxford University Press. New York, Oxford. ISBN 0-19-508328-8

U.S.S.L. (1954): Diagnosis and Improvement of Saline and Alkaline Soils. USDA Handbook No. 60. GPO, Washington D.C. (no ISBN)

Yong, R.N., Warkentin, B.P. (1966): Cohesive soil strength. p. 281–349. In G. Norbby (ed.): Introduction to soil behavior. Macmillan, New York. (no ISBN)

4. RHEOMETRY IN SOIL MECHANICS: MICROSTRUCTURAL CHANGES IN A CALCARIC GLEYSOL AND A DYSTRIC PLANOSOL

Wibke Markgraf, Rainer Horn

Advances in GeoEcology 38, pp.47-58 (2006)

Abstract

The application of rheological methods in soil mechanics provides an insight into microstructural changes on a particle to particle scale. Continuing previous investigations, amplitude sweep tests have been conducted with clay-rich and silty homogenised samples, which derive from a Calcaric Gleysol and Dystric Planosol. Rheological principles are based on fundamental mechanical laws of Hooke (elasticity) and Newton (lack of slipperiness), as well as Kelvin-Vogt (viscoelasticity). From the stress-strain relationship in oscillation, with preset deformation γ, specific parameters such as the storage modulus G' and loss modulus G", the linear viscoelastic (LVE) deformation range including a deformation limiting value γ_L were determined and calculated, respectively, defining transition stages from a predominantly elastic to a viscous state. Hence, structural effects of NaCl and $CaCl_2$ on the net work stability of clay platelets and single particles in a $CaCO_3$ and a Al^{3+} dominated system can be parameterised, depending on given physico-chemical characteristics. In order to quantify the strengthening effects, the link between Terzaghi's equation for effective stress and the salt concentration (osmotic pressure) has to be established, considering valency effects and hydration mechanisms.

Keywords: Rheology; amplitude sweep tests; soil microstructure; salt effects

4.1 Research objectives

In general, rheological techniques are adaptable not only in polymer science, but also in the quality control in food industries or in clay mineralogy (Jasmund and Lagaly, 1993). Markgraf et al. (2006) analysed the effect of texture, including clay mineralogy, and different NaCl salt concentrations on inter-particle forces as micromechanical aspects in soil mechanics for Na-bentonite suspensions (Ibeco Seal-80), clay rich soils from Brazil and $CaCO_3$ rich Avdat loess at a saturated stage and concluded that there are differences either in shear behaviour as well as in microstructural stability. In order to demonstrate fertiliser effects in dependency of the water content (saturated and drained @-60hPa), K^+-treated samples from Halle/ Saale, a loamy sand, and Kassel (Niestetal), a loamy silt, were tested (Markgraf and Horn, 2006) and compared with Avdat loess. Both textural effects and chemical mechanisms could be illustrated and quantified. Differences between ionic forces and those who are related to van der Waals mechanisms became obvious.

Young and Warkentin (1966), Mitchell and Soga (2005) have described the strengthening effect based on the hydration energy and ion radius, but the actual inter-particle forces as well as the main friction related processes were not quantified. As described in the DLVO theory according to Derjaguin and Landau (1941), Verwey and Overbeek (1948), and Osipov (1975) the interaction between the liquid and solid phase, especially when regarded to colloidal solutions, represents an important factor within these considerations. According to Mitchell and Soga (2005) ionic forces (Na^+) and Van der Waals bonds (Ca^{2+}, Mg^{2+}) are the major binding mechanisms (Peng et al., 2005). Further considerations have to be made regarding a link between Terzaghi's equation for effective stress (Fredlund and Rahardjo, 1993) and the salt concentration, or rather the osmotic potential Ψ_o.

In this context, the effective stress σ' (according to Terzaghi 1925, Fredlund and Rahardjo 1993, Horn and Baumgartl 1999, Bishop and Bjerrum (1960, 1961) in Mitchell and Soga 2005), depends at a given total stress not only on water pressure but should also be affected by potentials in soils with special regard to the osmotic potential. The latter depends on the salt content in the liquid phase and should affect internal strength.

As already mentioned in Markgraf and Horn (2006), Smith and Reitsma (2002), described the textural effects on strength and their changes with stress and strain, considering mineralogy, respectively. It can be postulated that the friction of internal strength remains high in kaolinitic clay, sandy, silty and Fe-rich soils (20 to 25 degrees) even at high deformation: the residual friction angle equals

the critical state friction angle. Turbulent shear behaviour is given, water menisci between single particles have a convex shape. In opposite to this case of compression or steady stress condition, the residual friction angle decreases in e.g. montmorillonitic clay soils with increasing deformation and results in a sliding shear behaviour with small values for the friction angle. Such behaviour can be attributed especially to platy clay platelets or, due to trafficking, aligned particles. It should be considered, that homogeneous terms are assumed. If however, steady stress conditions are applied for a naturally given structure it shows a higher resistance to the applied external, vertical stress even if in case of exceeding the internal structural strength by the external forces compaction, bulk density increases, and the (micro)pore system collapse can be determined. Such changes will be more pronounced if sliding shear behaviour occurs and results in a lower residual shear strength ϕ_R as was already described by Horn (1976). This state has a more finite, irreversible character in contrast to turbulent shear behaviour. In rheological terms the substrate dependent rigidity can be expressed by several characteristics, i.e. the stored elasticity, which is represented by the storage modulus, or an increase of viscosity, defined by the loss modulus.

With respect to the mechanical strength parameters, the applied mechanical tests or the effect of applied hydraulic stresses on internal strength have to be differentiated as also Ghezzehei and Or (2001, p. 624) stated, that "[…] there is a fundamental difference between soil deformation by farm implements (oscillatory stress) and capillary induced strains (steady stress) rooted in the inherent soil properties, manifested in the form of frequency-dependent rheological properties […]".

This work aims to corroborate the theory that rheometry is an appropriate method to quantify microstructural changes in soils on a particle-particle-scale, substantiated by SEM micrographs. Which effects occur due to changes in mineralogical, physical and chemical preconditions? Is it possible to elaborate NaCl and $CaCl_2$ affected microstructural changes? Furthermore, are there any (de)stabilising effects to be expected due to differences of the ion concentration?

4.2 Rheometry in soil mechanics: some remarks

Rheological parameters and their significance in soil mechanics have already been introduced by Markgraf et al. (2006), Markgraf and Horn (2006), based on works of Keedwell (1984), Whorlow (1992), Macosko (1994), Collyer and Clegg

(1998), Schulz (1998), Ghezzehei and Or (2001), Schramm (2002) and Mezger (2002). Viscoelastic natural substances i.e. soils of certain water contents (pF ≥1.8) and texture (clayey, silty), which show a complete or partial recovery from applied stress, consist of both, elastic and viscous compounds, which can be physically described by the Kelvin/Vogt model, a parallel combination of a spring and a dashpot. The latter ones are based on Hooke's law for ideal elastic substances and Newton's law for ideal fluids. The degree of viscoelasticity depends on physical and chemical properties, i.e. texture, porosity, water content, and ionic composition of the liquid phase. In rheology elasticity and viscosity are defined as mathematical expressions by the storage modulus G' [Pa] (dynamic rigidity) and the loss modulus G" [Pa]. For a complete mathematical description of viscoelasticity further parameters a needed. The LVE (linear viscoelastic) range and the deformation limit γ_L [%] can be calculated by using values from G', the real part of stored elasticity, in opposite to G", as the imaginary part of lost elasticity and representing viscosity (Markgraf et al., 2006, Markgraf and Horn, 2006). Natural viscoelastic substances react with a temporal delay. This is represented by the phase shift angle δ, whereas tan δ equals the relation of the loss modulus G" [Pa] to the storage modulus G' [Pa], defining the relation of lost and stored elasticity. If tan δ<1, G' prevails G", a gel character is given. Viscous behaviour is defined in case of tan δ>1 and G" predominates G'.

4.3 Material and Methods

Homogenised (grinded and sieved < 2 mm), soil substrates have been prepared according to Markgraf and Horn (2006) deriving from a (Calcic) Calcaric Gleysol (Ritzerau, E Schleswig-Holstein, Germany), taken from a G(c)o in 40 cm depths (Richter, 2005), and a Dystric Planosol, from a IISd in 60 cm depths, which originates from Wacken (SW Schleswig-Holstein, Germany).

Table 4-1 summarise physical and chemical properties of the tested material. The Calcaric Gleysol (soil 03) is characterised by a silt rich texture (58%) accompanied by a high clay content of 32% (moderate silty clay), as well as a basic pH value of 7.5 in average due to $CaCO_3$ and low content of organic matter. High pH values are typical for Calcaric (calcaric, calcic or gypsic) Gleysols. In opposite to this, a low pH value of about 4.5 (strongly acid) in average, influenced by Al^{3+} (58 $mmol_c/kg$) with exception of the $CaCl_2$ 1.0M treated sample, and a clay rich texture (65%, weekly sandy clay) are given in case of the Dystric Planosol (soil 04).

The electrical conductivity (EC) was measured in 1:5 w/w extract solutions. Exchangeable cations were extracted by 1M ammonium acetate. According to

standardised methods, K^+ and Na^+ were measured by flame emission; concentrations of Mg^{2+} and Ca^{2+} were detected by atomic absorption spectrophotometer.
For scanning electron microscopy (SEM) samples (all treatments) were oven-dried, prepared on a specimen stage and Au-metallised. SEM micrographs (***Fig. 4-4***) show an illitic clay mineralogy, agreeable to a low CEC.

4.3.1 Preparation of samples

The homogenised samples were repacked in 100 cm³ cylinders at a bulk density d_B of 1.5 g/cm³ and saturated with distilled water, NaCl (0.1, 1.0M) and $CaCl_2$ (0.1, 1.0M). Half of the prepared samples - one cylinder each treatment - were drained at -60 hPa (pF 1.8).

Tab. 4-1 *Physical and chemical properties of the investigated material, Soil 03, a Calcaric Gleysol, and Soil 04, a Dystric Planosol.*

Substrate	**Texture**			**pH**	**EC**	**C_{org}**	**CEC**	**K**	**Na**	**Mg**	**Ca**
	S	U	T	$CaCl_2$	[mS/cm]	[%]	[mmolc/kg]				
Soil 03											
DW				7.6	0.18		195.3	1.4	0.9	12.0	181.0
NaCl 0.1 M				7.5	3.10						
NaCl 1.0 M	7	58	35	7.7	9.01	1.4					
$CaCl_2$ 0.1 M				7.4	2.40						
$CaCl_2$ 1.0 M				7.3	15.89						
Soil 04											
DW				4.5	0.09		157.4	7.1	7.0	28.3	115.0
NaCl 0.1 M				4.6	1.98						
NaCl 1.0 M	20	15	65	4.4	4.40	0.5					
$CaCl_2$ 0.1 M				4.3	3.75						
$CaCl_2$ 1.0 M				6.3	17.65						

Soil 03: Calcaric Gleysol
Soil 04: Dystric Planosol

4.3.2 Amplitude sweep test

In order to quantify and to investigate structural changes of dispersions and/or soil substrates with a parallel plate rheometer (MCR 300, Paar Physica), oscillatory tests, amplitude sweep tests (AST), and a constant frequency are recommended. The term 'sweep' represents a function with a variable parameter. Amplitude sweep tests are conducted to achieve data regarding the flow behaviour of a substrate, especially its elastic part, the LVE deformation range, marked as area between the points of the parallel running curves of G' and G" and their transition. Representative curve progressions of G' and G" in an

amplitude sweep test with controlled shear deformation (CSD) are shown in ***Fig. 4-1***.

In an *initial or plateau phase*, an almost constant level is given. At this stage the elastic component prevails the plastic in case of (viscoelastic) substrates, which show a gel character in the resting state: G'>G". The LVE range is limited by a certain deformation value, the deformation limit γ_L [%]. This value is defined by material properties, especially elastic compounds. The deformation limit may be used synonymously to the term yield stress τ_y, considering that the shear stress τ [Pa] would be controlled (CSS) in this case, not the deformation (CSD). In the second stage, a phase of *transgression*, values of G' decrease, substances are in a state between elastic and viscous flow behaviour. Here, the slope of decline is significant. In phase 3, the *final stage*, a viscous character is given, γ_L has been exceeded: G'<G", substances are creeping, a structural break down has been induced.

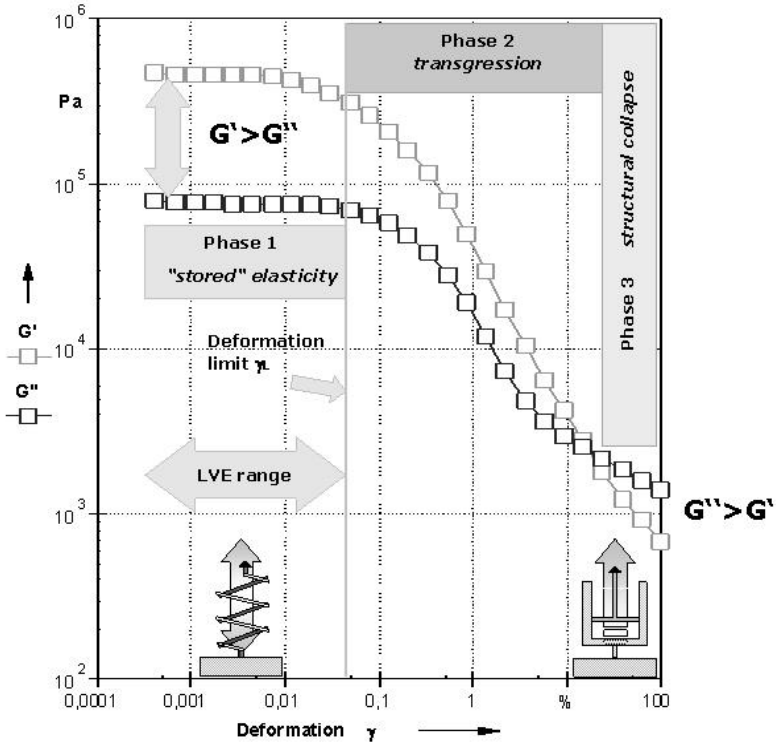

Fig. 4-1 *Representing result deriving from an amplitude sweep test with controlled shear deformation (CSD). The curve progressions of G' (storage modulus), light green blank rectangles, and G" (loss modulus), dark green blank rectangles, can be divided into three stages. In phase 1, the stored elasticity can be defined and quantified. The LVE deformation range, including the deformation limit is attributed to this state. Phase 2 is a stage of transgression, ending in phase 3, the state of an irreversible structural collapse.*

4.3.3 Test configuration

According to given textural conditions a plate distance of 4 mm was preset within the test control. Regarding the measuring system a rotating bob of 25 mm in diameter and a measuring plate, both with profiled surfaces, were chosen. During all tests a constant temperature of 20°C was regulated by a Peltier unit. The generated normal force averaged between 0 to 12 N. A resting period of 30 seconds in the beginning was inserted in the test software (USD 200) to ensure a reorientation of the particles and an undisturbed measurement. The deformation γ was preset as logarithmic range from 0.0001 to 100%, the frequency at a constant value of 0.5 Hz, or π 1/s in SI unit. One run, including 30 measuring points, lasted approximately 15 minutes. By calculating the LVE range after a "yield stress II"-analysis, the deformation limit γ_L as well as the corresponding values of yield stress τ_y were defined.

4.4 Results

Figures 4-2 and ***4-3*** show representatively resulting plots, from amplitude sweep tests conducted on the Calcaric Gleysol (Soil 03), treated with NaCl (***Fig. 4-2***) and $CaCl_2$ (***Fig. 4-3***) salt solutions. The three phases of elasticity loss are well defined: starting with the initial or plateau phase, including the LVE deformation range, which is separated by the deformation limit γ_L from stage two, the phase of transgression, passing into the intersection of G' and G", resulting in stage three, an irreversible structural collapse. These characteristics are less distinctive regarding the Dystric Planosol (not illustrated), i.e. the point of intersection, and phase three.
In ***Tab. 4-2*** the mean values of the deformation limit γ_L and the yield stress τ_y are summed up for both substrates and all treatments. Saturated and drained conditions are illustrated comparatively. Effects of water content as well as of ion concentrations can be observed.

Tab. 4-2 *Summarised collected data of amplitude sweep tests conducted on Soil 03, Calcaric Gleysol, and Soil 04, Dystric Planosol. For each treatment three passes were absolved (n = 3).*

treatment	γ_L [%]	τ_y [Pa]	γ_L [%]	τ_y [Pa]
Calcaric Gleysol (Soil 03)	saturated		-60 hPa	
DW	0.00912	42.5	0.03487	200.3
NaCl 0.1	0.00833	127.7	0.00845	161.0
NaCl 1.0	0.00808	40.8	0.00836	185.0
CaCl2 0.1	0.00813	83.8	0.00844	619.3
CaCl2 1.0	0.00798	38.8	0.00768	91.9

treatment	γ_L [%]	τ_y [Pa]	γ_L [%]	τ_y [Pa]
Dystric Planosol (Soil 04)	saturated		-60 hPa	
DW	0.01457	1568.0	0.01280	2006.7
NaCl 0.1	0.01167	603.7	0.01169	2176.7
NaCl 1.0	0.01183	1106.7	0.01063	859.5
CaCl2 0.1	0.01107	1058.7	0.01200	1455.0
CaCl2 1.0	0.01046	640.7	0.00966	1033.7

At lower water contents, the structural stability increases; the levels of G' and G" is higher in case of drained samples. In the initial phase G' prevails G", an elastic behaviour is given, a small plateau is formed clearly. Running through a stage of transgression and an intersection of G' and G", a structural breakdown occurs in the end. Levels of G' and G" of the samples, which were treated with NaCl 0.1M are higher under saturated conditions than those ones of NaCl 1.0M treated substrates (***Fig. 4-2a***). In addition, the deformation limit γ_L as well as the corresponding yield stress τ_y show conformable values. Lower NaCl concentrations have almost no sensitivity regarding changes in water content in opposite to higher concentrations. The deformation limit γ_L and the yield stress τ_y show a congruent curve progression of investigated NaCl 0.1M and 1.0M treated samples when drained @-60hPa (***Fig. 4-2b***). A similar development occurs in case of saturated, $CaCl_2$ treated samples, but become more distinctive under drained conditions. A $CaCl_2$ concentration of 0.1M leads to a noticeable rise of τ_y. Whereas the levels of $G'_{NaCl\ 0.1\ and\ 1.0M}$ and $G''_{NaCl\ 0.1\ and\ 1.0M}$ cover a relatively small range, the difference of $G'_{CaCl2\ 0.1M}$ and $G''_{CaCl2\ 0.1M}$ is one order of magnitude higher. Furthermore, the phase of transgression (phase 2) is characterised by a steeper slope; hence, a shift of the phase durations derives from this instance. A direct comparison of the Calcaric Gleysol and the Dystric Planosol makes clear that $G'_{soil\ 04}$ and $G''_{soil\ 04} >> G'_{soil\ 03}$ and $G''_{soil\ 03}$.

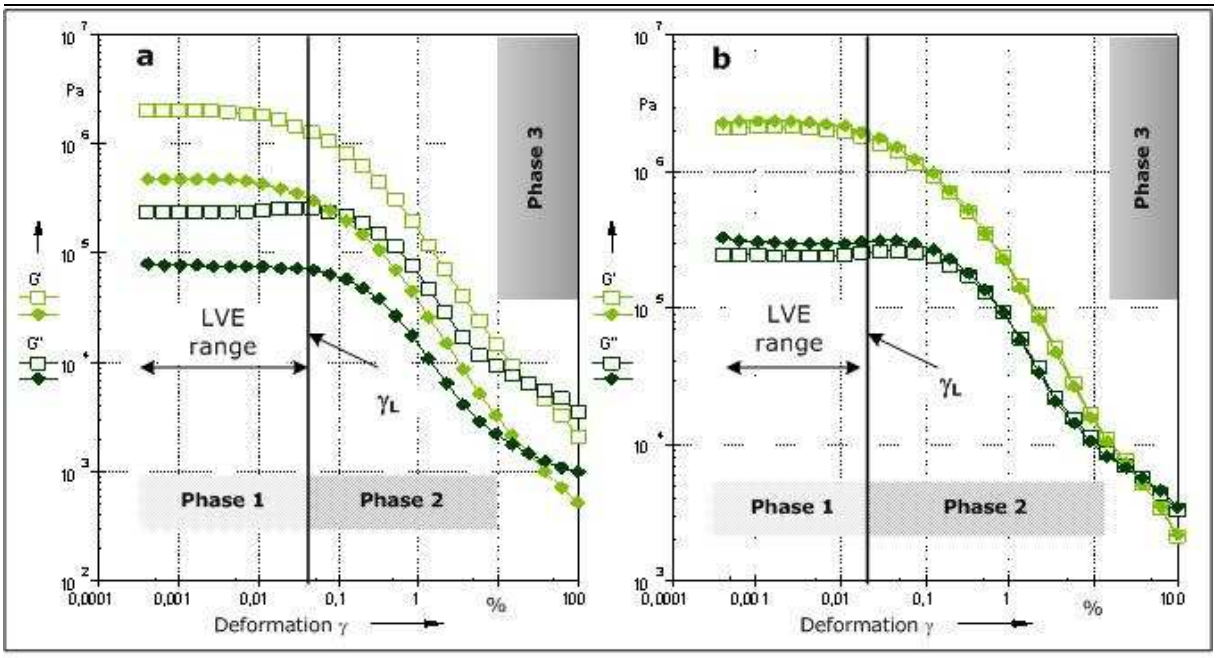

Fig. 4-2 *Plotted graphs of conducted AST (CSD) on NaCl treated Calcaric Gleysol (Soil 03). 0.1M (blank rectangles), storage modulus (light green □), loss modulus (dark green □) and 1.0M (filled rhombus'), storage modulus (light green ♦), loss modulus (dark green ♦), under saturated (a) and drained @ -60hPa conditions (b). (further explanations are given in the text)*

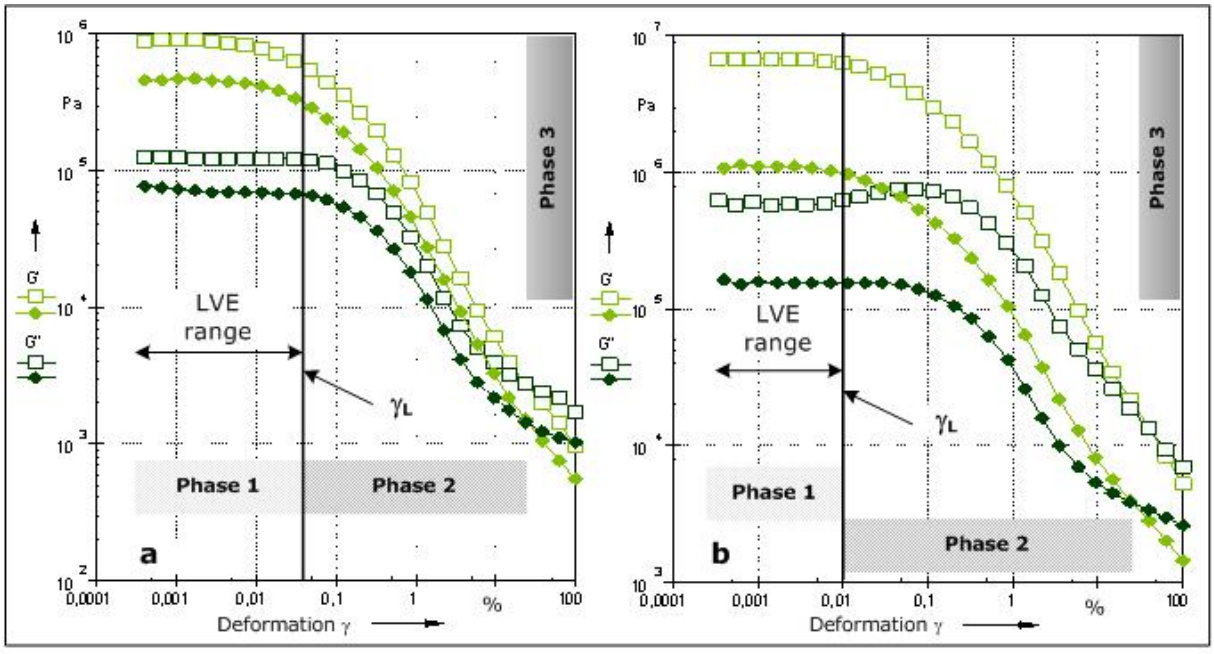

Fig. 4-3 *Plotted graphs of conducted AST (CSD) on $CaCl_2$ treated Calcaric Gleysol (Soil 03). 0.1M (blank rectangles), storage modulus (light green □), loss modulus (dark green □), and 1.0M (filled rhombus'), storage modulus (light green ♦), loss modulus (dark green ♦), under saturated (a) and drained @ -60hPa conditions (b). (further explanations are given in the text)*

SEM micrographs of Soil 04 (***Fig. 4-4***) illustrate exemplarily diverse effects of NaCl and $CaCl_2$ on the surface structure of illite (identification according to Henning and Störr, 1986), in a textural assemblage. In general, NaCl 0.1M retains the original structural state of illite and leads to an expansion of the

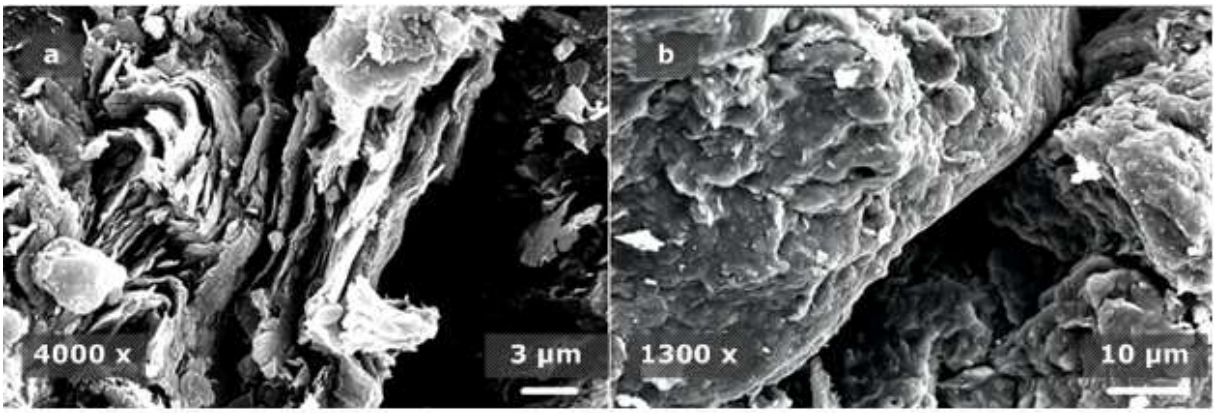

Fig. 4-4 *SEM micrographs of Soil 04 (Dystric Planosol), NaCl 0.1M (a) and $CaCl_2$ 0.1M (b) treated and oven dried, showing a typical illitic structure (ragged flakes), which is even intensified in case of NaCl salt solution treatment.*

border area at higher concentrations. In opposite to this, $CaCl_2$ has a smoothening influence. Single grains, either sand or silt, are encased by a more or less uniform, even clayey cover. A previously ragged flaky structure cannot be defined in this case.

4.5 Discussion

Microstructural effects of NaCl salt solutions of different concentrations have already been investigated in $CaCO_3$ rich, silty and/or clayey substrates by Markgraf and Horn (2006), in bentonite suspensions (Markgraf et al. 2006) as well as in K^+-treated samples. Beside rheological findings, additional information is needed to enable a more distinct interpretation. Hence, this work is not only based on amplitude sweep test results but also on SEM micrographs, which give an insight into the surface structure. Stabilising effects could be verified considering soil texture, and water content. Moreover, there is a corroborative evidence for the influence of NaCl on a $CaCO_3$ dominated system, in comparison to Avdat loess (Markgraf and Horn, 2006). Same tendencies could be observed in this study considering the Calcaric Gleysol. The addition of NaCl 1.0M solution leads to an increase of G' and G", a strengthening effect, which may be explained by the reaction of $2NaCl+CaCO_3 \rightarrow Na_2CO_3+CaCl_2$, is the consequence. In opposite to this, a lower concentration of $CaCl_2$ shows a higher sensitivity to changes in water content than those systems, which were treated with, $CaCl_2$ 1.0M solution. It can be postulated, furthermore, that $CaCO_3$ has a greater influence than other physico-chemical parameters, and reacts more sensitively than a $CaCO_3$ free but Al^{3+} influenced substrate, as results of conducted amplitude sweep tests on the Dystric Panosol proved. Here, besides strengthening effects due to Al^{3+}, effective parameters as e.g. the texture, clay

mineralogy or water content influence the micromechanical behaviour. With respect to collected rheological data, in NaCl 1.0M and $CaCl_2$ 1.0M treated samples (@-60hPa), tendencies of a deleterious effect can be found.
Providing the theory of salt effects (valency, hydration), mechanisms of attractive forces between clay (negatively charged) surfaces and cation selectivity according to the Gapon equation in sodic-saline systems are described in Rengasamy and Olssen (1991), Rengasamy and Sumner (1998), Peng et al. (2005). In opposite to Na, where an ionic linkage of clay surfaces and an extensive hydration are given, Ca^{2+} forms polar covalent bonds (Van der Waals bonds), with a limited state of hydration, determined by the polarisation (Rengasamy and Sumner, 1998). Considering these works and findings regarding rheological properties of unsaturated, non-swelling soils that were elaborated by Ghezzehei and Or (2001) data of microstructural changes under oscillatory shear can be added. Thus, by executing amplitude sweep tests, it is possible to point out physico-chemical properties, which have an influence on micromechanical parameters (G', G", LVE range).

4.6 Conclusions

Soils can be defined as a complex and sensitive viscoelastic material. Presented results demonstrated that rheometry is an appropriate method in micromechanics, especially when focused on salt effects. Different concentrations of NaCl and $CaCl_2$ in a $CaCO_3$ rich, Calcaric Gleysol are predominantly responsible for structural effects on the particle-particle-scale. In case of a Dystric Planosol, structural changes are induced by Al^{3+}, texture and water content, in the first instance. Auxiliary data of SEM micrographs corroborates Na^{+} and Ca^{2+} (de-) stabilising effects visually beside a rheological database. Furthermore, additional investigations, which are based on this work as well as on Markgraf et al. (2006) and Markgraf and Horn (2006) particularly with respect to altering effects, that are induced by texture, clay mineralogy, ion concentrations, need to be done, confirming the applicability of rheometry in soil mechanics.

4.7 Acknowledgments

Dr. Xinhua Peng for an inventive, enjoyable collaboration and his support as well as Mr. Stefan Büchner for technical advice, Mrs. Ute Schuldt and Claudia Ehlert for their engagement in SEM analyses.

4.8 References

Bishop, A.W. (1960): The principle of effective stress. *Publikasjon Norges Geotekniske Institutt*, **23**:1-5. ISSN 0078-1193

Bishop, A.W., Bjerrum, L. (1961): Bedeutung und Anwendbarkeit des Dreiachsial-versuches für die Lösung von Standsicherheitsaufgaben. 61pp. Dt. Ges. für Erd- und Grundbau e.V., Hamburg. *Publikasjon Norges Geotekniske Institutt*, **43**. ISSN 0078-1193

Collyer, A.A., Clegg, D.W. (eds.) (1998): Rheological Measurement. 2nd edition. 779 pp. Chapman & Hall, London. ISBN 0-412-72030-2

Derjaguin, B.V. and Landau L.D., (1941). Theory of the stability of strongly charged lyophobic sols and the adhesion of strongly charged particles in solutions of electrolytes. *Acta Physicochimica URSS.***14**: 633-662. (no ISSN)

Fredlund, D.G., Rahardjo, H. (1993): Soil Mechanics for Unsaturated Soils. 517 pp. John Wiley & Sons Inc., New York. ISBN 0-471-85008-X

Ghezzehei, T., Or, D. (2001): Rheological Properties of Wet Soils and Clays under Steady and Oscillatory Stresses. *Soil Sci. Amer. J.* **65**:624-637. ISSN 1435-0661

Henning, K.-H., Störr, M. (1986): Electron micrographs (TEM, SEM) of clays and clay minerals. *Schriftenreihe für Geologische Wissenschaften – Series in Geological Sciences* **25**. Gesell. Geol. Wiss. Akademie-Verlag, Berlin. ISBN 3-05-500168-0, ISSN 0323-8946

Horn, R. (1976): Festigkeitsänderungen infolge von Aggregierungsprozessen eines mesozoischen Tones.119 pp. PhD Thesis. Tech. Univ., Hannover.

Horn, R., Baumgartl, T. (1999): Dynamic properties of soils. Pages A19-A46 *in* M. E. Sumner, ed. Handbook of Soil Science. CRC Press, Boca Raton, FL. ISBN 0-8493-3136-6

Keedwell, M.J. (1984): Rheology and Soil Mechanics. 323 pp. MacMillan, London, New York. ISBN 0-8533-4285-7

Macosko, C.W. (1994): Rheology - Principles, Measurements, and applications. 550 pp. VCH Publishers, New York. ISBN 1-56081-579-5

Markgraf, W., Horn, R., Peth, S. (2006): An Approach to Rheometry in Soil Mechanics: Structural Changes in Bentonite, Clayey and Silty Soils. *Soi Till. Res.: doi 10.1016/j.still.2006.01.007* (in print) ISSN 0167-1987

Markgraf, W., Horn, R. (2006): Rheological Strength Analysis of K^+-treated and of $CaCO_3$-rich soils. *J. Plant Nutr. Soil Sci.* (in print). ISSN 1436-8730

Mezger, T. (2002): The Rheology-Handbook - For users of rotational and oscillatory rheometers. 252 pp. Vincentz Verlag, Hannover. ISBN 3-87870-745-2

Mitchell, J. K., Soga, K. 2005. Fundamentals of soil behavior, 3rd edition. 577 pp. John Wiley & Sons, Hoboken, NJ. ISBN 0-471-46302-7

Osipov, V.I. (1975): Structural Bonds and the Properties of Clay. *Bull. Intern. Assoc. Eng. Geol.* **12**:13-20. ISSN 0074-1612

Peng, X., Horn, R., Deery, D., Kirkham, M.B., Blackwell, J. (2005): Influence of soil structure on the shrinkage behaviour of a soil irrigated with saline-sodic water. *Austr. J. Soil Res.* **43**:555-563. ISSN 0004-9573

Rengasamy, P., Olssen, K.A. (1991): Sodicity and soil structure. *Austr. J. Soil Res.* **29**:935-952. ISSN 0004-9573

Rengasamy, P., Sumner,M.E. (1998): Processes Involved in Sodic Behavior. *In* Sumner, M.E., Naidu, R. (eds.): Sodic Soils – Distribution, Properties, Management, and Environmental Consequences. Oxford University Press, Oxford. ISBN 0-19-509655-X

Richter, F. (2005): Vergesellschaftung und Eigenschaften von Böden unterschiedlicher geomorpher Einheiten einer Jungmoränenlandschaft des Ostholsteinischen Hügellandes. PhD thesis. *Schriftenreihe des Institutes für Pflanzenernährung und Bodenkunde Universität Kiel*, **66.** 132 pp. (with appendices) ISSN 0933-680X

Schramm, R. (2002): Einführung in Rheologie und Rheometrie. 2nd edition. 360 pp. Haake GmbH, Karlsruhe. (no ISBN)

Schulz, O. (1998): Strukturell-rheologische Eigenschaften kolloidaler Tonmineral-dispersionen. Berichte aus der Chemie. 501 pp. PhD Thesis, Christian-Albrechts-University of Kiel, Shaker Verlag, Aachen. ISBN 3-8265-4439-0

Smith, D.W., Reitsma, M.G. (2002): Towards an explanation for the residual friction angle in montmorillonite clay soil., p. 27-44, *In* Vulliet, L., Laloui, L., Schrefler, B. (eds.): Environmental Geomechanics - Monte Veritá 2002. EPFL Press, Monte Veritá. ISBN 2-8807-4512-2

Terzaghi, K. (1925): Erdbaumechanik auf bodenphysikalischer Grundlage. 399 pp. Deuticke, Leipzig.

Verwey, E. J. W., Overbeek, J.T.G. (1948): Theory of the Stability of Lyophobic Colloids: the Interaction of Soil Particles having an Electric Double Layer. Elsevier, New York. (no ISBN)

Whorlow, R. W. (1992). Rheological Techniques, 2nd edition. 460 pp. Ellis Horwood Ltd., Chichester. ISBN 0-13-775370-5

Yong, R.N., Warkentin, B.P. (1966): Cohesive soil strength. p. 281–349. *In* G. Norbby (ed.): Introduction to soil behavior. Macmillan, New York. (no ISBN)

5. Interaction Between SEM/ EDS-Analyses and Rheological Investigations of South-Brazilian Soils

Wibke Markgraf, Rainer Horn

submitted to Soil Sci. Soc. Am. J. (2006)

Abstract

Scanning electron microscopy (SEM), including energy dispersive scan analyses and amplitude sweep tests (AST) with controlled shear deformation (CSD), were conducted on substrates derived from four kaolinitic, Fe-oxide-rich Brazilian Hapludox soils and one montmorillonitic Calciudert soil, to confirm results obtained from a parallel-plate-rheometer used in soil mechanics. In Brazilian Hapludox soils the occurrence of *pseudosand* (an aggregation of fine particles with a grain size of sand), due to Fe-(hydr)oxide cementation, had a significant effect on aggregation and microstructural stability. We could quantify the existence of hematite, goethite, and, in rare cases, halloysite, as the major stabilizing minerals in such soils.

The influences of soil organic matter (SOM), Fe-oxides, and clay minerals on micromechanical shear behavior under oscillation were tested under saturated and pre-drained (at -60 hPa) conditions. Collected data included G (shear modulus), G' (storage modulus), G" (loss modulus), linear viscoelastic (LVE) deformation range, deformation limit (γ_L), and yield stress (τ_y). From the data, the dissipation of elasticity in a viscoelastic substance (i.e., soil) was derived, and the values ranged from 200-1,000 Pa in all untreated samples, both Hapludox and Calciudert soils, to 50-500 Pa in SOM-leached Hapludox samples. Minimum τ_y values of 10-50 Pa occurred after a Na-dithionite treatment (Fe_d leached) of the four Hapludox samples. These findings show that Fe-(hydr)oxides have a more stabilizing effect than SOM.

Keywords: Rheology; Typic Hapludox; Typic Calciudert; pseudosand; micromechanics

ABBREVIATIONS

AST, amplitude sweep tests;
CN, campo natural (meadow);
CSD, controlled shear deformation;
C_t, total carbon content [g/g];
d_B, bulk density [g/cm³];
EDS, energy dispersive scan;
F, natural forest;
Fe_d, Na-dithionite soluble Fe;
γ, shear strain [%]; in AST deformation [%] or [1];
γ_L, deformation limit [%] or [ ];
ε, strain rate [%];
G, shear modulus [MPa];
G', storage modulus [Pa];
G", loss modulus [Pa];
HAC, high active clay;
LAC, low active clay;
LVE, linear viscoelastic;
MCR, modular compact rheometer;
NT, no tillage (at least five years);
RS, Rio Grande do Sul;
SEM, scanning electron microscopy;
SOM, soil organic matter;
τ_y, yield stress [Pa];
ω, angular frequency [s^{-1}];
XRD, x-ray diffractometry

5.1 Introduction

Micromechanical investigations can be related to geomechanical research. Soil mechanics is an intimate combination of solid and fluid mechanics. In these studies, the stiffness and strength of the skeleton, and the permeability and porosity of the pore space, are all highly significant and variable (Bolton, 2000). Type of soil, including its physicochemical compounds (i.e., soils with different clay mineralogy) and the shearing stress to which a soil is exposed, are of great importance.

Rheological investigations of bentonite suspensions (Na-bentonite Ibeco Seal-80 in Markgraf et al., 2006) and silt- and clay-rich substrates corroborate the hypothesis that the application of a parallel-plate-rheometer (MCR 300, Anton Paar, Stuttgart, Germany) is appropriate for the quantification of microstructural changes on a particle-to-particle scale (Markgraf et al. 2006). General stress-strain relations for soil mechanics are described by Mitchell and Soga (2005), who use terms such as the shear modulus G [MPa], shear strain γ [%], and the strain rate ε [%], which are dependent on time or frequency. Beside well established methods such as direct-shear or triaxial tests, rheometry appears to be another suitable method, whenever mechanical behavior between single particles (tactiles, platelets, and grains) needs to be measured. These measurements can include quantifying effects due to both soil physical and chemical factors or to pre-conditions that affect both of them.

Jasmund and Lagaly (1993), Schulz (1998), Mezger (2002), and Markgraf et al. (2006) introduced rheology to inorganic chemistry (clay suspensions), material science, and soil mechanics. Based on fundamental knowledge of soil mechanics, stress-strain relations with small strains can be transferred to rheological tests by using amplitude sweep tests under oscillatory conditions. Amplitude sweep tests include information about stress-strain relations, namely the relation of shear moduli G' (storage modulus) and G" (loss modulus) to a controlled shear deformation (CSD) γ. In amplitude sweep tests with CSD, the shear strain, as input, is set as a logarithmic ramp, and a constant frequency f or angular frequency ω is provided. Furthermore, calculations of a deformation limit γ_L - related to strain -, or a yield stress τ_y - related to stress -, determined from a collected database, lead to conclusions about the stress-strain relation on a micro-scale. In addition, graphs of G' and G" give specific characteristics of the material under study. The shear behavior is influenced by texture, clay content, clay mineralogy, and Fe-(hydr)oxides. Physicochemical properties and water content affect microstructural changes, (micro)aggregation, and microstructural stability. By interpreting curve characteristics of G' and G", the following can be

quantified: dissipating elasticity (= decrease of G') and frictional heat (= slight increase of G" prior to transition to creeping, which is related to an increase of contact points and structural break down). Rheology often has been applied to study the impact of (cat)ions on structureless clay pastes in concrete, where a defined structure exists between cement and larger particles (Szecsy, 1997; Akroyd and Nguyen, 2003a, 2003b; Phan and Chaouche, 2005). However, rheology has rarely been applied to soils to study the internal microstructure, particularly under arable conditions, where land management will have an impact (Horn and Baumgartl, 1999). Rheology also has not been related to descriptions of soil aggregation. The mechanisms that lead to a stabilization of soil by SOM and Fe-(hydr)oxides and the role of clay might be quantified by this method.

Markgraf et al. (2006) and Markgraf and Horn (2006a, 2006b) investigated the influence of texture, natural physicochemical properties, water content, and valency (hydration mechanisms) on the micromechanical shear behavior of soil. They based their studies on the work of Keedwell (1984), Vyalov (1986), and Ghezzehei and Or (2001). Markgraf and co-workers found that coarse, sandy substrates show a turbulent shear behavior compared to clay-rich materials, which show a sliding shear behavior. They defined clay mineralogical compounds like kaolinite as low-active (LAC) and smectites as high-active clay (HAC) minerals. They found that lower water contents (pre-drained at -60 hPa) lead to a higher structural stability, because menisci forces occur. With regard to hydration mechanisms, covalent bonds (Ca^{2+}, Mg^{2+}) are stronger than monovalent ionic forces (Na^{+}) (Markgraf and Horn, 2006a and 2006b). Markgraf and Horn (2006b) described results from scanning electron microscopy (SEM) studies and concluded that additional information about surface properties and shape of (micro)pores and cracks needs to be obtained to explain the rheological phenomena.

Application of SEM in clay mineralogy is common. For example, Abichou et al. (2002) investigated microstructural changes and hydraulic conductivity of simulated sand-bentonite mixtures. They applied two methods: photomicrographs using digital image acquisition software and scanning electron micrography. Such visual findings may explain the importance of soil microstructure and resulting differences in curves of G' and G". Differences in the relation of elastic and viscous parts of the curves, and in values of deformation limits γ_L (with a specific yield stress' τ_y in amplitude sweep tests), also can be determined from SEM studies. These visual findings may also lead to conclusions about the micromechanical behavior on a particle-to-particle scale. However, coupled mechanical and SEM measurements in soils are rare, although they can provide insight into geomechanical processes. SOM and Fe-(hydr)oxides

are well known to influence the structural stability and aggregation of soils across a wide range of types. Differences in the mechanical behavior of soil are also observed at larger scales. However, studies to determine soil-strength changes due to Fe-(hydr)oxide and SOM are few. Muggler et al. (1999) quantified differences in the grain-size distribution determined by laser diffraction after three pre-treatments. He followed up on studies of Deshpande et al. (1968), Tisdall and Oades (1982), Oades and Waters (1991), and Duiker et al. (2003). Duiker et al. (2003) shook samples with water, leaching them of organic matter, and then followed that treatment with deferration. Muggler et al. (1999), who studied Brazilian Oxisols from Minas Gerais, showed well defined differences in aggregation, depending on the parent material (either rock-saprolites or sediment) and the formation or remobilization of iron. However, the mechanical strength was not determined, although it was important in understanding the structure-formation processes and the corresponding effects on soil strength. This information is also important to understand the interaction between the physical and chemical processes that strengthen particles. Herein lies the importance of the use of a parallel-plate-rheometer in soil micromechanics. It provides information about aggregate stability (Breuer and Schwertmann, 1999) and pseudosand effects, as defined by Cornell and Schwertmann (2003). Duiker et al. (2003) used the method to demonstrate the effects of iron (hydr)oxide crystallinity on soil aggregation. By executing oscillatory tests (amplitude sweep tests) with controlled shear deformation (CSD), deformation effects due to vibrations, which are produced by farm implements, can be simulated (Horn and Baumgartl, 1999, Garciano et al., 2001).
However, such measurements have not been carried out, including quantification of the strength of the various bonding mechanisms. Thus, this study was done to prove or disprove the following hypotheses:

(1) Soil organic matter (SOM), as well as Fe-(hydr)oxides, increase the mechanical soil strength and result in the occurrence of pseudosand.
(2) Curve characteristics, as well as single parameters like G’ (storage modulus), G” (loss modulus), the calculated linear viscoelastic (LVE) deformation range, and deformation limit (γ_L), enable a quantification of dissipating elasticity (loss of rigidity) in soils on a microscale (particle-particle scale). As a result, amplitude sweep tests will show significant differences of these characteristics in Hapludox and Calciudert soils.

(3) SEM/ EDS analyses of untreated, H_2O_2-, and Na-dithionite treated samples facilitate the explanation of microstructural properties and changes. Results depend on these preceding treatments and affect the rheological properties.

5.2 Material and Methods

Measurements were carried out on two types of soil: four kaolinitic Typic Hapludox soils (USDA, 2003) (Latossolos Vermelho according to da Silva, 2004, and Streck et al. 2002), which contained variable compounds of hematite and/or goethite and different amounts of soil organic matter (SOM) and clay, and a montmorillonitic Typic Calciudert soil (USDA, 2003) (Vertissolo Ebânico according to Streck et al. 2002).

5.2.1 Geography and Geology

The southernmost state of Brazil, Rio Grande do Sul, is climatologically classified as humid subtropical (Cfa-climate according to Köppen, 1931). Temperate, natural grasslands cover the southern part of Rio Grande, and temperate Brazilian pine *(Araucaria angustifolia)* forests predominate in the northern, higher regions (*planalto*). These two major vegetation units have geomorphologically separate structural elements. They are divided by an escarpment into the upper *planalto* or *Serra Geral* and the lowlands, which include the *depressão periférica* and the *escudo*. These both belong to the *pampa* region. The Paraná basin was formed on the Brazilian shield in which marine and continental sediments have been deposited. At the southern border of this formation (Santo Ângelo 28°12'S, 54°13'W, região das Missões, and Cruz Alta 28°34'S, 53°06'W, região do Planalto Medio) (da Azevedo, 2003), sediments are covered by effusive basic rocks (Cretaceous basalt) of the *Serra Geral*. Santana do Livramento (31°06'S, 55°12'W), which is located at the Uruguayan border, has sedimentary rocks and fluvial Mesozoic *Botocatú* sandstones of the Brazilian shield as the parent material. Both *Serra Geral* and *Botocatú* belong to the *São Bento* formation (Pinto, 1966, FAO-Unesco, 1971, Silvério da Silva and Menegotto, 2002, West et al., 2004).

5.2.2 Substrates

Samples were taken from three locations: ≥40 cm depth under no tillage (NT) and campo-natural conditions (CN meadow, F natural forest) in Santo Ângelo

(Typic Hapludox, kaolinitic); in Cruz Alta (sandy and clayey Typic Hapludox, kaolinitic); and in Santana do Livramento under pasture (Typic Calciudert, smectitic). Homogenized air-dried samples were sieved to <2 mm and were repacked in 45 cm³ cylinders (n=3; d_B=1.4 g/cm³).

Tab. 5-1 *Physicochemical properties of investigated substrates from Cruz Alta (sandy and clayey Typic Hapludox), S. Ângelo (Typic Hapludox F and NT) and Santana do Livramento (Typic Calciudert).*

	Sand	Silt	Clay	Na	Mg	Ca	pH	C_t	Fe_2O_3	Fe_o	Fe_d	Fe_o/Fe_d
		[%]			[$mmol_c$/kg]		*$CaCl_2$*	%		‰		[ ]
Typic Calciudert	3	32	65	2.7	157	396	5.5	3.4	n.v.§	n.v.	n.v.	n.v.
Sandy Typic Hapludox	75	7	18	0.4	2	5	4.1	0.6	2.0	0.6	14	0.04
Clayey Typic Hapludox	46	9	45	0.3	17	28	5.5	1.0	2.6	1.1	59	0.02
Clayey Typic Hapludox F†	6	25	69	1.5	17	41	4.4	6.6	3.9	2.5	99	0.03
Clayey Typic Hapludox NT‡	5	19	75	1.1	21	43	4.9	1.1	4.1	2.6	102	0.03

† F natural forest ‡ NT no tillage § n.v. no value

Thereafter they were completely saturated with distilled water; parallel samples (n=3) were prepared and drained at -60 hPa (***Tab. 5-1***). Altogether, 78 samples were prepared: 30 of untreated, natural soil material from Santana do Livramento, Cruz Alta, and Santo Ângelo, 24 of H_2O_2- treated, and 24 of Fe_d-leached samples (Cruz Alta and Santo Ângelo).

5.2.2.1 Analyses

Analyses were conducted according to standard methods as described in Schlichting et al. (1995), and van Reeuwijk (2002). Sieved (<2 mm) and homogenized samples were taken to measure exchangeable cations, which were extracted by 1 M ammonium acetate. Concentrations of Ca^{2+} and Mg^{2+} were measured by an atomic absorption spectrometer, whereas K^+ and Na^+ were measured by flame emission. Iron oxides were extracted by Na-dithionite according to Mehra and Jackson (1960). Soil organic matter was removed with H_2O_2.

Typic Hapludox soils are dominated by a kaolinitic clay fraction, while Typic Calciudert soils have smectitic clay mineralogy and a typical, high content of Mg^{2+} and Ca^{2+} in a ratio of 1:2.5. Sandy and clayey Typic Hapludox soils from Cruz Alta show textural differences, whereas clayey Typic Hapludox soils from Santo Ângelo contain variable amounts of soil organic matter (here C_t) contents. X-ray diffractometry was carried out by Prof. Dr. R. Jahn, MLU Halle, and was

conducted according to standardized methods as described in Whittig and Allardice (1986).

5.2.2.2 Amplitude sweep tests (AST)

Markgraf et al. (2006) give a detailed description of amplitude sweep tests, including a theoretical background to rheology and its application. A parallel-plate-rheometer, MCR 300 (Anton Paar Company, Stuttgart, Germany), was used. During all tests a constant temperature of 20°C was maintained, regulated by a Peltier unit.
Amplitude sweep tests (AST) under oscillatory conditions were conducted, with controlled shear deformation (CSD) γ = 0.0001… 100% , an angular frequency ω = πs^{-1} (f = 0.5 Hz), and 30 measuring points, which led to an average test duration of 16 minutes. A plate distance of 4 mm was pre-set according to a plate radius of the rotating bob of 25 mm and the given texture (>2 µm). The tests were controlled by the software US 200 (Anton Paar Company, Stuttgart, Germany).
A representative result of an amplitude sweep test is shown in ***Fig. 5-1***. The plots of storage and loss modulus (G' and G") are generated automatically during a test. Three phases of elasticity loss can be identified:
Phase 1: initial or plateau phase, G'>G"; an elastic behavior is observed, represented by a spring for ideal elastic substances according to Hooke's law. A linear viscoelastic (LVE) range and the included deformation limit γ_L are parameters needed to quantify 'stored elasticity' of any viscoelastic substrate, e.g., soils.
Phase 2: stage of transgression or the intersection of G' and G".
Phase 3: final stage of structural collapse, G'<G"; a viscous character predominates; substances are creeping or running; this behavior can be represented by a dashpot (a device for damping shock or vibration), an analogue for ideal fluids according to Newton's law.

More parameters need to be identified for curve progressions:

(1) the duration of each phase of elasticity dissipation,
(2) characteristics of the plateau phase; distances between graphs of G' and G"; slope progression in phase 2; intersection of G' and G"; and
(3) whether the state G'<G" is reached or not in phase 3; this is the stage of microstructural collapse, where the final level of G' and G" is considered.

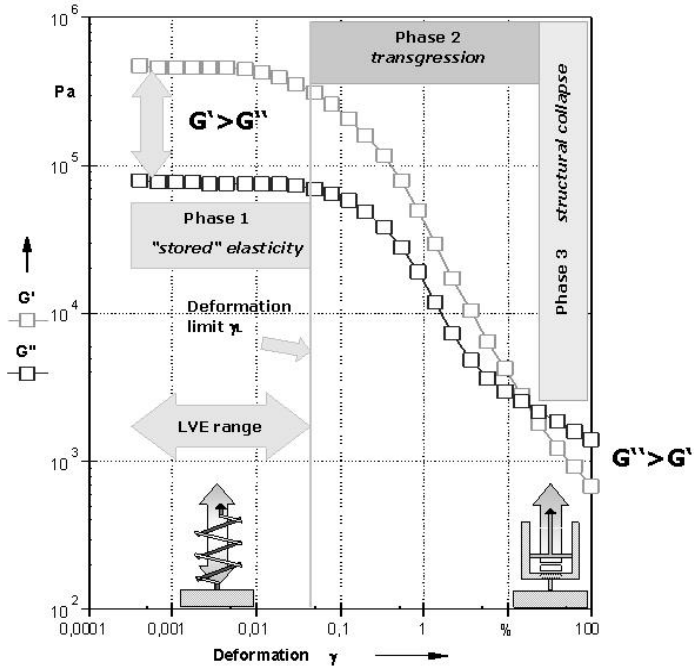

Fig. 5-1 *Generated plots of G' (storage modulus) □ and G"(loss modulus) □. Three stages of elasticity loss can be defined, showing a gradual transition of an elastic (G'>G") to a viscous (G'<G") character.*

For calculations of the linear viscoelastic (LVE) deformation range, deformation-limit γ_L and yield-stress τ_y (that is, the "yield stress II") analyses were executed after each completed test run (Ghezzehei and Or, 2001; Mezger, 2002; Markgraf et al. 2006; Markgraf and Horn 2006a, 2006b). To do this, under oscillatory conditions a tangent is fit to the G' curve, which is based on the minimum γ value and is limited by a decline of G' that has a deviation of >5% in relation to this calculated tangent.

5.2.2.3 Scanning electron microscopy (SEM)

Scanning electron microscopy (SEM) was done with a CamScan CS 44 (E.O. Electron-Optik Service GmbH, Dortmund, Germany), which also can be used to for energy dispersive scan investigations (EDS). Oven-dried (at 40 °C) samples and aluminum holders are connected with a self-adhesive carbon die. For SEM, required conductivity was achieved by applying a gold-palladium coating under high vacuum conditions (sputtering). SEM micrographs were obtained at 15 KeV at a working distance of 15 mm. Monochrome photographs were taken with a small picture reflex camera, which is integrated into the CamScan CS 44 working station as an external unit. A detailed description of SEM and microanalysis (and their applications) is given by Henning and Störr (1986; see their tables) and

Schmidt (1994). Visual images of polarizing microscopy were prepared according to the method of van Reeuwijk (2002).

5.2.2.4 Water content

The water content [w/w] was determined prior rheological tests according to standardized methods (Hartge and Horn, 1999).

5.2.2.5 Statistics

Seventy-eight samples were tested, including two repetitions (n=3). Seven to eight samples with different treatments - either saturated untreated, Fe_d- and SOM-leached, or pre-drained at -60 hPa - were measured per day, which resulted in twenty-one to twenty-four measurements per day, with 14 to 18 minutes for each test. From data of γ_L and τ_y, arithmetic mean values were calculated based on a pre-set range (in US 200) of tolerance with ±5% deviation included in "yield stress II" analyses. Hence, a high level of accuracy can be assumed. This is also shown by the fact that a minimum deformation of 0.0001% equals a deflection of 1 µm under oscillatory conditions.

5.3 Results

5.3.1 Amplitude sweep tests (AST)

Microstructural effects of SOM and Fe_d, which depended on the water content w/w [%], were obvious. Values of γ_L and τ_y showed significant differences (***Tab. 5-2***).
Untreated samples, including all natural compounds, were more stable compared to SOM or Fe_d-leached samples. In the latter case, both the deformation limit γ_L and the yield stress τ_y decreased noticeably, which can be summed up as follows: untreated > SOM leached > Fe_d leached (***Fig. 5-2 b to e***). In addition, in almost every case, γ_L and τ_y increased under pre-drained conditions (-60 hPa; ***Fig. 5-2a***, ***Fig. 5-3a to d***, and ***Tab. 5-2***). A secondary stabilizing effect was demonstrated: levels of G'_{-60hPa} and G''_{-60hPa} plots were higher than under saturated conditions. Increases of G' and G" showed a higher rigidity, assuming that G' is higher than G" in the first phase.

Tab. 5-2 *Summarized results from conducted amplitude sweep tests (with controlled shear deformation). Values of γ_L and τ_y are arithmetic means, n=3. Generally, under pre-drained conditions γ_L and τ_y increase, except untreated clayey Typic Hapludox samples from Santo Ângelo. Furthermore, a decrease of γ_L and τ_y becomes obvious, if untreated, SOM and Fe_d leached samples are compared.*

Untreated	γ_L	τ_y	w/w [%]	γ_L	τ_y	w/w [%]
	[%]	[Pa]	**saturated**	[%]	[Pa]	**-60hPa**
Calciudert (Santana do Livramento)	0.02630	255	44	0.02835	532	42
Sandy Typic Hapludox (Cruz Alta)	0.00682	437	32	0.00661	941	18
Clayey Typic Hapludox (Cruz Alta)	0.01037	499	37	0.01022	897	19
Typic Hapludox F (Santo Ângelo)	0.01677	1105	41	0.00917	*804*	22
Typic Hapludox NT (Santo Ângelo)	0.01277	1067	36	0.01277	*919*	18

SOM leached	γ_L	τ_y	w/w [%]	γ_L	τ_y	w/w [%]
	[%]	[Pa]	**saturated**	[%]	[Pa]	**-60hPa**
Sandy Typic Hapludox (Cruz Alta)	0.00287	52.0	31	0.00560	288	25
Clayey Typic Hapludox (Cruz Alta)	0.00584	101	46	0.00610	293	39
Typic Hapludox F (Santo Ângelo)	0.00679	149	43	0.00771	350	34
Typic Hapludox NT (Santo Ângelo)	0.00768	215	49	0.00856	502	43

Fe_d leached	γ_L	τ_y	w/w [%]	γ_L	τ_y	w/w [%]
	[%]	[Pa]	**saturated**	[%]	[Pa]	**-60hPa**
Sandy Typic Hapludox (Cruz Alta)	0.00295	9.6	25	0.01487	140	16
Clayey Typic Hapludox (Cruz Alta)	0.01413	49.7	37	0.02443	194	19
Typic Hapludox F (Santo Ângelo)	0.01903	40.4	26	0.00585	114	23
Typic Hapludox NT (Santo Ângelo)	0.02570	42.7	44	0.03423	208	17

An ideal curve is shown by the untreated saturated and pre-drained Calciudert samples (**Fig. 3a)**. A sliding shear behavior predominates, which results from a smectitic clay mineralogy. The plateau phase, which is characterized by a parallel run of G' and G", is well defined, followed by a typical progression in phase 2. It ends with the intersection of G' and G" - at a lower deformation input under pre-drained conditions - and finally leads into phase 3, the stage of viscoplastic behavior.

If patterns of the variously treated Hapludox samples are compared with the untreated Calciudert samples, characteristics regarding textural compounds, properties of micro cracks, cavities, and pores, and clay mineralogy (HAC, LAC) are evident. Single grains, kaolinite piles, and small roots are embedded as an assemblage with a Fe-oxide coat containing fissures. The latter are preferentially at connection points under untreated conditions. Organic matter is completely removed in H_2O_2- treated samples. It can be assumed that binding mechanisms, which have been affected by exudates, are reduced or disabled. After the Na-dithionite treatment, bare surfaces of single grains result. Kaolinite piles may function as single grains with regard to shear behavior, if one assumes stable structural conditions of partially sharp-edged grains. In this case, a direct

surface-to-surface or edge-to-edge contact can be assumed during AST, which leads to a higher angle of friction. This is indicated by a lower level of G' and G" and a decelerating set in phase 3. Based on such visual findings, a link to rheological parameters can be done, assuming that single grains show a different mechanical behavior compared to more coherent structures such as micro aggregates. When combined with SEM/ EDS findings, characteristics of G' and G" lead to an understanding of friction processes on a particle-to-particle scale.

Phase 1 is less pronounced with substrates that have much kaolinite or are of coarse texture (***Fig. 5-2b***). Results with these substrates show a more or less rapid loss of elasticity.

Increases of G" in phase 2 of all untreated Typic Hapludox samples (blank squares), either saturated or pre-drained, indicate frictional heat. It results from the reorientation of particles, e.g., kaolinite platelets, packages, and/or single grains. Consequently, deformation γ increases, because frictional heat needs to be generated to cause a structural breakdown in phase 3. In general, viscoelastic and cohesive substrates also show this micromechanical behavior. It typically reacts with a temporal delay (Mezger, 2002).

Intersections of G' and G" of Typic Hapludox samples (***Fig. 5-2 b to e***) occur within a range of 50 to 80% deformation under saturated conditions and 70 to >90% under pre-drained conditions (***Fig. 5-3 a to d***), respectively. In **Fig. 5-3b** and **d** intersections of G' and G" of untreated clay-rich Hapludox samples are absent, and G' is higher than G", which indicates a very rigid character of the substrates, despite a relatively rapid decline of G' and G" in the beginning.

Leaching effects occur in almost every case, depending on differences in texture, organic matter, clay, or iron oxide contents at different water contents. With regard to the sandy Typic Hapludox soil (***Fig. 5-2b***), SOM-leached samples show few deviations in comparison to untreated samples. The effect of frictional heat decreases gradually from untreated > SOM > Fe_d- leached substrates. This effect also can be derived from the curve behavior, which changes from a flat s-character (untreated) to a straightened graph (leaching), followed by a decreasing elastic behavior, a lowering of G' and G" levels, and a reduced distance between graphs of G' and G" in the plateau phase.

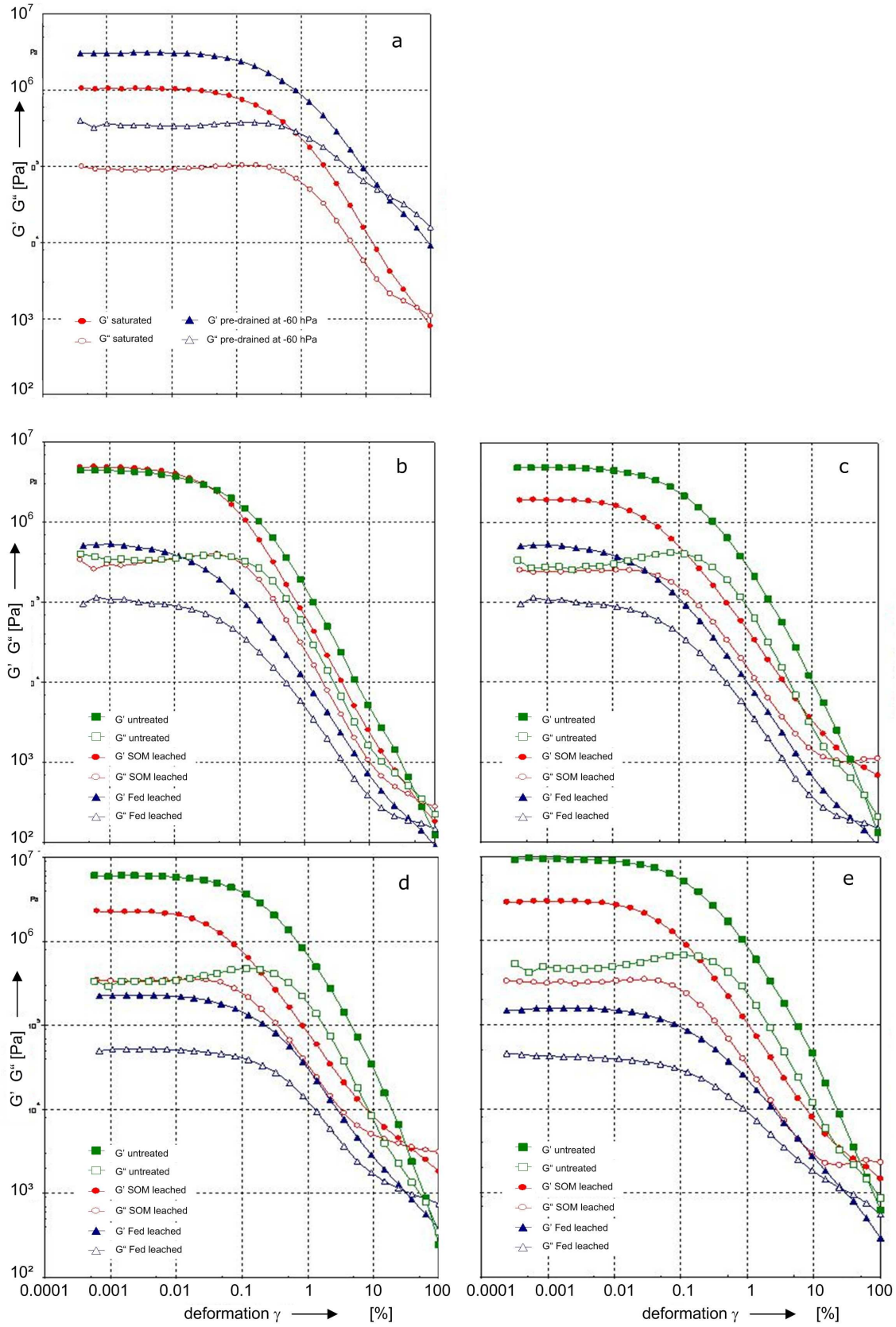

Fig. 5-2 *Results of conducted amplitude sweep tests with (distilled water) saturated samples of a) Calciudert (and under pre-drained conditions), Santana do Livramento, b) Sandy and c) Clayey Hapludox from Cruz Alta, d) Clayey Hapludox under natural forest (F), and e) Clayey Hapludox under no tillage (NT) conditions, both from Santo Ângelo.*

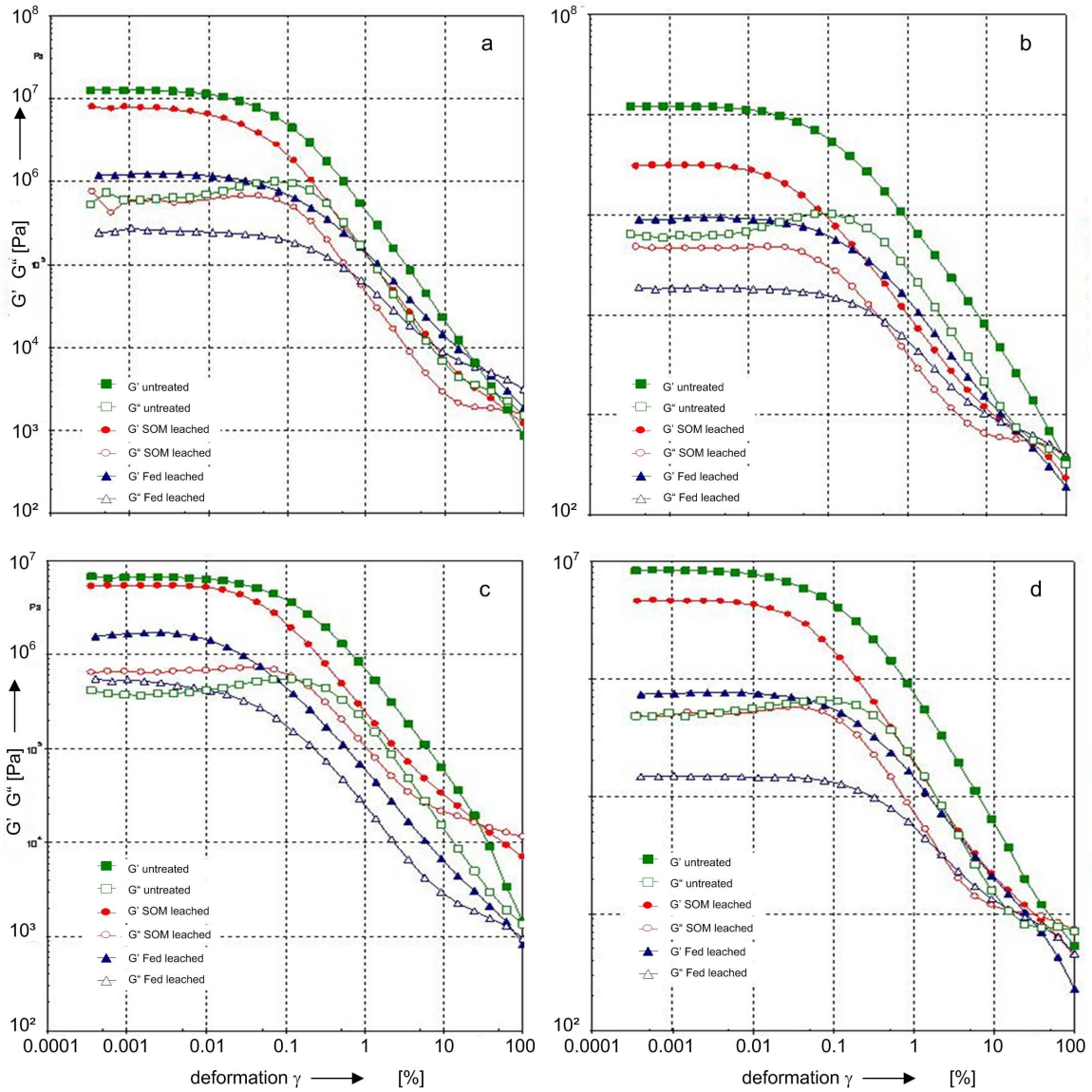

Fig. 5-3 *Results of conducted amplitude sweep tests with pre-drained (at –60hPa) samples of a) Sandy and b) Clayey Typic Hapludox from Cruz Alta, c) Clayey Typic Hapludox, Santo Ângelo, under natural forest (F), and d) Clayey Typic Hapludox, Santo Ângelo, under no tillage (NT) conditions.*

5.3.2 Detection of the mineral composition by SEM and EDS analyses, and XRD

To explain the rheological findings, SEM (scanning electronic microscopy) and EDS (energy dispersive scan) analyses were carried out. Based on visual findings of SEM micrographs, a typical smectitic (HAC) structure is given for the Typic Calciudert soil (Santana do Livramento) (***Fig. 5-4a***). X-ray diffractometry (XRD) graphs confirm these findings. High feldspar compounds, as well as kaolinite, occur with smaller contents of Fe-(hydr)oxides. Untreated kaolinitic samples of the Typic Hapludox soils from Cruz Alta and Santo Ângelo show the phenomenon

of *pseudosand* aggregation (***Fig. 5-4b, e, h*** and ***k***). Surfaces are covered with kaolinite and Fe-(hydr)oxides, whereas samples from Cruz Alta are dominated by hematite. This is in contrast to a greater number of goethite compounds in Hapludox samples from Santo Ângelo. Additionally, single basalt grains (***Fig. 5-4g***, after the Na-dithionite treatment) are stuck together by fine roots (***Fig. 5-4h, k***), which merge into micro cracks (***Fig. 5-4c***) and cavities on the surface and kaolinite piles (***Fig. 5-4d***). In ***Fig. 5-4j*** a single crystalline structure of magnetite is shown. Both samples from Santo Ângelo, which were treated with Na-dithionite, feature this structure. Light microscopy under polarized conditions gives the same results, because magnetite has an opaque character. Furthermore, EDS analyses corroborate these findings. High contents of elementary iron were detected with EDS, which support the existence of magnetite as well as various amounts of aluminum and silicon in the surrounding structures, i.e., kaolinite. In addition, halloysite, which is characterized by high aluminum contents (confirmed by EDS analyses), is shown in detail in ***Fig. 5-4n*** for the clayey Typic Hapludox soil from Santo Ângelo.

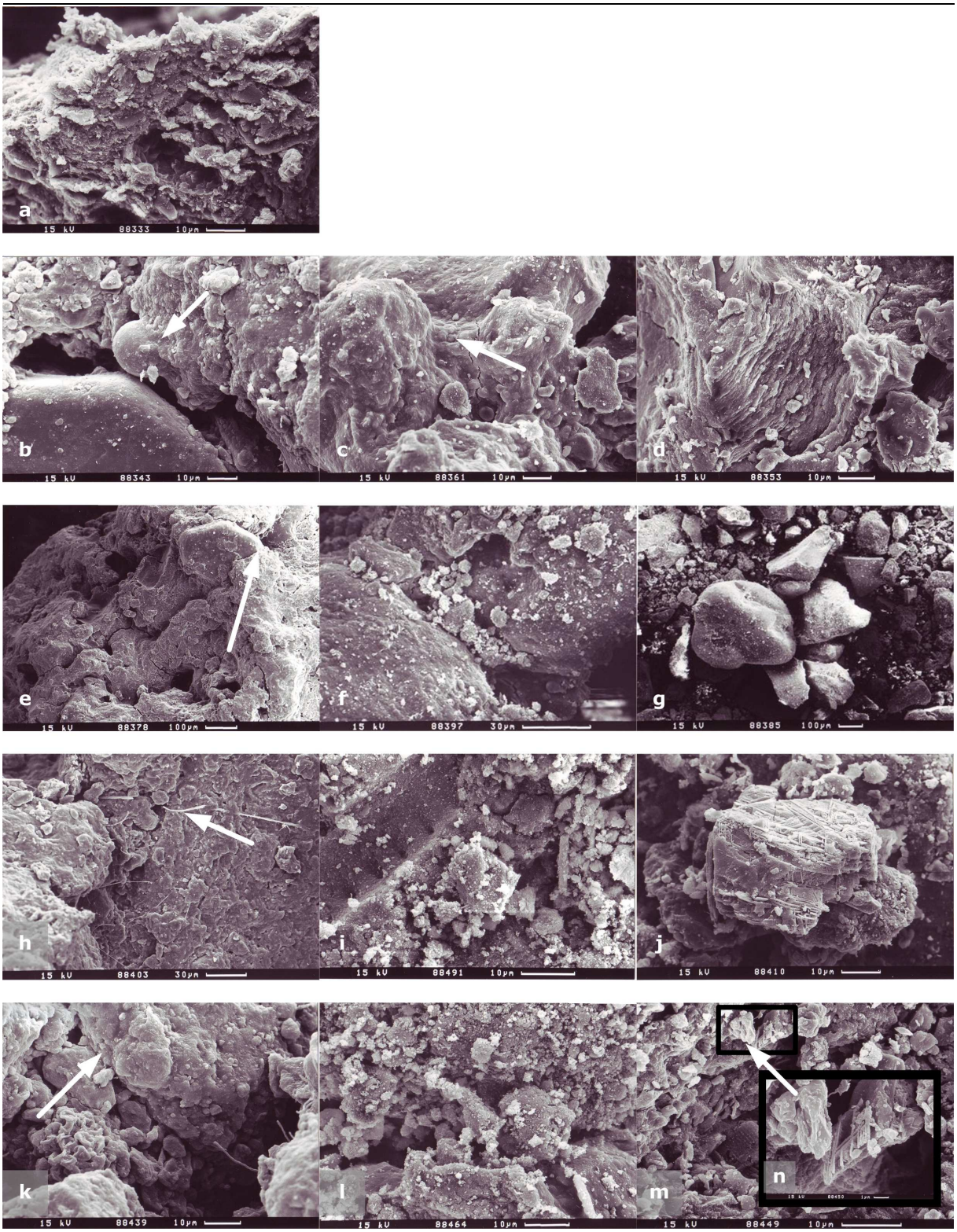

Fig. 5-4 *Scanning electron micrographs of a) Santana do Livramento Typic Calciudert, (Rio Grande do Sul) RS, untreated; b)-d) Cruz Alta, RS, sandy Typic Hapludox, b) untreated, c) SOM leached, d) Fe_d leached; e)-g) Cruz Alta, RS, clayey Typic Hapludox, e) untreated, f) SOM leached, g) Fe_d leached; h)-j) Santo Ângelo clayey Typic Hapludox, F, h) untreated, i) SOM leached, j) Fe_d leached; k)-n) Santo Ângelo, clayey Typic Hapludox, NT, k) untreated, l) SOM leached, m) and n) Fe_d leached, n) detail of m) s. arrow.*

5.4 Discussion

Rheological data confirm that organic matter content and Fe oxides influence aggregate stability and shear behavior under oscillatory loads. SEM micro graphs of differently treated samples (e.g., samples that have the organic matter removed) show transitions from a complex pseudosand aggregate to even surfaces of single, disconnected particles. Binding mechanisms that strengthen aggregates decrease stepwise from untreated, SOM leached to Fe_d-leached samples. These results are in agreement with the findings of Lamotte et al. (1997), Amado et al. (2001), Imhoff et al. (2002), and West et al. (2004), who considered friability of such soils. Additionally, Muggler et al. (1999) postulated diverging effects of iron oxides and organic matter in Oxisols. They demonstrated that aggregation by iron oxides is evident in soils that developed on (Tertiary) sediments compared to those that have rock-saprolite as parent material. Our findings support the idea that the effect of Fe-(hydr)oxides seems to be indirect, through binding with organic matter. However, aggregate formation and strengthening are strongly enhanced by the remobilization of iron and the conversion of ferrihydrite to hematite (Ohtsubo et al., 1991). Remnants of magnetite in Na-dithionite treated Typic Hapludox soils from Santo Ângelo (F and NT) show another aspect of pseudosand texture. An assemblage of single grains (e.g., silt) defines this phenomenon, as well as snatches of iron oxides (magnetite) or packages of kaolinite, which may function as single particles with respect to shear behavior. They result in altered curve progressions and phase characteristics, especially in phases 1 (plateau phase) and 2 (intersection of G' and G"). In general, such assemblages (***Fig. 5-4b, c, e, h, k***) lead to a more elastic behavior than single particles. Differences in shear behavior of such aggregates, in comparison to single grains, can, therefore, be parameterized and defined. Syres et al. (1971) investigated phosphate sorption parameters of representative soils from Rio Grande do Sul and also reported the mineralogical characteristics of soils from Cruz Alta and Santo Ângelo among other sites. They pointed out that SEM/EDS observations showed the appearance of interconnected voids between skeleton basalt and/or sand and silt grains coated with clay (kaolinite packages, smecititic layer structures) or iron (hydr)oxides. In this context, the phenomenon of wall-shaped bridges, shown by Lamotte et al. (1997), should be mentioned. They produced SEM micrographs of hard-setting, Fe-(hydr)oxide-rich soils from North Cameroon, which showed interconnected voids of broken surfaces and small fragments (compare ***Fig. 5-4c, f***). Effects of H_2O_2 and Na-dithionite treated samples, namely the gradual reduction of

functioning connectors or bridges between single grains, can be visualized and compared directly with untreated samples. These results are also consistent with the findings of Tisdall and Oades (1982), who, on one hand, noted defined micro aggregates in general as <250 µm and, on the other hand, the strengthening effect of organic matter for soil aggregation. Oades and Waters (1991) not only introduced a hierarchical system for aggregates or associations of clay aggregates, but also described a typical assemblage of kaolinite crystals. Thus, based on these SEM findings, results of the amplitude sweep tests confirm the assumption of stabilization effects caused by Fe-(hydr)oxides and SOM, when one considers the shear behavior and viscoelastic characteristics. Confirmation also is reflected in derived values of γ_L and τ_y (***Tab. 5-2***).

5.5 Conclusions

1) Amplitude sweep tests, made with a parallel-plate-rheometer, revealed microstructural changes in Oxisols, which are influenced by Fe-(hydr)oxide formations, textural differences (clay mineralogy), or water content. In agreement with hypothsis 1, results show that Fe-(hydr)oxides and SOM have an influence on microstructural stability.

2) Curve characteristics, as well as single parameters like G' (storage modulus), G" (loss modulus), the calculated linear viscoelastic (LVE) deformation range, and deformation limit (γ_L), enabled the quantification of dissipating elasticity (loss of rigidity) in soils on a microscale (particle-particle scale). By conducting amplitude sweep tests significant differences of these characteristics in Hapludox and Calciudert soils were elaborated. Untreated Typic Calciudert samples have relatively low values of γ_L and τ_y, as shown by these tests. This is because differences in clay mineralogical properties have a major influence. Microstructural stability of smectitic substrates is less than that of kaolinitic ones as presented in Hapludox soils, but they maintain a more or less stable level of viscoelasticity. The dissipation of elasticity occurs gradually. Sliding (platy or aligned particles) behavior is contrasted to a turbulent (rotund shape) shear behavior. Micro mechanical charactersitics under oscillatory conditions are parameterized by rheological data and complemented and visualized by SEM/ EDS findings.

3) Visual findings from SEM micrographs indicate transformations in aggregation due to different treatments: *pseudosand* aggregates in untreated samples; looser structures in SOM-leached samples; and single-particle conditions in Na-dithionite-treated Typic Hapludox samples. Micro pores and micro cracks increase in size until unconnected conditions are achieved.

Consequently, problems regarding up-scaling - from tactiles, grains, (micro)aggregates, or, as shown in this study, *pseudosand* structures, up to a meso (aggregate) or even macro scale (undisturbed samples) - can be resolved. A trend of (dis-)aggregation sequence can be distinguished, which is either influenced by given physicochemical properties, especially different clay contents and mineralogical compounds, or by laboratory-induced effects due to H_2O_2- or Na-dithionite treatments. The interaction of both SEM/EDS and rheological findings provides information about micromechanical processes and leads to a better understanding of shear behavior under oscillatory loads.

5.6 Acknowledgments

The first author thanks Mrs. U. Schuldt and Ms. C. Ehlert, SEM/ EDS laboratory, Institute for Geo Sciences, CAU Kiel, Prof. Dr. R. Jahn, MLU Halle/Saale, who supported XRD analyses, as well as DAAD and CAPES for the financial support of this research work, and Prof. M.B. Kirkham for her advice.

5.7 References

Abichou, T., C.H. Benson, and T.B. Edil. 2002. Micro-structure and hydraulic conductivity of simulated sand-bentonite mixtures. Clays and Clay Minerals 50:537-545.

Amado, T.J.C., D.J. Reinert, and J.M. Reichert. 2001. Soil quality of very fragile sandy soils from Southern Brazil. pp. 564-568 *In* Scott, D.E., R.H. Mohtar, and G.C. Steinhardt (eds.) 10th International Soil Conservation Organization Meeting, Purdue University.

Akroyd, T.J., and Q.D. Nguyen. 2003. Continuous rheometry for industrial slurries. Experimental Thermal and Fluid Science 27:507-514.

Beurlen, K. 1954. Paläogeographie und Morphogenese des Paraná-Beckens (Süd-Brasilien). ZDGG (German Geol. Soc. J.) 106:519-537.

Breuer, J., and U. Schwertmann. 1999. Changes to hardsetting properties of soil by addition of metal hydroxides. Eur. J. Soil Sci. 50:657-664.

Bolton, M.D. 2000. The role of micro-mechanics in soil mechanics. 24 pp. Cambridge University Press, Engineering Dept.

Cornell, R.M., and U. Schwertmann. 2003. The iron oxides – structure, properties, occurances and uses. 2nd edition. 664 pp. WILEY-VCH, Weinheim.

da Azevedo, A.C. 2003. Inferências sobre a gênese de agregados em Latossolos Vermelho distroférrico baseadas na distrubuição de agregados. Rev. Ciênc. Agroveter. (J. Agronomy Veter. Sci.) 1:1-7.

Deshpande, T.L., D.J. Greenland, and J.P., Quirk. 1968. Charges in soil properties associated with the removal of iron and aluminium oxides. J. Soil Sci. 19:108-122.

Duiker, S.W., F.E. Rhoton, J. Torrent, N.E. Smeck, and R. Lal. 2003. Iron (hydr)oxide crystallinity effects on soil aggregation. Soil Sci. Soc. Am. J. 67:606-611.

FAO-Unesco. 1971. Soil map of the world, South America, 1:5,000,000. 193 pp. FAO Unesco (printed by Tipolitografia F. Failli, Rome), Paris.

Garciano L., R. Torisu, J. Takeda, and J. Yoshida. 2001. Resonance identification and mode shape analysis of tractor vibrations. J. JSAM 63:45-50.

Ghezzehei, T.A., and D. Or. 2001. Rheological properties of wet soils and clays under steady and oscillatory stresses. Soil Sci. Soc. Am. J. 65:624-637.

Hartge, K.H., and R. Horn. 1999. Einführung in die Bodenphysik, 3., überarbeitete Auflage edition. 304 pp. Enke, Stuttgart.

Henning, K.-H., and M. Störr. 1986. Electron micrographs (TEM, SEM) of clays and clay minerals. Akademie-Verlag Berlin.

Horn, R., and T. Baumgartl. 1999. Dynamic properties of soils. A19-A46 *In* M. E. Sumner, ed. Handbook of Soil Science. CRC Press, Boca Raton, FL.

Imhoff, S., A. Pires da Silva, and A. Dexter. 2002. Factors contributing to the tensile strength and friability of oxisols. Soil Sci. Soc. Am. J. 66:1656-1661.

Jasmund, K., und G. Lagaly (eds.) 1993. Tonminerale und Tone: Struktur, Eigenschaften, Anwendungen und Einsatz in Industrie und Umwelt. 490 pp. Steinkopff-Verlag, Darmstadt.

Keedwell, M.J. 1984. Rheology and soil mechanics. 323 pp. MacMillan, London, New York.

Köppen, W. 1931. Grundriss der Klimakunde, 2nd edition. 388 pp. de Gruyter, Berlin.

Lamotte, M., A. Bruand, F.X. Humbel, A.J. Herbillon, and M. Rieu. 1997. A hard sandy-loam soil from semi-arid Northern Cameroon:I. Fabric of the groundmass. Eur. J. Soil. Sci. 48 :213-225.

Markgraf, W., R. Horn, and S. Peth. 2006. An approach to rheometry in soil mechanics: structural changes in bentonite, clayey and silty soils. Soil Till. Res. *(available online), doi 10.1016/j.still.2006.01.007*

Markgraf, W., and R. Horn. 2006a. Rheological stiffness analysis of K^+-treated and $CaCO_3$-rich soils. J. Plant Nutr. Soil Sci. 169: 411-419.

Markgraf, W., and R. Horn. 2006b. Rheometry in soil mechanics: microstructural changes in a Calcaric Gleysol and a Dystric Planosol. pp. 47-58 *In* Horn, R., H. Fleige, S. Peth, and Xh. Peng (eds.) Sustainability - Its Impact on Soil Management and Environment. Advances in GeoEcology 38. Catena Verlag.

Mehra, O.P., and M.L. Jackson. 1960. Iron oxide removal from soils and clays by a dithionite-citrate system buffered with sodium bicarbonate. pp. 317-327 *In* A. Swineford (ed.) 7th National Conference on Clays and Clay Minerals. Adlard & Son Ltd., Washington, D.C.

Mezger, T. 2002. The Rheology-Handbook - For users of rotational and oscillatory rheometers. 252 pp. Vincentz Verlag, Hannover. ISBN 3-87870-745-2

Mitchell, J.K., and K. Soga. 2005. Fundamentals of soil behavior, 3rd edition. 577 pp. John Wiley & Sons, Hoboken, NJ.

Muggler, C.C., C. van Griethuysen, P., Buurman, and T. Pape. 1999. Aggregation and organic matter, and Fe-(hydr)oxide morphology in oxisols from Minas Gerais, Brazil. Soil Sci. 164:759-770.

Oades, J.M., and A.G. Waters. 1991. Aggregate hierarchy in soils. Austr. J. Soil Res. 29:815-828.

Ohtsubo, Y.A., A. Yoshimura, S.-I. Wada, and R.N. Yong. 1991. Particle interaction and rheology of illite-iron oxide complexes. Clays Clay Min. 39: 347-354.

Phan, T.H., and M. Chaouche. 2005. Rheology and stability of self-compacting concrete cement pastes. Applied rheology. 15:336-343.

Pinto, I.D. 1966. Geology of the State of Rio Grande do Sul - Brasil. Esc. Geol. P. Alegre 11:1-22.

Reeuwijk, L.P. van. 2002. Procedures for soil analysis, 6th edition. International Soil Reference and Information Centre (ISRIC), Wageningen.

Schlichting, E., H.-P. Blume, and K. Stahr. 1995. Bodenkundliches Praktikum - Eine Einführung in pedologisches Arbeiten für Ökologen, insbesondere Land- und Forstwirte, und für Geowissenschaftler, 2nd edition. 295 pp. Blackwell Wissenschafts-Verlag Berlin, Wien.

Schmidt, P.F. 1994. Praxis der Rasterelektronenmikroskopie und Mikrobereichsanalyse. Kontakt & Studium 444. 810 pp. Expert Verlag, Esslingen.

Schulz, O. 1998. Berichte aus der Chemie - Strukturell-rheologische Eigenschaften kolloidaler Tonmineraldispersionen.501 pp. PhD. Christian-Albrechts-Universität zu Kiel.

Silva, V.R. da, J.M. Reichert, and D.J. Reinert. 2004. Variabilidade espacial da resistência do solo à penetração em plantio direto. Ciência Rural 34:399-406.

Silvério da Silva, J.L., and E. Menegotto. 2002. Aspectos mineralógicos de silicificações em rochas sedimentares mesozóicas no Rio Grande do Sul. Revista Brasiliera de Geociências 32:317-326.

Streck, E.V., N. Kämpf, R.S.D. Dalmolin, E. Klamt, P.C. de Nascimento, and P. Schneider. 2002. Solos do Rio Grande do Sul. UFRGS Editora, Porto Alegre.

Syres, J.K., T.D. Evans, J.D.H. Williams, and J.T. Murdock. 1971. Phosphate sorption parameters of representative soils from Rio Grande do Sul, Brazil. Soil Sci. **122**:267-275.

Szecsy, R.S. 1997. Concrete rheology. 215 pp. Ph. D. Thesis. Urbana-Champaign, University of Illinois.

Tisdall, J.M., and J.M. Oades. 1982. Organic matter and water-stable aggregates in soils. Soil Sci. 33:141-163.

USDA. 2003. Keys to Soil Taxonomy. 9th edition. NRCS, Washington D.C.

Vyalov, S.S. 1986. Rheological fundamentals of soil mechanics. XII + 564 pp. Elsevier, Amsterdam.

West, S.L., G.N. White, Y. Deng, K.J. McInnes, A.S.R. Juo, and J.B. Dixon. 2004. Kaolinite, halloysite, and iron oxide influence on physical behavior of formulated soils. Soil Sci. Soc. Am. J. 68:1452-1460.

Whittig, L.D., and W.R. Allardice. 1986. X-Ray diffraction techniques. 331-362. *In* A. Klute, ed. Methods of Soil Analysis: Part 1. Physical and Mineralogical Methods. ASA, SSSAJ, Madison, Wisconsin.

PART III

Discussion and Conclusions
Outlook

6. Discussion and Conclusions

In the following section, the general relevance of rheology in soil micromechanics will be discussed and concluded, besides aspects of texture, effects due to physicochemical properties and cultivation, Fe(hydr)oxides and soil organic matter, the combined applicability of scanning electron microscopy and rheological methods, and soil-tool interface considerations.

6.1 General

In this work it could be proved that rheological methods are adaptable to soil mechanical considerations. Based on well established methods for pastes and liquids of low viscosity as used in food industries, polymer science or inorganic chemistry, a method which can be adapted to granular systems was developed. Moreover, the application of a parallel-plate rheometer leads to new aspects of soil mechanics on the microscale.
Amplitude tests were modified and conducted with a modular compact rheometer MCR 300. Knowledge of soil micromechanics, including single particle considerations was intertwined with rheological principles. In conducted amplitude sweep tests, small stress-strain relationships have been considered. Stiffness degradation as introduced by i.e. Jardine (1992) was transferred to results deriving from collected data and plotted graphs of storage and loss modulus G' and G"; those show significant curve characteristics. Further parameters as the shear modulus G, the complex shear modulus G*, tan δ, the ratio of G"/G', deformation γ, strain ε, the shear stress τ, and the shear rate $\dot{\gamma}$ are of relevance, if correlated with general aspects of shear behaviour and strength analyses not only in particular in soil physics, but also in geotechnical research. With respect to scale considerations, terms such as the cohesion of soil, the angle of inner friction, residual friction, stiffness, particle forces, and intergranular stress are of interest in the practice of geoengineering in general. Besides a general adaptation of a parallel-plate rheometer to soil micromechanics, the applicability was proved by testing a variety of soil materials. One of the main features that was considered is related to textural effects.

6.2 Textural effects

Regarding shear behaviour considerations, textural effects have been worked out. It was observed that coarser materials with average grain sizes between 630µm and 2mm tend to turbulent shear behaviour in opposite to fine or very fine substrates (≤630µm). Data was presented of a high variety of substrates with loamy sand, loamy silt, loess, clayey to very clayey texture (kaolinitic, illitic, and smectitic) and of pure bentonites. It could be demonstrated that microstructural stability of smectitic substrates is lower than of kaolinitic or illitic ones. However, stiffness degradation occurs gradually in smectitic soils, which leads to a higher structural stability in the end, if compared to a more rapid dissipation of stiffness in kaolinitic or illitic soils. Furthermore, kaolinitic soils show, similar to sandy or silty soils turbulent shear behaviour, whereas sliding shear behaviour is evident for smectitic, montmorillonitic soils. Reasons for these different shear behaviours can be found in both, particle properties and particle forces. These findings are in consensus with investigations of Smith and Reitsma (2002), who refer to aspects of different friction angles, as well as of Kézdi (1974), Fredlund and Rahardjo (1993), Mitchell and Soga (2005). Based on works that are more specified to rheological aspects as presented e.g. in Ghezzehei and Or (2000, 2001) a link between soil mechanics in general and rheology could be made.

6.3 Water content

In proving the significance of water content lies a second important aspect of this soil micromechanical approach to rheometry. Although technical properties are limited to specimens that need to have a minimum water and/or certain clay contents, and have to be a more or less homogeneous paste of a maximum volume of 4-5 cm³, - a flow or creeping character has to be obtained - a methodological advance was achieved by using pre-drained samples (-60hPa). In this case, it could be assumed that particle forces – adhesion, changes of the surface tension of capillary water due to cation effects – occur. Increasing values of G', G", the deformation limit γ_L and significant differences in curve characteristics and the linear viscoelastic deformation range confirm this hypothesis. With respect to Bishop's equation for effective stress, Li (2003) concluded that a fabric factor needs to be examined carefully and involved into any effective stress consideration, in particular with respect to microstructural analysis in unsaturated soils. Rheology can be adapted with appropriate

modification of measuring systems, which allow i.e. an online measurement of the matric potential (including the osmotic potential), to effective stress considerations (χ-factor in Bishop's equation for effective stress).

6.4 Physicochemical and cultivation effects

With regard to salt affected microstructural changes that were introduced in Rimmer and Greenland (1976), Shani and Dudley (2001) or Peng et al. (2005), valency effects could be proved. By adding NaCl or $CaCl_2$ solution in different concentrations to pure, natural or already salt affected substrates, it was shown that strengthening effects, induced by ionic forces (monovalent) have a smaller influence than van der Waals bonds (covalent).
Data of conducted amplitude sweep tests with Na-bentonite (Ibeco Seal-80) as introduced in chapter 2, confirm that the microstructural stability was increased due to higher NaCl concentrations, especially when regarded to $CaCO_3$ rich (Avdat Loess) substrates. In Chapter 3 fertilising effects were presented. Critical values of K^+ and $CaCl_2$, are responsible for different structural changes on the particle-particle scale due to valency effects. Similar to this experiment, NaCl and $CaCl_2$ solutions were added to a $CaCO_3$ rich Calcaric Gleysol and an Al^{3+} rich Dystric Planosol. Microstructural changes were caused by different concentrations of Na^+ and Ca^{2+} dissolved in distilled water, high $CaCO_3$ and Al^{3+} contents, clay mineralogical – with geological background - and textural constituents and water content (saturated, pre-drained).
Moreover, effects of cultivation systems and associated fertilising concepts to the microstructure could be demonstrated for samples that originate from Germany (Halle, Kassel) and Brazil (Rio Grande do Sul). In the latter case, the influence of Fe-(hydr)oxides, variations of clay contents and characteristics, as well as differences in organic matter compounds were considered, and led to significant conclusions. Findings corroborate the hypothesis that Fe(hydr)oxides are in first instance responsible for microstructural stability, followed by soil organic matter. In addition, as soil organic matter content is also correlated to cultivation systems – conventional tillage, no tillage, natural conditions under forest or grassland – a first approach to up-scaling could be made.
A link contribution to research works of Emerson (1967, 1983), Tisdall and Oades (1982), Rengasamy and Olssen (1991), Oades and Waters (1991), Ohtsubo et al. (1991), Schwertmann et al. (2005) is given. The different significances of soil compounds for soil aggregation were elaborated, taking scale considerations into account. The association of particles to microaggregates in comparison to aggregation on a mesoscale, induced by the same factors: clay mineral compounds, pH values, soil organic matter, Fe-(hydr)oxides, cations (salts) etc.

With respect to these relevant factors of aggregation and particle association, visualising methods were comprised. In dependency on particle shape, size, roughness, sphericity, and degree of aggregation curve characteristics of G' and G", and decline in stiffness were parametrised and related to information that derived from scanning electron microscopy. Based on fundamental findings of i.e. Santamarina (2001) and Cho et al. (2006), who showed a significant influence of the particle shape to the shear behaviour with respect to soil-tool interface models, the rheological data and SEM micrographs as presented in chapter 5 could be intertwined to these considerations.

6.5 Rheology and scanning electron microscopy

Due to a combination of this modified amplitude sweep test with methods that are commonly used in clay mineralogy such as x-ray diffractometry (XRD), scanning electron microscopy (SEM), and energy dispersive scans (EDS), the applicability in other research fields could be demonstrated. Hence, for instance SEM can not only be used for the identification of specimen compounds (clay minerals), but also for microstructural characteristics: particle associations, particle shape, roughness and/or size, connectors as e.g. micro roots, clay mineral features, physical changes as affected by NaCl or $CaCl_2$ solution treatments, micro fractures and fissures etc. By taking SEM micrographs as an auxiliary information source for the interpretation of microstructural changes, (de-)stabilising effects in a Dystric Planosol and a Calcaric Gleysol could be detected. In addition, an even closer interrelationship of rheology and SEM/EDS analyses was pointed out in chapter 5. Structural compounds, in particular Fe-(hydr)oxides, single grains, clay minerals, particles in assemblages, microaggregates and the aggregation phenomenon of pseudosand could be identified in four South Brazilian kaolinitic Hapludox soils (Oxisols) and a smectitic, montmorillonitic Calciudert (Vertisol). Further microstructural features as micro roots, micro cracks and micro pores are of importance for aspects that are regarded to swelling and shrinkage, the interaction at the plant-root-soil interface, and to structural processes as aggregate formation, including pores. Micro mechanical behavior under oscillatory conditions is on the one hand parameterized by rheological data and on the other hand complemented and visualized by SEM/EDS findings.

6.6 Soil-tool interface and up scaling considerations

Due to improving the applicability of amplitude sweep tests in soil mechanical testing, soil-tool interface aspects that were introduced by Santamarina (2001, 2003), Tong (2004) and Cho et al. (2006), intertwined with meso- or even macroscale considerations, as farm implements have a defined surface with occurring forces between soil (particles) and the tool. Conclusion regarding the influence of particle shape to shear behaviour were made, which derived from observations in amplitude sweep tests. Increases of the loss modulus G" in the end of phase 1 and the beginning of the transgression state indicated clearly frictional heat: The contact points of coarser particles were increased according to this phenomenon. Comparable aspects could be transferred to clay mineralogical aspects; former existing card house structures collapsed under oscillatory shear conditions, but show a significant resistance against strain, which was also indicated by this rise of G" values.

The detected normal force F_N showed significant differences that depend on substrate specifications. Higher values, partly >25N, were measured in very stiff or coarse and pre-drained material, in which turbulent shear behaviour predominated. In the initial state, in which the linear viscoelastic (LVE) deformation range is defined, a parallel run of G' and G" is not well pronounced. Whereas lower F_N values (0-12N) were evident in case of fine textured, clay rich and saturated substrates. A state of sliding shear behaviour is either given from the beginning (smectitic clay mineralogy) or reached at the end of phase 1. Due to oscillatory shear a reorientation and alignment of particles is caused. In a final state of stiffness degradation a complete structural collapse was reached. If compared to turbulent shear behaviour, the state of creeping is reached earlier (=intersection of G' and G") in fine textured and/or saturated material.

A rotational rheometer can be integrated to the soil-tool interface theory (Appendix A). The parallel-plate measuring device exposes two surfaces, which are in contact with a soil testing specimen. In addition, vibration effects can be simulated that may be produced by any instrument; frequencies up to 10Hz are common for farm implements (Garciano et al., 2001). In the present studies the frequency was kept constantly at 0.5 Hz throughout conducted amplitude sweep tests, however, preliminary test results, which included variations of frequencies, show a trend of vibration effects. With increasing frequency not only the tests duration was shortened, but levels of G' and G" decrease, or in other words, stiffness degradation occurs. In this context, it has also to be considered that homogenised samples (<2mm) were prepared and tested. Thus, if transferred to natural soil structures, a higher degree of stiffness can be assumed considering a

higher degree of aggregation, which also lead to different hydraulic properties. At present primarily a methodological approximation of rheological measurements to soil mechanics was done starting with paste-like substrates. The water content had been reduced stepwise, in order to simulate in-field conditions. Due to technical limitations, measurements with undisturbed cylinder samples and water contents lower than 20 w/w [%] were not applied. Problems occurred due to fringe effects in cylinder samples, the limited specimen volume of 4-5cm³ and a minimum water content that is needed for any rheological investigations; under (slightly wet to) dry conditions particle movement is frustrated (Santamarina 2001), and a high degree of friction is generated by the contact of bare particles. This finally leads to incorrect results. Nevertheless, it can be assumed that the functionality of microaggregates and single particles was kept. Intact microaggregates were observed in SEM micrographs. Hence, the focus of upcoming research will be extended from microscale considerations (rheometer-soil interface) to the macroscale (in field).

7. OUTLOOK

Rheometry was introduced and adapted successfully as a testing method of soil micromechanics,
There are several advantages that result from an application of a rotational rheometer in oscillatory mode:

(1) the high degree of accuracy and sensitivity,
(2) detection of particle specific characteristics,
(3) replicability,
(4) small specimen volume,
(5) test duration,
(6) ease of operation,
(7) number of resulting test parameters, and the
(8) comparability of collected data to common parameters of soil mechanics.

The high degree of sensitivity of the measuring system implies a careful preparation. Physical parameters of the testing specimen as the volume, particle size and distribution, water content and degree of homogeneity influence test progression, resulting plots and parameters, as well as the interpretation of the results. Thus, same basic conditions should be given at any time, in particular with respect to the

a) preparation and treatment of samples: degree of saturation, homogeneity, number of replicates (n=3, saturated and pre-drained);
b) the amplitude sweep test setup (***Appendix B***): measuring plate system, plate diameter and distance, preset deformation, constant frequency;
c) test procedure (application of samples), repetitions (3<n<5), and the
d) calculation set-up: LVE range, yield stress II-analysis.

But there are still a few open questions regarding technical limitations, which need to be investigated and answered. From presented results the following aspects for further investigations are deduced:

(1) According to the present state of research, there is no possibility for online-measurements of changes in water content (matric potential) during any rheometrical test that is conducted with a parallel-plate rheometer (modular

compact rheometer MCR 300), neither under rotational nor under oscillatory condition. For this approach a modification of a new measuring plate needs to be developed (***Appendix C, Fig. C-1***) by integrating a pF measuring device into the plate system.

(2) In this work methodological aspects were focused. Practical applications were demonstrated by conducting amplitude sweep tests on substrates with varying characteristics: industrial produced pure bentonites, substrates with changed microstructural properties that are induced by e.g. salt effects due to fertilising or laboratory produced conditions. In context with the development of a modified measuring system that may be adapted to matric potential measurements, further investigations are needed of several more substrates, which show varying compounds in texture, physicochemical properties, treatment, cultivation, including fertilisation and other preconditions

(3) Furthermore, statistical significance has to be confirmed. Thus, an appropriate amount of repetitions have to be produced. Due to the high accuracy of the instrument three repetitions (n=3) are sufficient; nevertheless, additional tests are of great importance to corroborate collected data from these results.

8. SUMMARY - ZUSAMMENFASSUNG

Summary

In this work rheometry was introduced as method, which can be adapted to microstructural studies.
Purpose of this work was to adapt well established rheological methods that are applied in polymer sciences, food industries, inorganic chemistry, coating industries, and familiar research areas as well as in geoengineering, to soil mechanical methods. According to the recent state of research, undisturbed cylinder specimens are commonly taken for conducting oedometer, triaxial or direct shear tests to achieve data regarding deformation or compression behaviour of soils, but neglecting contact point considerations. An important aspect of this approach is related to upscaling processes. Rheometry as very sensitive measuring procedure enables the detection of microstructural processes and changes. This instant is distributed to the specimen volume, which is small, indeed, if compared to common cylinder samples. According standardised field methods the average sample volume of a cylinder is 100cm³, the volume of a rheometer testing sample 4-5cm³ only. Furthermore, methodological differences with respect to water contents had to be elaborated, as rheology is applied for substances of low viscosity, clay suspensions, oils or slurries, as well as of concrete; but in this case with respect to other rheological considerations.
So called amplitude sweep tests in oscillation mode were conducted with a compact modular rheometer MCR 300 with a parallel-plate measuring system. Associated principles, parameters, and methods had been transferred and adapted and introduced to soil mechanical considerations.
To prove the applicability of a rheometer, numerous tests had been conducted with various soils.
In advance, homogenised Na-bentonite pastes were produced to keep comparability to well established methods. Under field conditions water contents that equal or are above the yield point throughout a longer time period hardly occur. Limited by technical frame conditions, disturbed soil material were analysed, which had been sieved to <2mm and prepared in 45cm³ cylinders, saturated and in parallels pre-drained at -60hPa. Amplitude sweep tests were conducted with saturated and pre-drained samples. Regarding salt affected changes of the matric potential, NaCl and $CaCl_2$ solutions were produced; a

major part of the samples had been treated with these solutions. Clay and silt-rich substrates as Ibeco Seal-80, a Na-Bentonite, a carbonate-rich loess from Israel, a Chernozem derived from loamy sand, Halle/ Kassel ("Eternal Rye Grow"), a Luvisol derived from loamy silt, Kassel – both with special respect to Potassium fertilising -, a Gleysol from Ritzerau as well as a Planosol from Wacken, Schleswig-Holstein, South-Brazilian Oxisols (Hapludox) and a Vertisol (Calciudert), Rio Grande do Sul, belong to the investigated materials.

Microstructural changes that are influenced by the texture, physicochemical properties and cultivation systems could be elaborated. Besides a high variability of substrates, investigations were focused on textural, water content and salt effects.

Presuming a comparability of results it was necessary to apply a uniform measuring method. On the basis of empirical collected and calculated data, significant interpretations of the database could be done. This method was accompanied by scanning electron microscopy.

Due to the modification of microstructural analysis by such visual investigations, structural changes and consequences for upscaling considerations become evident as well as the need of research in soil mechanical processes on the particle-particle scale.

Thus, rheology can be seen as technical procedure that is appropriate for this research area of soil mechanics, besides practical application for the investigation of soil-tool interface considerations. An adaptation of elaborated mathematical models of such research areas are obtained by applying rheological measurement techniques, as introduced here. By the modification of amplitude sweep tests in oscillation mode, a plentifold applicability of a rotational rheometer is given. A wide range of soil micromechanics can be comprised; collected rheological data is appropriate to be transferred to the next larger scale.

It was shown that rheometry is an applicable method to detect microstructural changes by using a rotational rheometer.

Zusammenfassung

Im Rahmen der vorgelegten Arbeit wurde Rheometrie als Messmethode vorgestellt, die sich dazu eignet, mikrostrukturelle Studien zu betreiben.
Ziel der Arbeit war es, bereits bekannte rheologische Methoden aus den Bereichen der Polymerwissenschaften, der Nahrungsmittelbranche, der anorganischen Chemie, Lack- und Farbenindustrie, verwandten Forschungsbereichen sowie den Geoingenieurswissenschaften an bodenmechanische Methoden anzupassen. Bislang war es in der Bodenmechanik nur möglich, über Oedometer-, Triaxial- oder direkte Schertests das Deformations- und Drucksetzungsverhalten von Böden anhand von ungestörten Stechzylinderproben zu untersuchen, ohne weitere Berücksichtigung von Kontaktpunktmechanismen. Ein wichtiger Aspekt dieser Arbeit bezieht sich auf skalenübergreifende Prozesse. Die Rheometrie als ein äußerst sensitives Messverfahren, ermöglicht es, mikrostrukturelle Prozesse und Veränderungen zu erfassen. Ein einfacher Vergleich der zu untersuchenden Probenvolumina macht das deutlich. Gemäß standardisierter Feldmethoden umfasst das durchschnittliche Probenvolumen eines Stechzylinders 100cm³, das einer zu untersuchenden Rheometerprobe lediglich 4-5cm³. Des weiteren galt es, methodische Unterschiede hinsichtlich der Wassergehalte zu erarbeiten, da sich die Rheologie als solche mit der Untersuchung niederviskoser Substanzen, wie Tonsuspensionen, Ölen oder Schlämmen befasst, daneben ebenfalls von Mörteln; diesbezüglich jedoch unter einem anderen rheologischen Aspekt.
Es wurden so genannte Amplitudentests im Oszillationsmodus an einem Compact Modular Rheometer MCR 300 mit einem Platte-Platte Messsystem durchgeführt. Dazugehörige Prinzipien, Kenngrößen und Methoden wurden auf Belange der Bodenmechanik übertragen, modifiziert und vorgestellt.
Um die tatsächliche Anwendbarkeit eines solchen Rheometers zu überprüfen, wurden zahlreiche Untersuchungen an Böden mit unterschiedlichsten Variationen getestet. Es wurden zunächst homogenisierte Na-Bentonit Pasten hergestellt, um eine Vergleichbarkeit zu bekannten Methoden zu bewahren. Unter Feldbedingungen sind Wassergehalte, die über einen längeren Zeitraum dem der Fleißgrenze gleichkommen, kaum gegeben. Limitiert durch messtechnische Rahmenbedingungen wurde auf 2mm gesiebtes, gestörtes Probenmaterial in 45cm³ großen Zylindern präpariert, gesättigt und in Parallelen auf -60hPa vorentwässert. Amplitudentests wurden an gesättigten wie vorentwässerten Proben durchgeführt. Unter dem Aspekt des Einflusses von Salzen auf das Matrixpotenzial, wurden zusätzlich NaCl und $CaCl_2$-Lösungen hergestellt, mit

denen ein Großteil der Proben behandelt wurde. Zu den untersuchten ton- und schluffreichen Substraten gehören Ibeco Seal-80, ein reiner Na-Bentonit, carbonathaltiger Löß aus Israel, ein Chernozem aus lehmigem Sand aus Halle/Saale („Ewiger Roggenanbau"), ein Luvisol aus lehmigem Schluff, Kassel (Kalidüngung), ein Gleysol aus Ritzerau sowie ein Planosol aus Wacken, Schleswig-Holstein, Oxisole und ein Vertisol aus Südbrasilien (Rio Grande do Sul). Herausgearbeitet wurden mikrostrukturelle Veränderungen, die auf Einflüsse der Textur, physikochemischer Eigenschaften und von Bearbeitungsmethoden zurückzuführen sind. Neben dieser hohen Variabilität an Substraten, wurden Untersuchungsschwerpunkte hinsichtlich von Textur-, Wassergehalts- und Salzeffekten gesetzt. Um eine Vergleichbarkeit der Ergebnisse zu gewährleisten, war es notwendig, eine einheitliche Messmethode anzuwenden. Auf der Basis der empirisch gewonnenen wie auch kalkulierten Daten, konnten recht eindeutige Interpretationen der Datensätze vorgenommen werden. Begleitet wurde diese Methode von Rasterelektronenmikroskopie. Durch die visuelle Erweiterung mikrostruktureller Analyse werden nicht nur skalenübergreifende strukturelle Veränderungen und Konsequenzen verdeutlicht, sondern auch die Notwendigkeit der Erforschung bodenmechanischer Prozesse auf der Partikel-Partikel-Ebene. Rheologie kann somit als ein technisches Verfahren angesehen werden, das für diesen Bereich der Bodenmechanik geeignet ist; darunter auch unter dem Gesichtspunkt der praktischen Anwendung für die Untersuchung der Kontaktebene Boden und Bodenbearbeitungsinstrument ("soil-tool interface"). Eine Umsetzung bereits existierender Modellierungen derartiger Forschungsbereiche kann mit Hilfe rheologischer Messtechniken, wie sie hier vorgestellt wurden, erzielt werden. Durch die Modifikation von Amplitudentests im Oszillationsmodus, ist die vielfältige Einsetzbarkeit eines Rotationsrheometers gegeben. Weite Bereiche der Bodenmikromechanik können somit einbezogen werden; die gewonnen Daten sind ebenfalls dazu geeignet, auf die jeweils nächst größere Skala transferiert zu werden. Es konnte belegt werden, dass Rheometrie eine anwendbare Methode ist, mikrostrukturelle Veränderungen mit Hilfe eines Rotationsrheometers zu untersuchen.

9. DANKSAGUNG

Ich möchte an erster Stelle meinem Doktorvater Herrn Prof. Dr. R. Horn danken, der mir die Erarbeitung dieses interessanten und innovativen Themas überlassen hat. Während meiner Doktorandenzeit stand er mir mit Rat und Tat zur Seite, fand stets die richtigen Worte der Motivation; in Gesprächen ergaben sich immer wieder Aspekte, die die Vielfältigkeit des Themas herausstellten, und zu dem Ergebnis dieser Arbeit geführt haben.

Des weiteren danke ich Prof. em. Dr. Dr. hc. H.-P. Blume, Dr. Stephan Peth, Dr. Heiner Fleige, Dr. Xinhua Peng sowie Dr. Holger Wetzel für ihre Hilfe und die wissenschaftlich-erforschenden Diskussionen. All meinen Kollegen danke ich für eine sehr angenehme und kurzweilige Zeit hier am Institut, in der sich gerade das „Perkolationslabor" als einer der favorisierten Treffpunkte herausgestellt hat. Des weiteren möchte ich allen wissenschaftlichen Gästen danken, die mir in dieser Zeit begegnet sind, und für einen regen internationalen Wissensaustausch gesorgt haben.

Dem Laborteam der Bodenkunde möchte ich für die äußerst zuverlässige Arbeit danken; durch die Mithilfe konnten nicht nur teilweise entstandene, zeitliche Engpässe bewältigt werden, sondern vor allen Dingen Daten gewonnen werden, die einen wichtigen Beitrag zu neuen Erkenntnissen geliefert haben. Frau Hoyer sei ein besonderer Dank für Ihre Arbeit „hinter den Kulissen" gewidmet.

Dr. H. Frahm gebührt Dank für eine erste Annäherung an die Rheologie. Herrn S. Büchner sei für die technische Unterstützung und Einführung am Rheometer gedankt; ebenso Herrn Th. Mezger für die theoretische Heranführung. Für die messtechnische Unterstützung am Rasterelektronenmikoskop danke ich sehr Frau Dr. B. Bader, Frau U. Schuldt und Claudia Ehlert. Durch ihr Interesse an dieser Arbeit und die Einbringung von Ideen kam es zu einer sehr produktiven Zusammenarbeit, die zugleich eine methodische Erweiterung mit sich brachte.

Prof. Dr. Dalvan Reinert, Prof. Dr. José Miguel Reichert, Dr. Elena Blume, Dr. Milton da Veiga und Carlos Streck möchte ich für die schöne Zeit in Santa Maria, Rio Grande do Sul, Brasilien, danken; sie haben den Aufenthalt zu einem Erlebnis werden lassen.

Für einen philosophischen Einblick in die Bodenkunde und seinen fachlichen Rat in tonmineralogischen Belangen danke ich Prof. Dr. G.J. Churchman.

Ein sehr persönliches Dankeschön möchte ich meiner Familie, darunter ganz besonders meiner Mutter widmen, die mir in schwierigen Zeiten zur Seite stand, - und Gerd, der mir gezeigt hat, dass es manchmal auch gut sein kann, den Boden unter den Füßen zu verlieren, nicht zuletzt, um alles aus einer anderen Perspektive betrachten zu können.

DANKESCHÖN!

Mercí, thank you, xie xie, obrigada, maururu!

10. REFERENCES

DIN 53018. 1976. Measurements of the dynamic viscosity of Newtonian fluids using rotational viscometers.

Abichou, T., C.H. Benson, and T.B. Edil. 2002. Micro-Structure and Hydraulic Conductivity of Simulated Sand-Bentonite Mixtures. Clays and Clay Minerals **50**:537-545. ISSN 0009-8604

Akroyd, T.J., and Q.D. Nguyen. 2003a. Continuous on-line rheological measurements for rapid settling slurries. Minerals Engineering **16**:731-738. ISSN 0892-6875

Akroyd, T.J., and Q.D. Nguyen. 2003b. Continuous rheometry for industrial slurries. Experimental Thermal and Fluid Science **27**:507-514. ISSN 0894-1777

Amado, T.J.C., D.J. Reinert, and J.M. Reichert. 2001. Soil Quality of Very Fragile Sandy Soils From Southern Brazil. Pages 564-568 *in* D. E. Scott, Mohtar, R.H., Steinhardt, G.C., editor. 10th INternational Soil Conservation Organization Meeting, Purdue University.

Atterberg, A. 1914. Die Eigenschaften der Bodenkörner und die Plastizität der Böden. Kolloidchemische Beihefte. **6**:55-89. (1913-1961 ISSN 0368-6590; since 1962 ISSN 0023-2904)

Barrett, P.J. 1980. The shape of rock particles, a critical review. Sedimentology **27**:291-303. ISSN 0037-0746

Barnes, H.A., J.F. Hutton, and K. Walters. 1989. An Introduction to Rheology. 199 pp. Elsevier, Amsterdam, Oxford, New York, Tokyo. ISBN 0-444-87469-0

Bekkour, K., H. Ern, and O. Scrivener. 2001. Rheological Characterization of Bentonite Suspensions and Oil-In-Water Emulsions Loaded with Bentonite. Appl. Rheol. **11**:178-187. ISSN 1430-6395

Berilli, M., T.A. Ghezzehei, and D. Or. 2002. Modeling Bulk Soil Compaction Using A Rheologically-Based Pore Closure Model. *In* L. Vulliet, Laloui, L., Schrefler, B., ed. Environmental Geomechanics - Monte Verità 2002. EPFL Press, Lausanne, Monte Verità. ISBN 2-88074-512-2

Beurlen, K. 1954. Paläogeographie und Morphogenese des Paraná-Beckens (Süd-Brasilien). ZDGG (German Geol. Soc. J.) **106**:519-537.

Bishop, A.W., and L. Bjerrum. 1960. The Relevance of the Triaxial Test to the Solution of Stability Problems. *in* ASCE, editor. Proc. ASCE Research Conference on Shear Strength of Cohesive Soils, Boulder, Colorado.

Bishop, A.W. 1960. The principle of effective stress. Publikasjon Norges Geotekniske Institutt **23**:1-5. ISSN 0078-1193

Bishop, A.W., und L. Bjerrum. 1961. Bedeutung und Anwendbarkeit des Dreiachsialversuches für die Lösung von Standsicherheitsaufgaben. 61 pp. Norges Geotekniske Institutt, Oslo. ISSN 0078-1193

Bohor, B.F., and R.E. Hughes. 1971. Scanning Electron Microscopy of Clays and Clay Minerals. Clays Clay Miner. **19**:49-54. ISSN 0009-8604

Boivin, P., P. Garnier, and D. Tessier. 2004. Relationship between Clay Content, Clay Type, and Shrinkage Properties of Soil Samples. Soil Sci. Soc. Am. J. **68**:1145-1153.

Bolton, M.D. 2000. The role of micro-mechanics in soil mechanics. 24 pp. Cambridge University Press, Engineering Dept. ISSN 0309-7439

Brandenburg, U. 1990. Fließverhalten von Bentonit-Dispersionen.268 pp. PhD Thesis. Christian-Albrechts-Universität zu Kiel, Kiel.

Bresler, E., B.L. McNeal, and D.L. Carter. 1982. Saline and Sodic Soils: Principles-Dynamics-Modeling. 236 pp. Springer-Verlag., Berlin, Heidelberg, New York. ISBN 3-540-11120-4

Breuer, J., and U. Schwertmann. 1999. Changes to hardsetting properties of soil by addition of hydroxides. Eur. J. Soil Sci. **50**:657-664. ISSN 1351-0754

Cho, G.-C., J. Dodds, and J.C. Santamarina. 2006. Particle Shape Effects on Packing Density, Stiffness, and Strength: Natural and Crushed Sands. J. Geotech. Geoenv. Eng. **132**:591-602. ISSN 1090-0241

Chorom, M., P. Rengasamy, and R.S. Murray. 1994. Clay Dispersion as Influenced by pH and Net Particle Charge of Sodic Soils. Austr. J. Soil Res. **32**:1243-1252. ISSN 0004-9573

Collyer, A.A., and D.W. Clegg, ed. 1998. Rheological Measurement. 2nd edition. 779 pp. Chapman & Hall, London. ISBN 0-412-72030-2

Cornell, R.M., and U. Schwertmann. 2003. The Iron Oxides - Structure, Properties, Reactions, Occurences and Uses second, completely revised and extended edition edition. 664 pp. WILEY-VCH, Weinheim. ISBN 3-527-30274-3

Cristescu, N.D., and G. Gioda, ed. 1994. Visco-Plastic Behaviour of Geomaterials. 1st edition. International Centre for Mechanical Sciences, Courses and Lectures No. 350. 289 pp. Springer Verlag, Wien, New York. ISBN 3-211-82586-X, 0-387-82586-X

Cundall, P.A., and O.D.L. Strack. 1979. A Discrete Numerical Model for Granular Assemblies, Géotechnique, **29**:47-65. ISSN 0016-8505

Dafarmos, C.M., and J.A. Nohel. 1980. A nonlinear hyperbolic Volterra equation in viscoelasticity. Mathematics Research Center, Madison, Wisconsin.

Davey, B.G. 1979. Soil Structure as Revealed by Scanning Electron Microscopy. 97-102 *In* W. W. Emerson, R.D. Bond, and A.R. Dexter (eds.), Modification of Soil Structure. John Wiley & Sons, Chichester, N.Y., Brisbane, Toronto. ISBN 0-471-99530-4

de Azevedo, A.C. 2003. Inferências sobre a gênese de agregados em Latossolos Vermelho distroférrico baseadas na distrubuicao de agragados. Rev. Ciências Agroveterniárias (J. Agronomy Veter. Sci.) **1**:1-7. ISSN 1676-9732

Derjaguin, B.V., and L.D. Landau. 1941. Theory of the stability of strongly charged lyophobic sols and the adhesion of strongly charged particles in solutions of electrolytes. Acta Physicochimica URSS **14**:633-662. (no ISSN)

Deshpande, T.L., D.J. Greenland, and J.P. Quirk. 1968. Charges in soil properties associated with the removal of iron and aluminium oxides. J. Soil Sci. **19**:108-122.

Diamond, S. 1970. Pore size distribution in clays. Clays Clay Miner. **18**:7–23. ISSN 0009-8604

Diamond, S. 1971. Microstructure and pore structure of impact-compacted clays. Clays Clay Miner. **19**:239-250. ISSN 0009-8604

Dörfler, H.-D. 2002. Grenzflächen und kolloid-disperse Systeme: Physik und Chemie. 989 pp. Springer, Berlin. ISBN 3-540-42547-0

Drescher, J., R. Horn, und M. de Boodt, (eds.) 1988. Impact of Water and External Forces on Soil Structure. Catena Supplement **11**. 171 pp. Catena Verlag, Cremlingen. ISSN 0722-0723 / ISBN 3-923381-11-5

Duiker, S.W., F.E. Rhoton, J. Torrent, N.E. Smeck, and R. Lal. 2003. Iron (Hydr)Oxide Crystallinity Effects on Soil Aggregation. Soil Sci. Soc. Am. J. **67**:606-611. ISSN 1435-0661

Emerson, W.W. 1954. The determination of the stability of soil crumbs. J. Soil. Sci. **5**:235-250. ISSN 0022-4588

Emerson, W.W. 1962a. The Swelling of Ca-Montmorillonite due to Water Absorption, I: Water Uptake in the Vapour Phase. J. Soil. Sci. **13**:31-39. ISSN 0022-4588

Emerson, W.W. 1962b. The Swelling of Ca-Montmorillonite due to Water Absorption, II: Water Uptake in the Liquid Phase. J. Soil Sci. **13**:40-45. ISSN 0022-4588

Emerson, W.W. 1967. A classification of soil aggregates based on their coherence in water. Austr. J. Soil Res. **5**:47-57. ISSN 0004-9573

Emerson, W.W., and A.C. Bakker. 1973. The comparative effects of exchangeable calcium, magnesium, and sodium in physical properties of red-brown earth subsoils. II. The spontaneous dispersion of aggregates in water. Austr. J. Soil Res. **11**:151-157. ISSN 0004-9573

Emerson, W.W., R.D. Bond, and A.R. Dexter (eds.) 1978. Modification of Soil Structure. 438 pp. John Wiley & Sons, Chichester, New York, Brisbane, Toronto. ISBN 0-471-99530-4

Emerson, W.W. 1983. Inter-particle bonding. p. 928 *In* CSIRO, ed. Soils: An Australian Viewpoint. Academic Press, London. ISBN 0-6430-0400-9

Emerson, W.W. 1994. Aggregate Slaking and Dispersion Class, Bulk Properties of Soil. Austr. J. Soil Res. **32**:173-184. ISSN 0004-9573

FAO-Unesco. 1971. Soil Map of the World, South America, 1 : 5,000,000. 193 pp. FAO Unesco (printed by Tipolitografia F. Failli, Rome), Paris. (no ISBN)

Fiés, J.C., and A. Bruand. 1998. Particle packing and organization of the textural porosity in clay-silt-sand mixtures. Eur. J. Soil Sci. **49**:557-567. ISSN 1351-0754

FitzPatrick, E.A. 1993. Soil Microscopy and Micromorphology. 304 pp. Wiley, Aberdeen. ISBN 0-471-93859-9

Fredlund, D.G., and H. Rahardjo. 1993. Soil Mechanics for Unsaturated Soils. 517 pp. John Wiley & Sons, Inc., New York. ISBN 0-471-85008-X

Garciano, L., R. Torisu, J. Takeda, and J. Yoshida. 2001. Resonance Identification and Mode Shape Analysis of Tractor Vibrations. J. JSAM **63**:45-50. ISSN 0285-2543

Garz, J., Scharf, H., Stumpe, H., Scherer, H.W., Schliephake, W. 1993. Effect of potassium fertilization on some chemical properties in a long-term trial on sandy loess. Potash Review **3**:1-12. ISSN 0032-5546

Ghezzehei, T.A., and D. Or. 2000. Dynamics of soil aggregate coalescence governed by capillary and rheological processes. Water Resour. Res. **36**:367-379. ISSN 0148-0227

Ghezzehei, T.A., and D. Or. 2001. Rheological Properties of Wet Soils and Clays under Steady and Oscillatory Stresses. Soil Sci. Soc. Amer. J. **65**:624-637. ISSN 1435-0661

Grant, C.D., A.R. Dexter, and C. Huang. 1990. Roughness of soil fracture surfaces as a measure of soil microstructure. J. Soil Sci. **41**:95-110. ISSN 0022-4588

Grant, C.D., P.H. Groenevelt, and G.H. Bolt. 2002. On Hydrostatics and Matristatics of Swelling Soils. 345 *In* Raats, P.A.C. D. Smiles, and A.E. Warrick, ed. Environmental Mechanics - Water, Mass and Energy Transfer in the Biosphere. The Philip Volume. American Geophysical Union, Washington. ISBN 0-87590-988-4

Güven, N., and R.M. Pollastro, (eds.) 1992. Clay-Water Interface and its Rheological Implications. T. C. M. Society. CMS Workshop Lectures 244 pp. The Clay Mineral Society, Boulder, Colorado. ISBN 1-881208-04-4

Hadas, A., D. Swartzendruber, P.E. Rijtema, M. Fuchs, and B. Yaron, ed. 1973. Physical Aspects of Soil Water and Salts in Ecosystems. Ecological Studies 4. 460 pp. Springer Verlag, Berlin. ISBN 3-540-06109-6

Hartge, K.H., und R. Horn. 1999. Einführung in die Bodenphysik 3., überarbeitete Auflage edition. 304 pp. Enke, Stuttgart. ISBN 3-432-89683-2

Hartge, K.H., und R. Horn. 2002. Strength and deformation of arable soils and consequences for sustainable land use. Wasser & Boden **54**:34-38. ISSN 0043-0951

Heller, H., and R. Keren. 2002. Anionic Polyacrylamide Polymers Effect on Rheological Behavior of Sodium-Montmorillonite Suspensions. Soil Sci. Soc. Amer. J. **66**:19-25. ISSN 1435-0661

Horn, R. 1976. Festigkeitsänderungen infolge von Aggregierungsprozessen eines mesozoischen Tones.119 pp. PhD Thesis. Tech. Univ., Hannover.

Horn, R., K.H. Hartge, H. Flühler, R. Schulin, R., B. Buchter, und K. Roth. 1990. Methoden und Konzepte der Bodenphysik. Teil A: Mechanische Eigenschaften von Bodenprofilen und Bodenstruktureinheiten. Teil B: Modellierung des Stofftransportes im Boden. Teil A: 45 pp.; Teil B: 192 pp. *in* Weiterbildungsseminar der Deutschen Bodenkundlichen Gesellschaft in Kandersteg, 4.-7.4.1989, Zürich.

Horn, R. 1995a. Bedeutung von Auflast und Entwässerungsgrad für die Bodenwassercharakteristik von mineralischen Abdichtungen: BMBF-Verbundvorhaben Weiterentwicklung von Deponieabdichtungssystemen Teilvorhaben 45. Kiel.

Horn, R. 1995b. Aggregate strength of differently structured soil and its alteration with external stress application. Pages 177-182 *In* B. H. So, Smith, G.D., Raine, S.R., Schafer, B.M., Loch, R.J., (eds.) Sealing, Crusting and Hardsetting Soils: Productivity and Conservation. Proceedings of the 2nd International Symposium. Australian Society of Soil Science, Inc. - Queensland Branch, University of Queensland, Brisbane, Australia, 7-11 Feb. 1994. 0-646-23011-5

Horn, R., T. Baumgartl, W. Gräsle, and B.G. Richards. 1995. Stress induced changes of hydraulic properties in soils. 123-128 *In* E. E. Alonso, Delage, P., ed. Unsaturated Soils. Balkema Verlag, Rotterdam, Berlin. ISBN 9-0541-0583-6

Horn, R., and T. Baumgartl. 1999. Dynamic properties of soils. A19-A46 *In* M. E. Sumner, ed. Handbook of Soil Science. CRC Press, Boca Raton, FL. ISBN 0-8493-3136-6

Horn, R. 2004. Time Dependence of Soil Mechanical Properties and Pore Functions for Arable Soils. Soil Sci. Soc. Amer. J. **68**:1131-1137. ISSN 1435-0661

Imhoff, S., A. Pires da Silva, and A. Dexter. 2002. Factors Contributing to the Tensile Strength and Friability of Oxisols. Soil Sci. Soc. Amer. J. **66**:1656-1661. ISSN 1435-0661

Ingles, O.G. 1962. Bonding Forces in Soils - Part 3, Vol. 1. Pages 1025-1047 *in* Proc. of the First Conference of the Australian Road Research Board.

Jamiolowski, M., R. Lancellotta, and D.C.F. Lo Presti. 1995. Remarks on the stiffness at small strains of six Italian clays. pp. 817-836 *In* S. Shibuya, T. Mitachi, and S. Miura, eds. Pre-failure deformation of Geomaterials. Balkema, Rotterdam.

Jardine, R.J. 1992. Some observations on the kinematic nature of soil stiffness. Soils and Foundations **32**:11-124.

Jardine, R.J., D.M. Potts, and K.G. Higgins (eds.). 2004. Advances in Geotechnical Engineering: The Skempton Conference. Proceedings of the Skempton Memorial Conference on Advances in Geotechnical Engineering, held at the Royal Geographical Society. 1400 pp. pp. American Society of Civil Engineers (Thomas Telford Ltd.), London, United Kingdom. ISBN 0-7277-3264-1

Jasmund, K., und G. Lagaly, ed. 1993. Tonminerale und Tone: Struktur, Eigenschaften, Anwendungen und Einsatz in Industrie und Umwelt. 490 pp. Steinkopff-Verlag, Darmstadt. ISBN 3-7985-0923-9

Jia, X. 2004. Theoretical analysis of the adhesion force of soil to solid materials. Biosystems Eng. **87**:489-493. ISSN 1537-5110

Keedwell, M.J. 1984. Rheology and Soil Mechanics. 323 pp. MacMillan, London, New York. ISBN 0-8533-4285-7

Keedwell, M.J., ed. 1988. International Conference on Rheology and Soil Mechanics. International Conference on Rheology and Soil Mechanics 371 pp. Elsevier Applied Science, London and New York. ISBN 1-85166-273-1

Kézdi, Á. 1974. Handbook of soil mechanics - Volume 1: Soil Physics. 1st edition. 294 pp. Akadémiai Kiadó, Budapest. ISBN 963-05-0088-4

Köppen, W. 1931. Grundriss der Klimakunde 2nd edition. 388 pp. pp. de Gruyter, Berlin.

Kosmulski, M., J. Gustafsson, and J.B. Rodenholm. 1999a. Ion specificity and viscosity of rutile dispersions. Colloid Polym. Sci. **277**:550-556. ISSN 0023-2904

Kosmulski, M., J. Gustafsson, and J.B. Rodenholm. 1999b. Correlation between the Zeta Potential and Rheological Properties of Anatase Dispersions. J. Colloid Interface Sci. **209**:200-206. ISSN 0021-9797

Kosmulski, M. 2001. Chemical Properties of Material Surfaces. 753 pp. Marcel Dekker, Inc., New York, Basel. ISBN 0-8247-0560-2

Krumbein, W.C. 1941. Measurement and geological significance of shape and roundness of sedimentary particles. J. Sediment. Petrol. **11**:64-72. ISSN 0022-4472

Krumbein, W.C., and L.L. Sloss. 1963. Stratigraphy and Sedimentation. 497 pp. Freeman and Company, San Fransisco, CA. no ISBN

Kuhn, M.R. 1999. Structured deformation in granular materials. Mechanics of Materials **31**:407-429.

Kutílek, M. 1964. The influence of soil colloids upon the values of some hydrolimits. Rostlinná výroba **10**:605-623. ISSN 0370-663X

Kutílek, M. 1967. The affinity of water to kaolinites and montmorillonites. Pages 73-82 *in* Proc. Int. Soil Water Symp., Prague.

Kutílek, M. 1973. The influence of clay minerals and exchangeable cations on soil moisture potential. pp. 153-160 *In* A. Hadas, Swartzendruber, D., Rijtema, P.E., Fuchs, M., Yaron, B., ed. Physical Aspects of Soil Water and Salts in Ecosystems. Ecological Studies. Springer-Verlag, Berlin. ISBN 3-540-06109-6

Kutílek, M., and D.R. Nielsen. 1994. Soil Hydrology. 370 pp. Catena, Cremlingen. ISBN 3-923381-26-3

Lagaly, G., O. Schulz, und R. Zimehl. 1997. Dispersionen und Emulsionen - Eine Einführung in die Kolloidik feinverteilter Stoffe einschließlich der Tonminerale. 560 pp. Steinkopff, Darmstadt. ISBN 3-7985-1087-3

Lamotte, M., A. Bruand, F.X. Humbel, A.J. Herbillon, and M. Rieu. 1997. A hard sandy-loam soil from semi-arid Northern Cameroon:I. Fabric of the groundmass. Eur. J. Soil. Sci. **48**:213-225. ISSN 1351-0754

Le Bissonnais, Y., and D. Arrouays. 1996. Aggregate stability and assessment of soil crustability and erodibility: I. Theory and methodology. Eur. J. Soil Sci. **47**:425-437. ISSN 1351-0754

Le Bissonnais, Y., and D. Arrouays. 1997. Aggregate stability and assessment of soil crustability and erodibility: II. Application to humic loamy soils with various organic carbon contents. Eur. J. Soil Sci. **48**:39-48. ISSN 1351-0754

Li, X.S. 2003. Technical notes - Effective stress in unsaturated soil: A microstructural analysis. Géotechnique **53**:273-278. ISSN 0016-8505

Loveday, J., and J. Pyle. 1973. The Emerson Dispersion Tests and Its Relationship to Hydraulic Conductivity. CSIRO Australian Devision of Soils, Technical Paper **15**:1-7.

Macosko, C.W. 1994. Rheology - Principles, Measurements, and applications. 550 pp. VCH Publishers, New York. ISBN 1-56081-579-5

Markgraf, W., and R. Horn. 2005. Rheology in soil mechanics - structural changes in soils depending on salt and water content. 149-154 *In* S. L. Mason, ed. Papers presented at the Nordic Rheology Conference, Tampere, Finland, June 1-3, 2005. IKON, Vallensbaek. 87-988486-5-8

Markgraf, W., R. Horn und S. Peth. 2005. Einführung der Rheometrie in die Bodenmechanik: (Mikro-)Strukturelles Verhalten von Böden in Abhängigkeit von Salzkonzentration und Wassergehalt. Mitt. Dt. Bodenk. Ges. **106**:43-44.

Markgraf, W., R. Horn, and S. Peth. 2006. An Approach to Rheometry in Soil Mechanics: Structural Changes in Bentonite, Clayey and Silty Soils. Soil Till. Res. **(available online)**. ISSN 0167-1987

Markgraf, W., and R. Horn. 2006a. Rheological Stiffness Analysis of K^+-treated and $CaCO_3$-rich Soils. J. Plant Nutr. Soil Sci. **169**:411-419. ISSN 1436-8730

Markgraf, W., and R. Horn. 2006b. Rheometry in Soil Mechanics: Microstructural Changes in a Calcaric Gleysol and a Dystric Planosol. 47-58 *In* R. Horn, H. Fleige, S. Peth, and Xh. Peng, (eds.) Sustainability - Its Impact on Soil Management and Environment. Catena Verlag. ISBN 3-923381-52-2

Mehra, O.P., and M.L. Jackson. 1960. Iron Oxide Removal From Soils and Clays by a Dithionite-Citrate System Buffered With Sodium Bicarbonate. Pages pp. 317-327 (369 pp) *in* A. Swineford, editor. 7th National Conference on Clays and Clay Minerals. Adlard & Son Ltd., Washington, D.C.

Meichsner, G., T. Mezger, and J. Schröder. 2003. Lackeigenschaften messen und steuern: Rheologie - Grenzflächen - Kolloide 1st edition. 236 pp. Vincentz Verlag, Hannover. 3-87870-739-8

Mezger, T. 2002. The Rheology-Handbook - For users of rotational and oscillatory rheometers. 252 pp. Vincentz Verlag, Hannover. ISBN 3-87870-745-2

Mitchell, J.K. 1993. Fundamentals of Soil Behavior 2nd edition. 437 pp. John Wiley & Sons, New York. ISBN 0-471-85640-1

Mitchell, J.K., and K. Soga. 2005. Fundamentals of soil behavior 3rd edition. 577 pp. John Wiley & Sons, Hoboken, NJ. ISBN 0-471-46302-7

Muggler, C.C., C. van Griethuysen, P. Buurman, and T. Pape. 1999. Aggregation and Organic Matter, and Iron Oxide Morphology in Oxisols from Minas Gerais, Brazil. Soil Sci. **164**:759-770. ISSN 0038-075C

Myers, D. 1999. Surfaces, Interfaces, and Colloids: Principles and Applications 2nd edition. 501 pp. Wiley-VCH, New York. ISBN 0-471-33060-4

Neaman, A., and A. Singer. 2000. Rheological Properties of Aqueous Suspensions of Palygorskite. Soil Sci. Soc. Amer. J. **64**:427-436. ISSN 1435-0661

Oades, J.M., and A.G. Waters. 1991. Aggregate Hierarchy in Soils. Austr. J. Soil Res. **29**:815-828. ISSN 0004-9573

Ohtsubo, Y.A., A. Yoshimura, S.-I. Wada, and R.N. Yong. 1991. Particle Interaction and Rheology of Illite-Iron Oxide Complexes. Clays and Clay Minerals **39**:347-354.

Or, D., and M. Tuller. 1999. Liquid retention and interfacial area in variably saturated porous media: Upscaling from pore to sample scale model. Water Resour. Res. **35**:3591-3605. ISSN 0043-1397

Or, D., and J.M. Wraith. 1999. Temperature effects on soil bulk dielectric permittivity measured by time domain reflectometry: A physical model. Water Resour. Res. **35**:371. ISSN 0043-1397

Or, D., and M. Tuller. 2000. Flow in unsaturated fractured porous media: Hydraulic conductivity of rough surfaces. Water Resour. Res. **36**:1165-1177. ISSN 0043-1397

Osipov, V.I. 1975. Structural Bonds and the Properties of Clay. Bull. Int. Assoc. Eng. Geol. **12**:13-20. ISSN 0074-1612

Peng, X., R. Horn, D. Deery, M.B. Kirkham, and J. Blackwell. 2005. Influence of soil structure on the shrinkage behaviour of a soil irrigated with saline-sodic water. Austr. J. Soil Res. **43**:555-563. ISSN 0004-9573

Phan, T.H., and M. Chaouche. 2005. Rheology and Stability of Self-Compacting Concrete Cement Pastes. Applied rheology. **15**:336-343. ISSN 0939-5059

Pinto, I.D. 1966. Geology of the State of Rio Grande do Sul - Brasil. Esc. Geol. P. Alegre **11**:1-22.

Powers, M.C. 1953. A new roundness scale for sedimentary particles. J. Sediment. Petrol. **23**:117-119. ISSN 0022-4472

Raats, P.A.C., D. Smiles, and A.E. Warrick (eds.) 2002. Environmental Mechanics - Water, Mass and Energy Transfer in the Biosphere. The Philip Volume. American Geophysical Union, Washington. ISBN 0-87590-988-4

Ravina, I. 1973. The Mechanical and Physical Behavior of C-Clay Soil and K-Clay Soil. 131-141 *In* A. Hadas, D. Swartzendruber, P.E. Rijtema, M. Fuchs, and B. Yaron, (eds.) Physical Aspects of Soil Water and Salts in Ecosystems. Springer Verlag, Berlin.

Reed, S.J.B. 2005. Electron Microprobe Analysis and Scanning Electron Microscopy in Geology. 2nd edition. 192 pp. Cambridge University Press, Cambridge. ISBN 0-521-84875-X

Rengasamy, P., R.S.B. Greene, G.W. Ford, and A.H. Mehanni. 1984. Identification of Dispersive Behaviour and the Management of Red-brown Earth. Austr. J. Soil Res. **22**:413-431. ISSN 0004-9573

Rengasamy, P., and K.A. Olssen. 1991. Sodicity and soil structure. Austr. J. Soil Res. **29**:935-952. ISSN 0004-9573

Richter, F. 2005. Vergesellschaftung und Eigenschaften von Böden unterschiedlicher geomorpher Einheiten einer Jungmoränenlandschaft des Ostholsteinischen Hügelandes. PhD Thesis. 132 pp. Institut für Pflanzenernährung und Bodenkunde, Kiel. ISSN 0933-680X

Rimmer, D.L., Greenland, D.J. 1976. Effects of $CaCO_3$ on swelling behavior of a soil clay. J. Soil Sci. **27**:129-139. ISSN 0022-4588

Rosenqvist, I.T. 1959. Physico-chemical properties of soils; soil-water systems. J. Soil Mech. Found. Div., Proc. Am. Soc. Civil Engrs. **85**:285-312. ISSN 0044-8001

Rosenqvist, I.T. 1962. The influence of physico-chemical factors upon the mechanical properties of clays. Clays Clay Miner. **9**:12-27. ISSN 0009-8604

Santamarina, J.C. 2001. Soil Behavior at the Microscale: Particle Forces. Pages 1-32 *in* Proc. Symp. Soil Behavior and Soft Ground Construction, in honor of Charles C. Ladd., MIT.

Santamarina, J.C. 2003. Soil behavior at the microscale: particle forces. Pages 25-56 *in* Germaine, J.T., T.C. Sheahan, and R.V. Whitman (eds.) Soil Behavior and Soft Ground Construction. ASCE Geotechnical Special Publications No. 119, ASCE, Reston, VA.

Schlichting, E., H.-P. Blume, und K. Stahr. 1995. Bodenkundliches Praktikum - Eine Einführung in pedologisches Arbeiten für Ökologen, insbesondere Land- und Forstwirte, und für Geowissenschaftler. 2., neubearbeitete Auflage edition. 295 pp. Blackwell Wissenschafts-Verlag, Berlin, Wien. ISBN 3-8263-3042-0

Schmidt, P.F. (ed.) 1994. Praxis der Rasterelektronenmikroskopie und Mikrobereichsanalyse. W. J. Bartz. Kontakt & Studium 444. 810 pp. Expert Verlag, Esslingen. ISBN 3-8169-1038-6

Schramm, G. 2002. Einführung in Rheologie und Rheometrie. 2nd edition. 360 pp. Haake GmbH, Karlsruhe. no ISBN

Schulz, O. 1998. Berichte aus der Chemie - Strukturell-rheologische Eigenschaften kolloidaler Tonmineraldispersionen. 501 pp. PhD. Christian-Albrechts-Universität zu Kiel.

Schwertmann, U., F. Wagner, and H. Knicker. 2005. Ferrihydrite-Humic Associations: Magnetic Hyperfine Interactions. Soil Sci. Soc. Am. J. **69**:1009-1015. ISSN 1435-0661

Shainberg, I., J.D. Rhoades, and R.J. Prather. 1981a. Effect of low electrolyte concentration on clay dispersion and hydraulic conductivity of a sodic soil. Soil Sci. Soc. Am. J. **24**:273-277. ISSN 0361-5995

Shainberg, I., J.D. Rhoades, and R.J. Prather. 1981b. Effect of mineral weathering on clay dispersion and hydraulic conductivity of sodic soils. Soil Sci. Soc. Am. J. **45**:287-291. ISSN 0361-5995

Shainberg, I., and G.J. Levy. 1992. Physico-chemical effects of salts upon infiltration and water movement in soils. Interacting processes in soil science. 37-94 *In* R. J. Wagenet, P. Baveye, and B.A. Stewart, (eds.) Advances in Soil Science. Lewis Publications., Boca Raton, FL. ISBN 0-87371-889-5

Shani, A., and L.M. Dudley. 2001. Field Studies of Crop Response to Water and Salt Stress. Soil Sci. Soc. Amer. J. **65**:1522-1528. ISSN 1435-0661

Sharpley, A.N. 1990. Reaction of Fertilizer Potassium in Soils of Differing Mineralogy. Soil Sci. **149**:44-51. ISSN 0038-075X

Shi-qiao, D., R. Lu-quan, L. Yan, and H. Zhi-Wu. 2005. Tangent Resistance of Soil on Moldboard and the Mechanism of Resistance Reduction of Bionic Moldboard. J. Bionics Eng. **2**:33-46. ISSN 1672-6529

Silva, V.R. da, J.M. Reichert, and D.J. Reinert. 2004. Variabilidade espacial da resistência do solo à penetração em plantio direto. Ciência Rural **34**:399-406.

Silvério da Silva, J.L., and E. Menegotto. 2002. Aspectos mineralógicos de silicificações em rochas sedimentares mesozóicas no Rio Grande do Sul. Revista Brasiliera de Geociências **32**:317-326. ISSN 0375-7535

Skempton, A. 1960. Effective stress in soils, concrete and rocks. Pages 4-16 *In* Pore Pressure and Suction in Soils: Conference organised by the British National Society of the Internatational Society of Soil Mechanics and Foundation Engineering at the Institution of Civil Engineers held on March 30. and 31., 1960. Butterworths, London.

Smith, D.W., and M.G. Reitsma. 2002. Towards an explanation for the residual friction angle in montmorillonite clay soil. 27-44 *In* Vulliet, L., L. Laloui, and B. Schrefler, (eds.) Environmental Geomechanics - Monte Veritá 2002. EPFL Press, Monte Veritá. ISBN 2-8807-4512-2

Sonderegger, U.C. 1985a. Das Scherverhalten von Kaolinit, Illit und Montmorillonit. 165 pp. PhD Thesis. ETH Zurich, Zurich.

Sonderegger, U.C. 1985b. Interpretationsversuch des Scherverhaltens reiner Tone auf Basis von Texturuntersuchungen. Beiträge zur Geologie der Schweiz, Kleinere Mitteilungen - Matériaux pour la Géologie de la Suisse, Bulletin **76**:137-149.

Streck, E.V., N. Kämpf, R.S.D. Dalmolin, E. Klamt, P.C. de Nascimento, and P. Schneider. 2002. Solos do Rio Grande do Sul. 107 pp. + 117 maps. UFRGS Editora, Porto Alegre. ISBN 85-7025-648-5

Suklje, L. 1969. Rheological aspects of soil mechanics. 571 pp. Wiley Interscience, London. ISBN 0-471-83550-1

Sumner, M.E., and R. Naidu. 1998. Sodic Soils: distribution, properties, management and environmental consequences. 207 pp. Oxford University Press, New York. ISBN 0-19-509655-X

Syres, J.K., T.D. Evans, J.D.H. Williams, and J.T. Murdock. 1971. Phosphate sorption parameters of representative soils from Rio Grande do Sul, Brazil. Soil Sci. **122**:267-275. ISSN 0022-4588

Szecsy, R.S. 1997. Concrete rheology. 215 pp. PhD Thesis. Urbana-Champaign, University of Illinois.

Talsma, T., and J.R. Philip. 1971. Salinity and Water Use. 296 pp. MacMillan, London. ISBN 0-4718-4430-6

Tanner, R.I., and K. Walters. 1998. Rheology: an historical perspective. 255 pp. Elsevier, Amsterdam. ISBN 0-4448-2945-8

Tanner, R.I. 2000. Engineering Rheology. 2nd edition. 559 pp. Oxford University Press, New York. ISBN 0-1985-6473-2

Tarchitzky, J., and Y. Chen. 2002. Rheology of Sodium-montmorillonite suspensions: Effect of humic substances and pH. Soil Sci. Soc. Amer. J. **66**:406-412. ISSN 1435-0661

Tariq, A.U.R., and D.S. Durnford. 1993a. Analytical volume change model for swelling clay soil. Soil Sci. Soc. Amer. J. **57**:1183–1187. ISSN 1435-0661

Tariq, A.U.R., and D.S. Durnford. 1993b. Soil volumetric shrinkage measurements, a simple method. Soil Sci. **155**:325–330. ISSN 1435-0661

Terribile, F., and E.A. Fitzpatrick. 1995. The application of some image-analysis techniques to recognition of soil micromorphological features. Eur. J. Soil Sci. **46**:29-46. ISSN 1351-0754

Terzaghi, K. 1925. Erdbaumechanik auf bodenphysikalischer Grundlage. 399 pp. Deuticke, Leipzig. (no ISBN)

Terzaghi, K. 1936. The shearing resistance of saturated soils. Pages 54-56 *in* Proceedings of the 1st International Conference on Soil Mechanics., Cambridge, MA.

Terzaghi, K., and R. Jelinek. 1954. Theoretische Bodenmechanik. 505 pp. Springer Verlag, Berlin, Göttigen, Heidelberg. (no ISBN)

Throe, F.R., and L.M. Thompson. 1993. Soil and Soil Fertility 5th edition. 462 pp. Oxford University Press., New York, Oxford. ISBN 0-19-508328-8

Tisdall, J.M., and J.M. Oades. 1982. Organic matter and water-stable aggregates in soils. Soil Sci. **33**:141-163. ISSN 0022-4588

Tong, J., L. Ren, B. Chen, and A.R. Qaisrani. 1994. Charactersitics of Adhesion Between Soil and Solid Surfaces. J. Terramechanics **31**:93-105. ISSN 0022-4898

Tseng, W. 2003. Sedimentation, rheology and particle-packing structure of aquaeous Al_2O_3. Ceramics International: CI **29**:821-828. ISSN 0272-8842

Tuller, M., D. Or, and L.M. Dudley. 1999. Adsorption and capillary condensation in porous media: Liquid retention and interfacial configurations in angular pores. Water Resour. Res. **35**:1949-1964. ISSN 0043-1397

Tuller, M., and D. Or. 2001a. Hydraulic functions for macroporous soils. ASAE Proceedings of the 2nd International Symposium on Preferential Flow. Pages 37-40

in The 2nd International Symposium on Preferential Flow. ASAE, St. Joseph, MI, Honolulu, HI.

Tuller, M., and D. Or. 2001b. Hydraulic conductivity of varaibly saturated porous media - Film and corner flow in angular pore space. Water Resour. Res. **37**:1257-1276. ISSN 0043-1397

Tuller, M., and D. Or. 2002. Unsaturated Hydraulic Conductivity of Structured Porous Media. Vadose Zone J. **1**:14-37. ISSN 1539-1663

Tuller, M., and D. Or. 2003. Hydraulic functions for swelling soils: pore scale considerations. J. Hydrol. **272**:50-71. ISSN 0022-1694

Tuller, M., and D. Or. 2005. Water films and scaling of soil characteristic curves at low water contents. Water Resour. Res. **41**:W09403 (09401-09406). ISSN 0043-1397

USDA. 2003. Keys to Soil Taxonomy. 9th edition. NRCS, Washington D.C.

U.S.S.L. 1954. Diagnosis and Improvement of Saline and Alkaline Soils. USDA Handbook No. 60. GPO, Washington D.C.

Valdes, J.R. 2002. Fines Migration and Formation Damage. PhD Thesis, Georgia Institute of Technology.

van Olphen, H. 1977. An Introduction to Clay Colloid Chemistry 2nd edition. 318 pp. John Wiley & Sons, New York, London, Sydney, Toronto. ISBN 0-471-01463-X

van Reeuwijk, L.P. 2002. Procedures for soil analysis. 6th edition. International Soil Reference and Information Centre (ISRIC), Wageningen. ISBN 90-6672-044-1

Verwey, E.J.W., and J.T.G. Overbeek. 1948. Theory of the Stability of Lyophobic Colloids: the Interaction of Soil Particles having an Electric Double Layer. pp. Elsevier, New York.

Vulliet, L., L. Laloui, and B. Schrefler (eds.) 2002. Environmental Geomechanics - Monte Veritá 2002. 423 pp. EPFL Press, Lausanne, Monte Veritá. ISBN 2-8807-4512-2

Vyalov, S.S. 1986. Rheological fundamentals of soil mechanics. XII + 564 pp. Elsevier, Amsterdam. ISBN 0-444-42223-4

Wadell, H. 1932. Volume, shape, and roundness of rock particles. J. Geol. **40**:443-451.

Warkentin, B.P., and R.N. Yong. 1962. Shear strength of montmorillonite and kaolinite related to interparticle forces. Clays Clay Miner. **9**:210-218. ISSN 0009-8604

Warkentin, B.P., and R.K. Schofield. 1962. Swelling Pressure of Na-Montmorillonte in NaCl solutions. J. Soil Sci. **13**:98-105. ISSN 0022-4588

West, S.L., G.N. White, Y. Deng, K.J. McInnes, A.S.R. Juo, and J.B. Dixon. 2004. Kaolinite, Halloysite, and Iron Oxide Influence on Physical Behavior of Formulated Soils. Soil Sci. Soc. Amer. J. **68**:1452-1460. ISSN 1435-0661

Whittig, L.D., and W.R. Allardice. 1986. X-Ray Diffraction Techniques. 1188 pp. *In* A. Klute, ed. Methods of Soil Analysis: Part 1. Physical and Mineralogical Methods. ASA, SSSAJ, Madison, Wisconsin. ISBN 0-89118-088-5 (pt. 1)

Whorlow, R.W. 1992. Rheological Techniques 2nd edition. 460 pp. Ellis Horwood Ltd., Chichester. ISBN 0-13-775370-5

Yimsiri, S., and K. Soga. 1999. Effect of surface roughness on small-strain modulus: Micromechanics view. Pages 597-602 *in* Pre-failure Deformation Characteristics of Geomaterials. Balkema, Rotterdam.

Yimsiri, S., and K. Soga. 2000. Micromechanics-based stress-strain behaviour of soils at small strains. Géotechnique: the international journal of soil mechnaics. **50**:559-572. ISSN 0016-8505

Yimsiri, S., and K. Soga. 2002. Application of Micromechanics Model to Study Anisotropy of Soils at Small Strains. Soils and Foundations **42**:15-26. ISSN 0038-0806

Yoder, R.E. 1936. A direct method of aggregate analysis of soils and a study of the physical nature of erosion losses. J. Amer. Soc. Agronomy **28**:337-351. ISSN 0095-9650

Yong, R.N., and B.P. Warkentin. 1966. Introduction to soil behavior. pp. 281-349 *In* G. Norbby, ed. Macmillan series in civil engineering. Macmillan, New York. (no ISBN)

Yong, R.N., and B.P. Warkentin. 1975. Soil properties and behaviour. 449 pp. Elsevier, Amsterdam. ISBN 0-444-41167-4

Zeil, W. 1986. Südamerika. 160 pp. Ferdinand Enke Verlag, Stuttgart. ISBN 3-432-95861-7

PART IV

APPENDICES

APPENDIX A

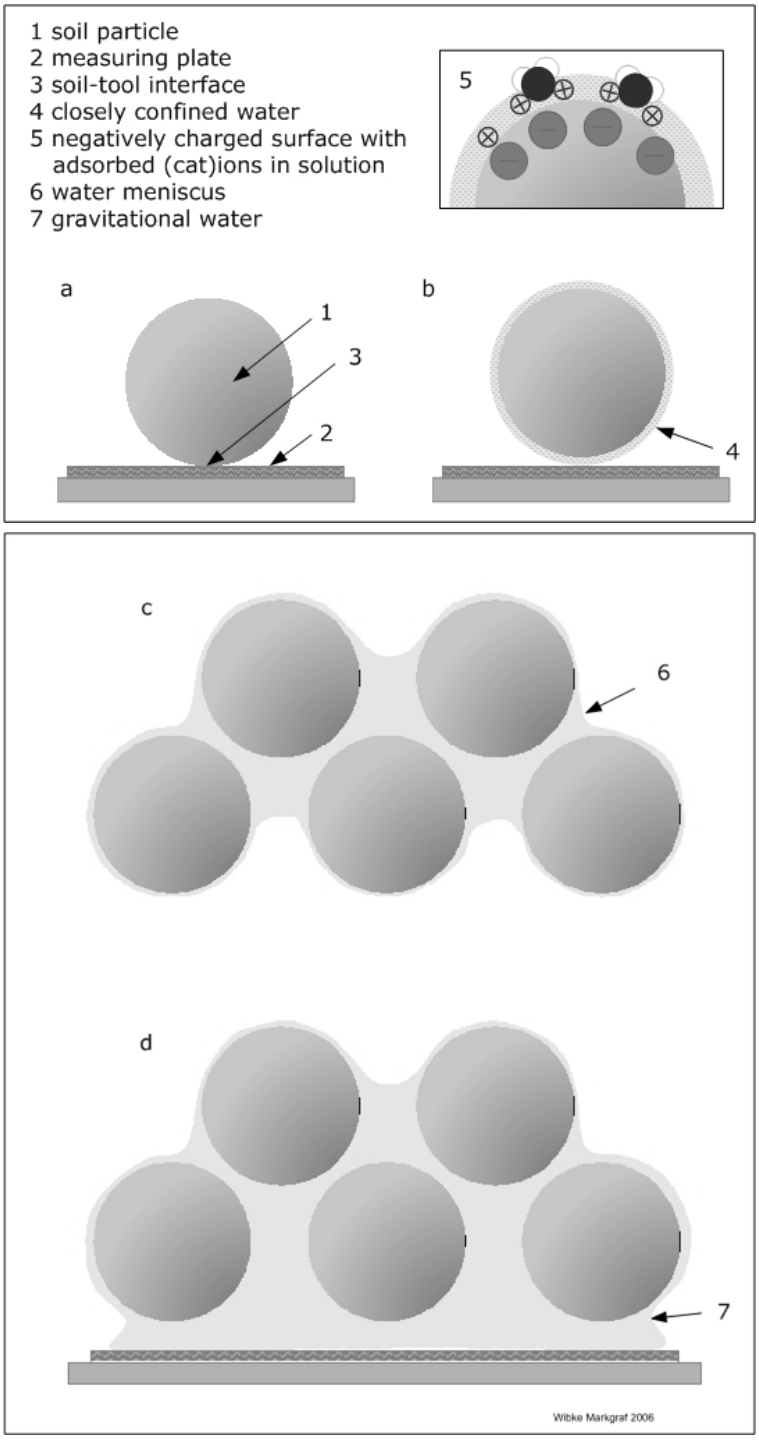

Fig. A-1 *Interaction between a soil particle (idealised) and a tool. a) adsorption water: direct contact between an air-dried soil particle (without water film); b) molecular water: contact between a with distilled water saturated or partly (pre-)drained soil particle; menisci may be formed at the soil particle-tool interface. Inlet: salts (cations in a certain concentration) may lead to a change of menisci forces (hydration mechanisms). c) water menisci: loose arrangement of single grains with continuous water film; neither internal nor external stress is applied or effective; d) gravitational water: particles are surrounded by a continuous water film (saturated), water menisci are formed at the soil-tool interface.*

A.1 Explanations and concepts for Fig. A-2 and Fig. A-3

A.1.1 Normal adhesion caused by intermolecular attraction of bare soil particles (N_{As})

Fig. A-2, **1** and **2**

$$W_A = E(d_e) = E_A = \frac{h\omega}{16\pi^2 d_e^2} \quad \text{(A.1)}$$

$$E_A = \frac{h\omega}{8\pi}\left[\frac{R}{d_0^2} - \ln\left(\frac{(d_0 + R)}{d_0}\right)\right] \quad \text{(A.2)}$$

$$N_{As} = \frac{-\partial E_A}{\partial d_0} = \frac{-h\omega}{8\pi}\left[\frac{R}{d_0^2} - \frac{R}{d_0(d_0 + R)}\right] \quad \text{(A.3)}$$

W_A : work of adhesion [J]
$E(d_e)$: interaction energy per unit area of separation [J/m²]
E_A :energy of adhesion [J/m²]
$h\omega$: Lifshitz van der Waals constant [J]
d_e : equilibrium intermolecular distance (shortest possible distance) [m]
d_0 : separation between the summit tip and tool surface [m]
R : radius of the soil particle asperity [m]
N_{As} : normal adhesion

A.1.2 Normal adhesion caused by water meniscus (N_{Am})

Water ring formed between the soil particle an planer tool surface as illustrated in ***Fig.A-2,*** **3** and **4** results in meniscus tensile force, acting in the direction of surface tension i.e. tangent at the meniscus-tool contact (Jia, 2004). The magnitude of adhesion force F_{AM} is expressed by

$$F_{AM} = \frac{2\pi R\gamma}{\left[1 + \frac{d_0}{b}\right]}(1 + \cos\theta) \quad \text{(A.4)}$$

with

F_{AM} = Adhesion force of water meniscus, in the direction of surface tension

b = vertical distance between soil particle surface to the lowest tip.

The normal adhesive force (***N*****$_{Am}$**), between the soil particle and plate can be computed as per the cncept of capillary rise, which states that the adhesion will be equal to the contact perimeter (2*2πR), surface tension (γ)and the cosine of the contact angle (θ). Thus,

$$N_{Am} = \pi R \gamma \cos\theta \qquad \text{(A.5)}$$

A.1.3 Normal adhesion caused by attraction of water film due to viscosity (***N*****$_{Av}$**)

For the contact model with water film between two parallel solid planes (***Fig. A-2, 5*** and ***Fig. A-3***) an analogy of two circular discs of Radius R, immersed in a liquid of viscosity η can be applied (Jia, 2004). If subjected to tensile forces ***N*****$_{Av}$** their separation increases from ***h*****$_1$** to ***h*****$_2$**, right before the liquid film does not break during pull. Furthermore, if the time required to pull is ***t***, the ***N*****$_{Av}$** can be expressed as,

$$N_{Av} = \left(\frac{3\pi\eta R^4}{4t}\right)\left(\frac{1}{h^2} - \frac{1}{h_2^2}\right) \qquad \text{(A.6)}$$

A.1.4 Normal adhesion due to capillary negative adsorption (***N*****$_{ca}$**)

Capillary negative adsorption is based on the well known Young-Laplace equation

$$\Delta P = \frac{2\gamma\cos\theta}{R_c} \qquad \text{(A.7)}$$

P = pressure inside liquid column near the meniscus

R_c = capillary radius

γ = tension of liquid

θ = contact angle

A. 2 Normal friction force (N_f)

$$N = N_G + N_A + N_f \quad \text{(A.8)}$$

N = total normal force
N_G = normal gravitational force
N_A = normal adhesion force
N_f = normal friction

and

$$N = (N_p+N_s)+ (\boldsymbol{N_{As}+N_{Am}+N_{Av}+N_{ca}}) + N_{wfm}$$

p = soil pores
s = soil particles
wfm = wet friction meniscus

A.3 Tangential forces acting at soil-tool interface

$$\tau = \tau_f + \tau_{drag} + \tau_A \quad \text{(A.10)}$$

τ = total tangential force
τ_f = tangential frictional resistance
τ_{drag}= tangential drag resistance
τ_A= tangential adhesive resistance

whereas the drag resistance τ_{drag} is mainly influenced by the tangential viscidity at the interface.
As Newton showed, the viscous force is directly proportional to the surface area (S) of the layer and velocity, and inversely proportional to its distance (***x***) from the stationary layer. If the coefficient of proportionality is h, which is the coefficient of viscosity, then,

$$\tau_{drag} = \tau_{tv} = -\eta\, S\, d_v/d_x \quad \text{(A.11)}$$

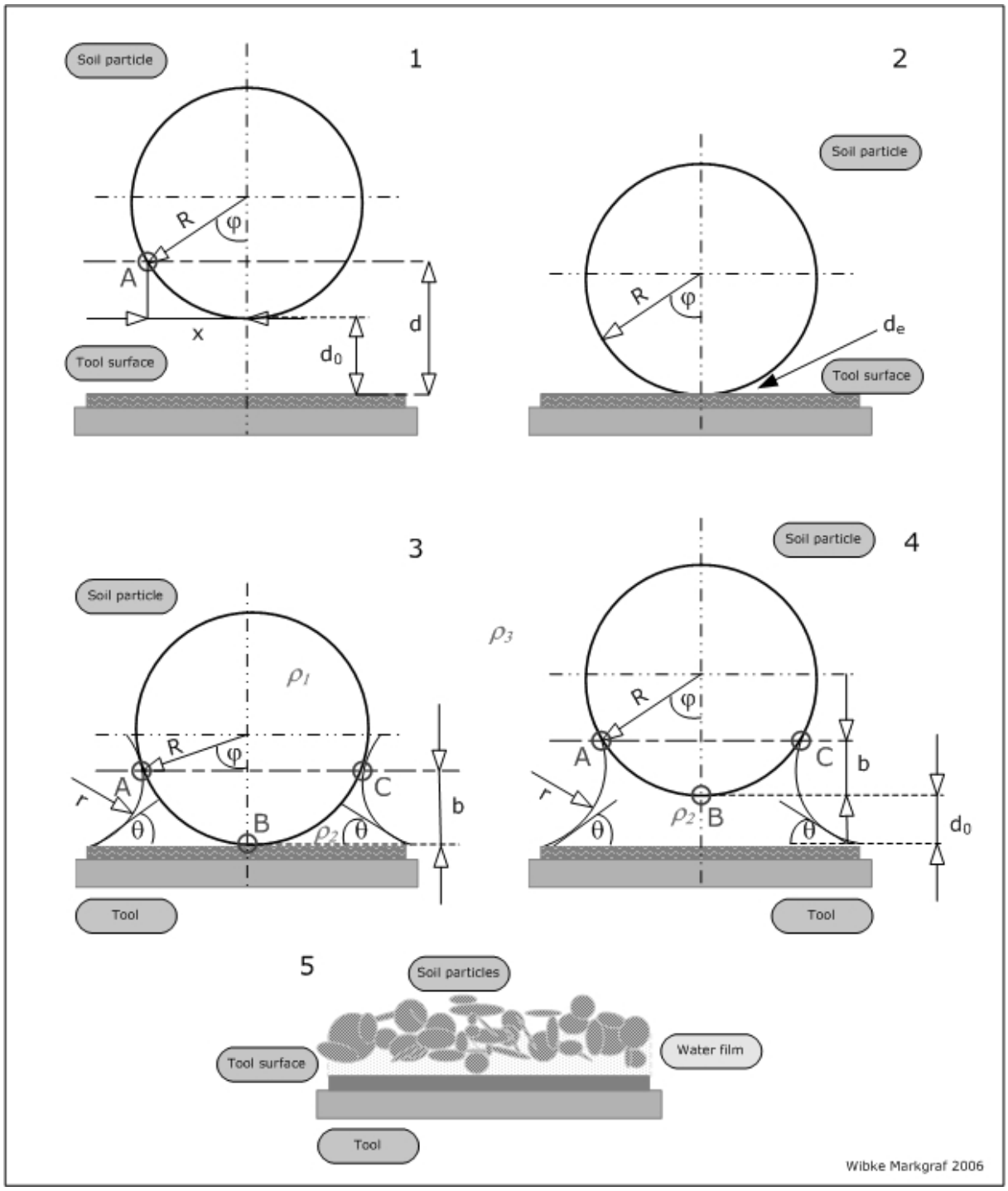

Fig. A-2 *Contact models of soil-tool interface: 1 completely non-contacting asperity without water ring; 2 water-point contacting asperity without water ring; 3 water-ring contacting asperity; 4 water-loop contacting asperity and 5 continiuous water film (redrawn after Jia, 2004)*

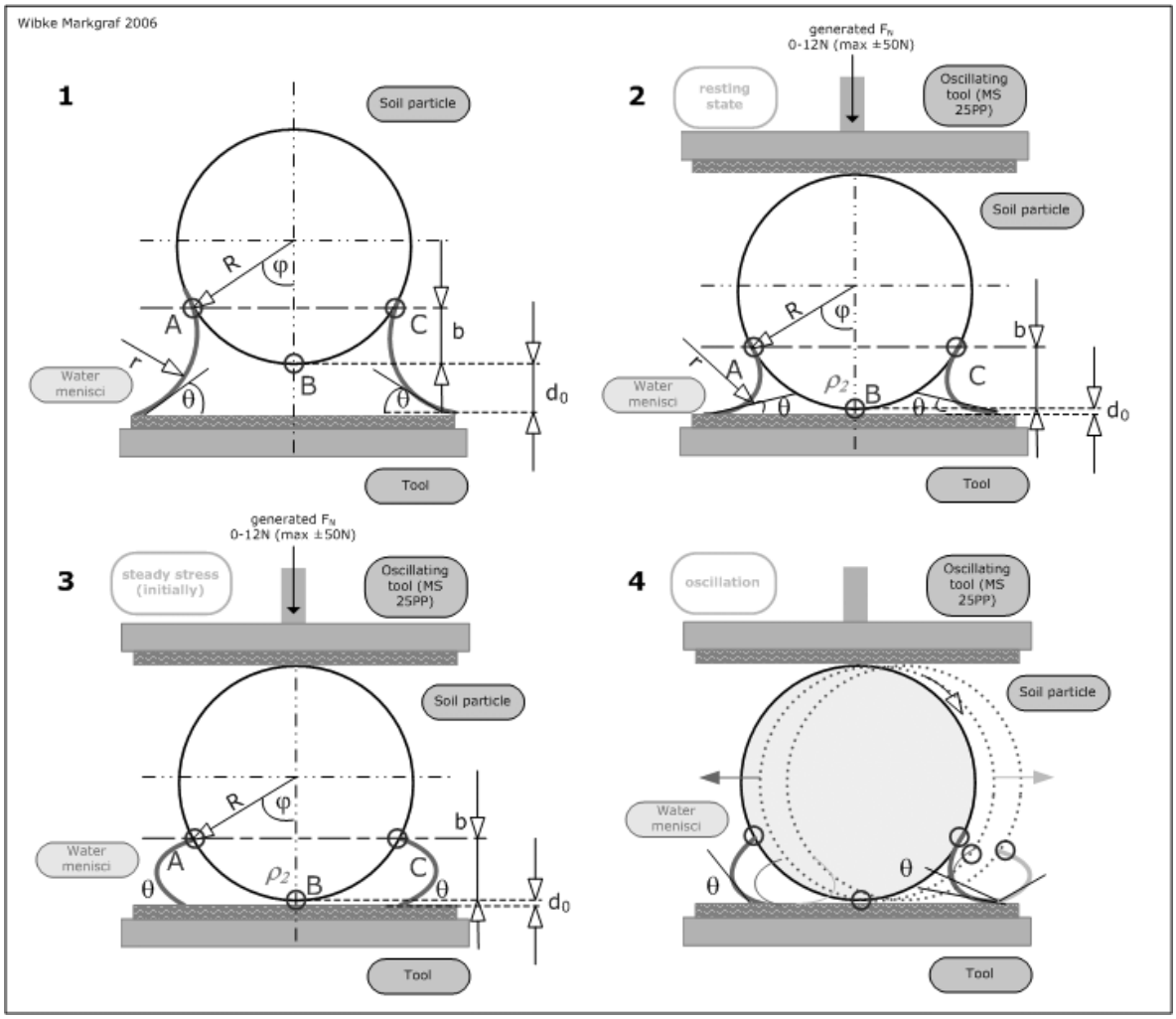

Fig. A-3 *representative illustration of a soil particle-tool interface.1 and 2 Initial and resting state: Single particle i.e. sand or silt in rest. 3 Under steady stress conditions, compression is caused; a convex menisci shape is evident. 4 Under oscillation (between to parallel plates) a direct contact between soil particle and tool is given; the contact angle changes due to oscillatory shear.*

APPENDIX B

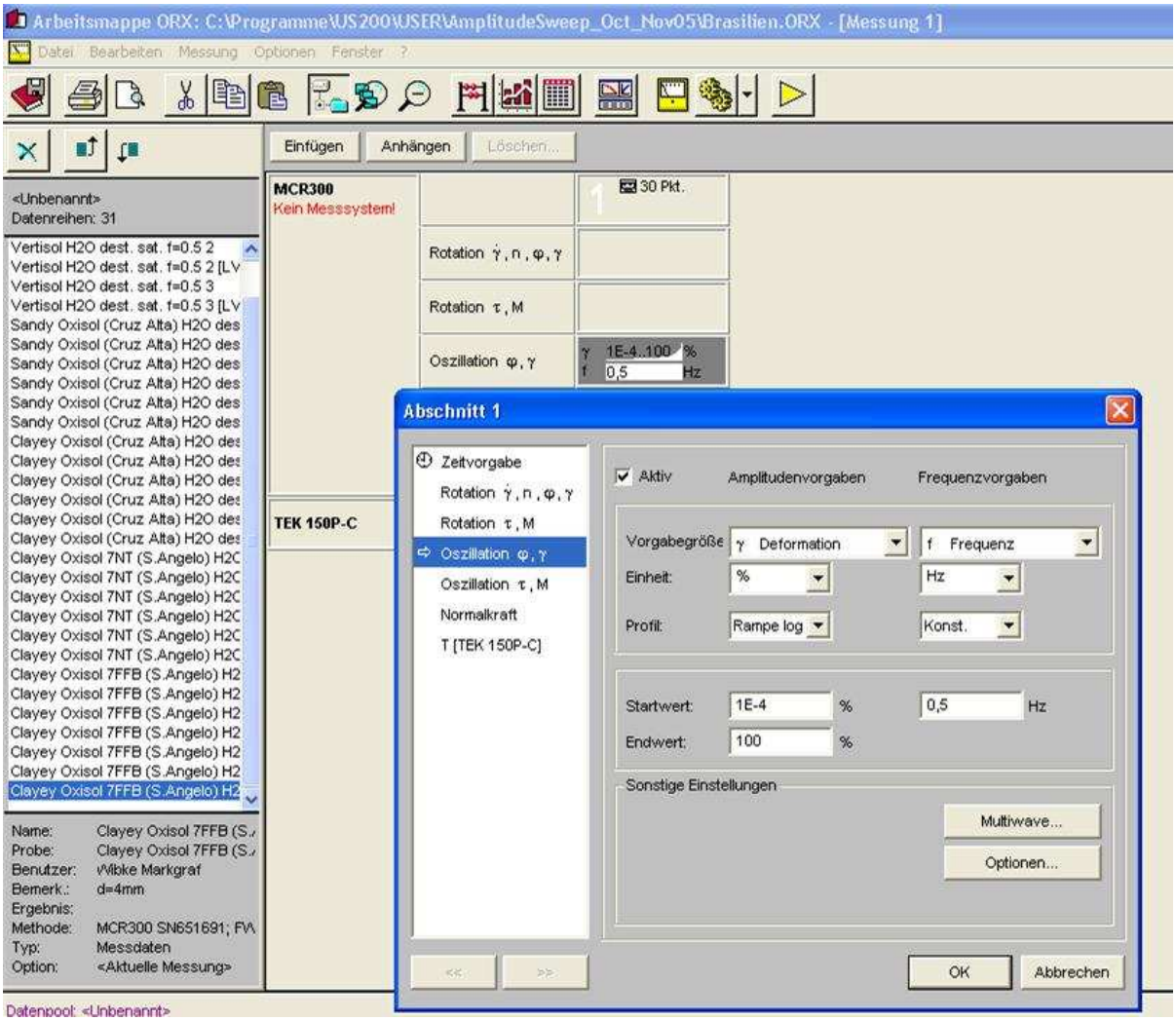

Fig. B-1 *Test configuration of an amplitude sweep test with a constant frequency f = 0.5HZ, and a controlled shear deformation(CSD) γ = 0.0001… 100% in oscillation (Software US200).*

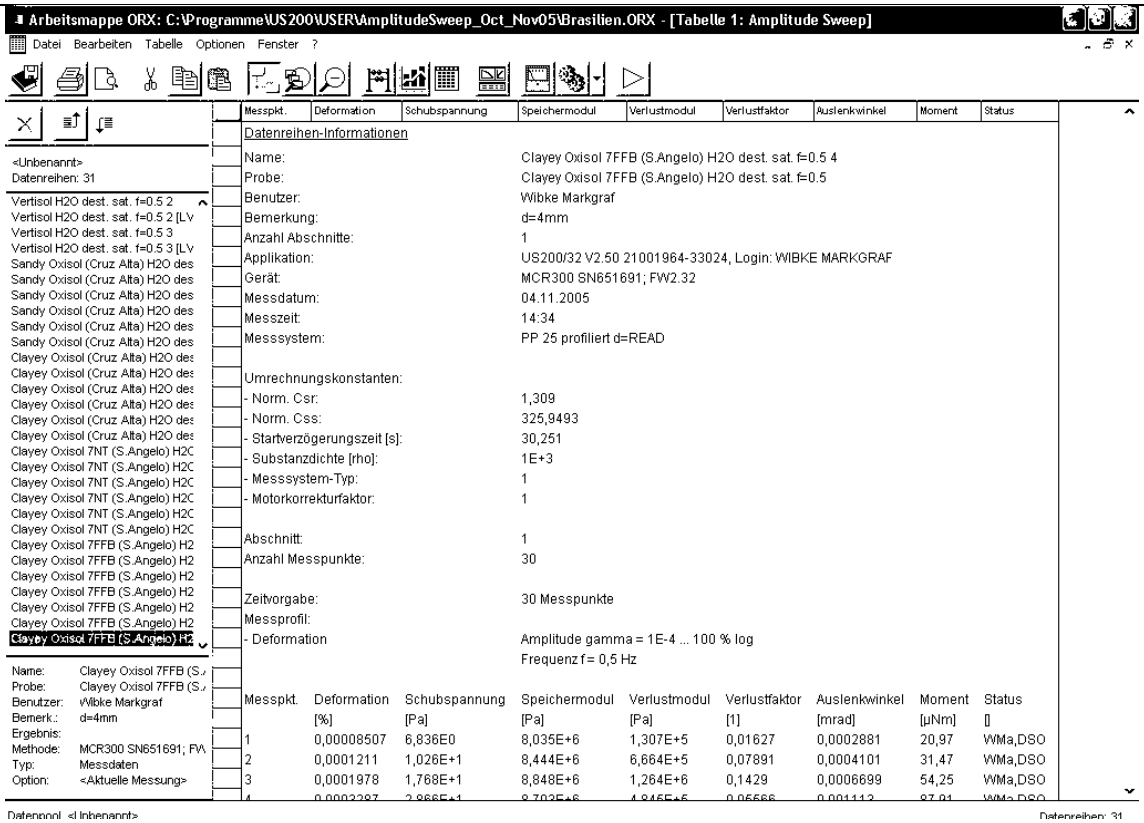

Fig. B-2 *Data sheet of collected parameters in amplitude sweep test.*

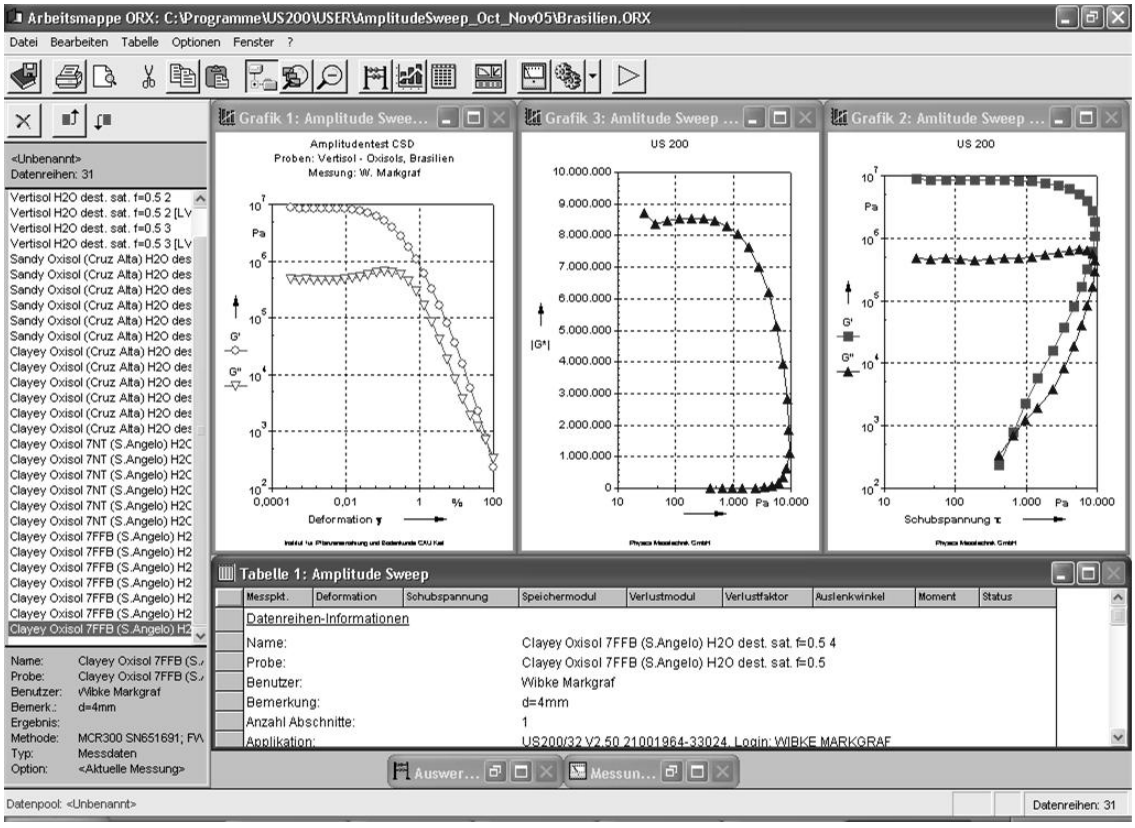

Fig. B-3 *Resulting graphs from a conducted amplitude sweep test. A variety of displaying stress-strain relationships is given, based on one database as presented here (see marked data description on the left sight "Clayey Oxisol 7FFB (S. Angelo) H2O dest.").*

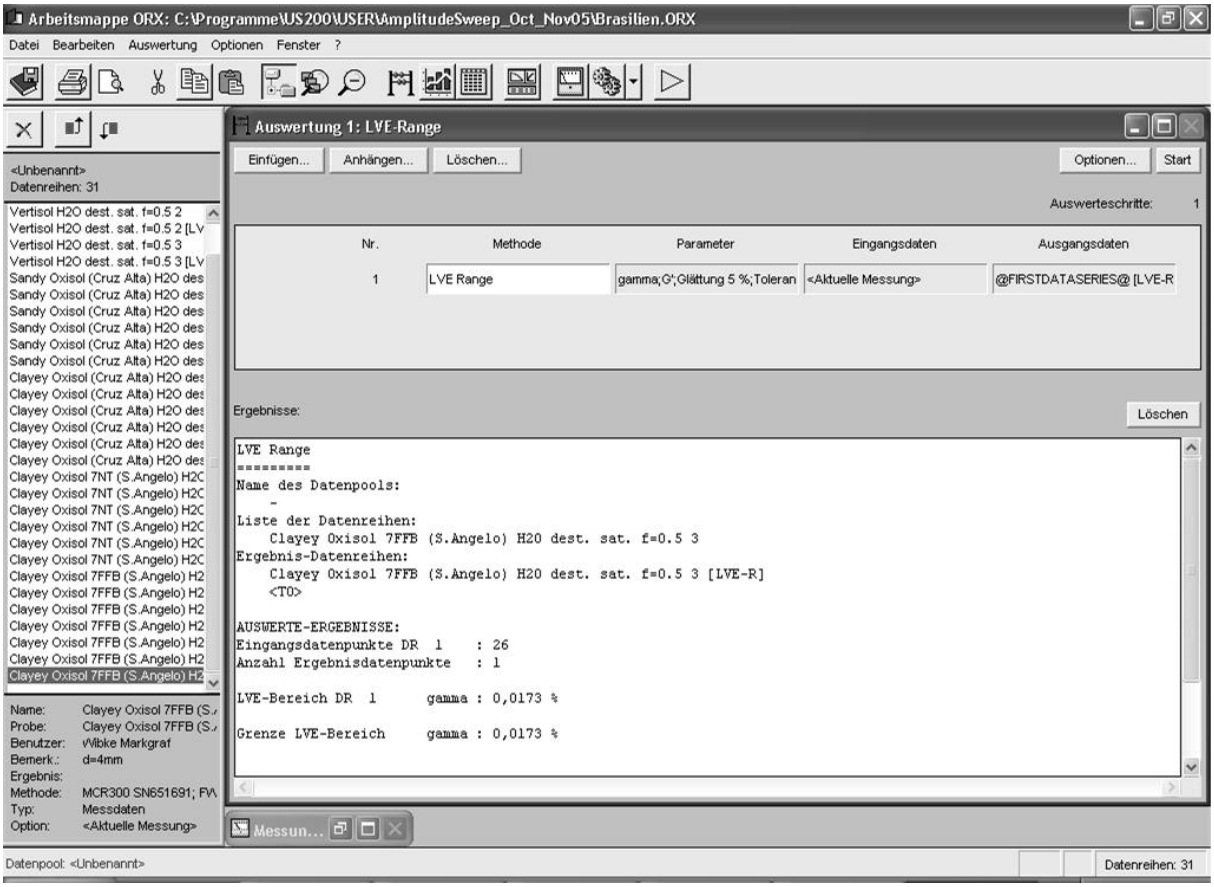

Fig. B-4 *The linear viscoelastic deformation range is calculated automatically after each completed test run, by selecting an appropriate method, parameters, and the data set. Hence the yield stress* τ_γ *and an analogue deformation limit* γ_L *derive from such calculations.*

APPENDIX C

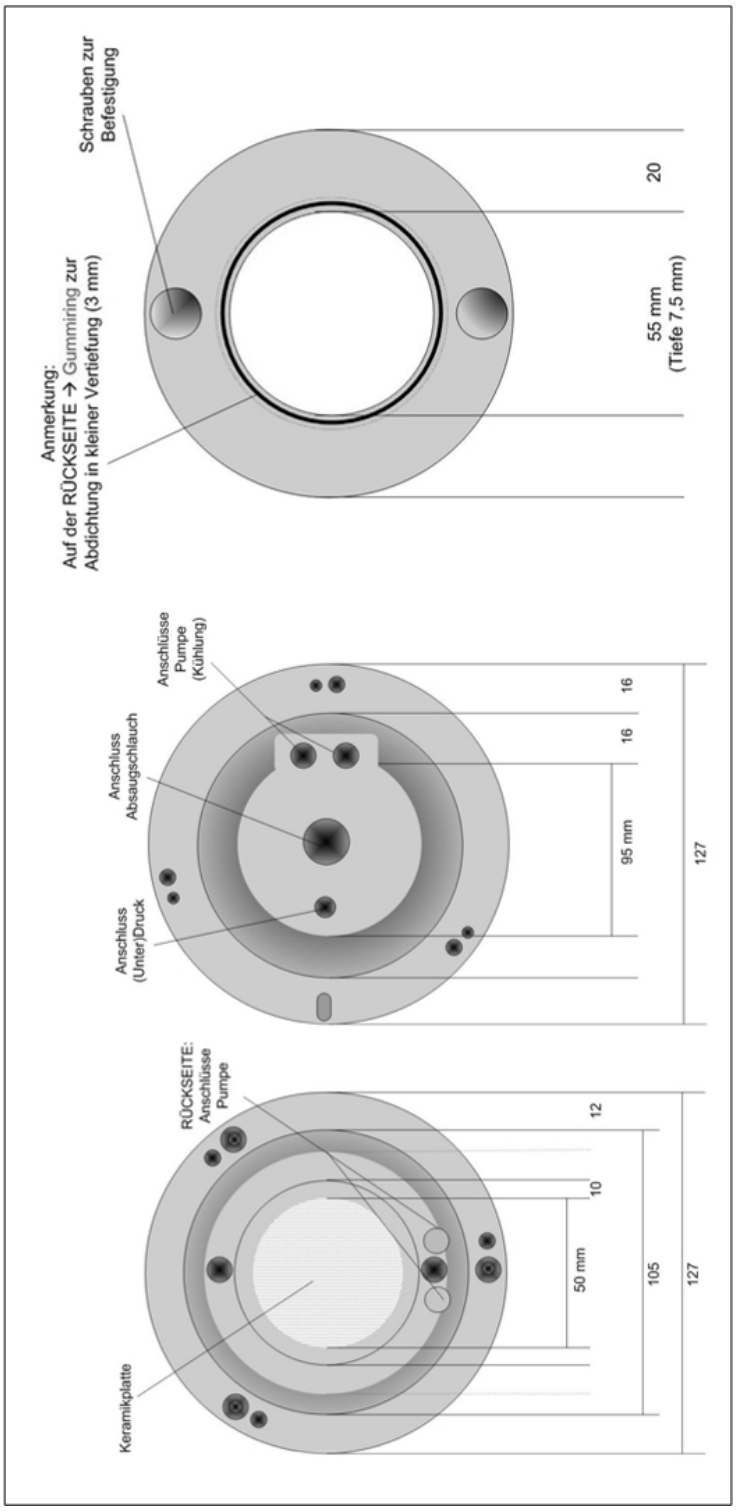

Fig. C-1 *Modified measuring plate system with pF-device (perforated ceramic plate). Front and backside are shown with interfaces, as well as an additional adapter for filter specimen. (W. Markgraf, 2006)*

APPENDIX D

IBECO SEAL 80 (saturated, 1:5)

	C0	C1	C3
γL [%]	2,23	2,28	1,96
τy [Pa]	952,70	881,00	800,10

C0 distilled water; **C1** NaCl 0.02M; **C2** NaCl 0.2M

sample	γL [%]	τy [Pa]	Mw γL [%]	Mw τy [Pa]	Stabw γL [%]	Stabw τy [Pa]
C0 12.07.2005	1,95	922,0	2,30	930,6	1,17	52,1
	1,92	975,0				
	5,64	955,0				
	1,49	841,0				
	2,24	969,0				
	2,25	1000,0				
	2,50	952,0				
	2,29	935,0				
	2,67	924,0				
	1,68	847,0				
C0 13.07.2005	2,64	951,0	2,16	1008,3	0,42	168,7
	2,44	924,0				
	2,64	947,0				
	1,88	827,0				
	2,26	1310,0				
	1,48	1250,0				
	2,39	1000,0				
	1,82	948,0				
C0 14.07.2005	2,81	1070,0	2,23	919,2	0,41	105,7
	1,92	885,0				
	2,88	1030,0				
	1,93	819,0				
	1,80	818,0				
	1,67	811,0				
	2,63	1030,0				
	2,35	1020,0				
	2,06	1010,0				
	2,42	827,0				
	2,46	851,0				

sample	γL [%]	τy [Pa]	Mw γL [%]	Mw τy [Pa]	Stabw γL [%]	Stabw τy [Pa]
C1 02.07.2005	2,32	853,0	2,34	823,6	0,21	97,1
	2,20	886,0				
	2,76	728,0				
	2,36	671,0				
	2,34	867,0				
	1,98	816,0				
	2,54	910,0				
	2,33	867,0				
	2,18	712,0				
C1 05.07.2005	2,46	979,00	2,21	938,4	0,26	75,6
	1,79	859,00				
	2,51	895,00				
	2,23	851,00				
	2,35	1020,00				
	2,24	997,00				
	2,46	1030,00				
	1,98	935,00				

sample	γL [%]	τy [Pa]	Mw γL [%]	Mw τy [Pa]	Stabw γL [%]	Stabw τy [Pa]
C3 07.07.2005	1,65	730	1,86	812,8	0,98	119,9
	1,64	757				
	4,75	747				
	1,79	782				
	1,83	763				
	1,61	742				
	1,67	1010				
	1,74	1070				
	1,90	827				
	1,36	770				
C3 08.07.2005	1,91	752	1,98	775,8	0,23	118,0
	1,56	728				
	1,89	862				
	2,20	971				
	1,92	792				
	1,91	809				
	2,00	866				
	1,93	859				
	2,40	615				
	2,17	588				
C3 09.07.2005	1,87	894	2,04	811,8	0,24	156,2
	1,92	915				
	1,97	1030				
	1,68	985				
	2,18	773				
	2,10	764				
	2,45	630				
	2,24	611				

Halle - Kassel saturated

sample	γL [%]	τy [Pa]	Mw γL [%]	Mw τy [Pa]	Stabw γL [%]	Stabw τy [Pa]	WC w/w [%]
H1	0,00537	7,72	0,00473	4,88	0,00058	2,60	30
	0,00426	2,63					
	0,00455	4,28					
H7	0,00559	3,90	0,00540	4,02	0,00071	1,16	33
	0,00462	2,92					
	0,00600	5,24					
H15	0,00587	4,86	0,00452	5,28	0,00155	2,96	30
	0,00487	2,55					
	0,00283	8,42					
KA2	0,0068	8,59	0,00668	4,50	0,00049	3,62	45
	0,00709	3,20					
	0,00614	1,72					
KA5	0,00750	7,93	0,00701	9,13	0,00056	2,95	46
	0,00640	6,97					
	0,00713	12,50					
KA8	0,00638	7,54	0,00697	10,20	0,00053	3,23	45
	0,00741	13,80					
	0,00713	9,27					
KA15	0,01170	7,53	0,01725	8,48	0,01134	1,41	47
	0,03030	7,82					
	0,00975	10,10					

Halle - Kassel -60hPa

sample	γL [%]	τy [Pa]	Mw γL [%]	Mw τy [Pa]	Stabw γL [%]	Stabw τy [Pa]	WC w/w [%]
H1	0,00587	422	0,00631	601	0,00069	196,34	19
	0,00596	570					
	0,00710	811					
H7	0,00747	644	0,00676	429	0,00106	212,08	21
	0,00728	422					
	0,00554	220					
H15	0,00276	198	0,00380	185	0,00094	27,87	23
	0,00405	204					
	0,00459	153					
KA2	0,00603	164	0,00642	123	0,00112	78,36	30
	0,00554	173					
	0,00768	33					
KA5	0,00904	272	0,00795	190	0,00108	81,02	33
	0,00792	188					
	0,00689	110					
KA8	0,00494	206	0,00626	137	0,00121	59,77	31
	0,00730	109					
	0,00655	97					
KA15	0,00813	679	0,00791	311	0,00037	319,32	28
	0,00812	147					
	0,00748	107					

Calcaric Gleysol (Soil 03) satur. H2O dest.

sample	γL [%]	τy [Pa]	Mw γ L [%]	Mw τ y [Pa]	Stabw γ L [%]	Stabw τ y [Pa]	WC w/w [%]
S03 DW	0,00919	40,6	0,00912	42,5	0,00033	10,8	33
	0,00876	32,7					
	0,00940	54,1					
S03 NaCl 0.1	0,00867	141,0	0,00833	127,7	0,00042	32,1	33
	0,00845	91,1					
	0,00786	151,0					
S03 NaCl 1.0	0,00821	39,2	0,00808	40,8	0,00024	4,3	32
	0,00780	45,6					
	0,00822	37,5					
S03 CaCl2 0.1	0,00762	63,7	0,00813	83,8	0,00045	18,0	32
	0,00846	89,3					
	0,00831	98,3					
S03 CaCl2 1.0	0,00784	34,3	0,00798	38,8	0,00012	13,6	33
	0,00807	54,0					
	0,00803	28,0					

Calcaric Gleysol (Soil 03) - 60hPa

sample	γL [%]	τy [Pa]	Mw γ L [%]	Mw τ y [Pa]	Stabw γ L [%]	Stabw τ y [Pa]	WC w/w [%]
S03 DW	0,00849	179,0	0,03487	200,3	0,04540	23,8	30
	0,00883	226,0					
	0,08730	196,0					
S03 NaCl 0.1	0,00858	172,0	0,00845	161,0	0,00016	30,0	26
	0,00828	127,0					
	0,00850	184,0					
S03 NaCl 1.0	0,00832	185,0	0,00836	185,0	0,00007	3,0	30
	0,00831	182,0					
	0,00844	188,0					
S03 CaCl2 0.1	0,00826	699,0	0,00844	619,3	0,00021	71,2	31
	0,00867	562,0					
	0,00839	597,0					
S03 CaCl2 1.0	0,00740	79,1	0,00768	91,9	0,00071	26,2	29
	0,00715	74,5					
	0,00848	122,0					

Dystric Planosol (Soil 04) satur. H2O dest.

sample	γ L [%]	τ y [Pa]	Mw γ L [%]	Mw τ y [Pa]	Stabw γ L [%]	Stabw τ y [Pa]	WC w/w [%]
S04 DW	0,01360	1580,0	0,01457	1568,0	0,00404	588,1	47
	0,01900	974,0					
	0,01110	2150,0					
S04 NaCl 0.1	0,00914	538,0	0,01167	603,7	0,00552	350,1	46
	0,01800	982,0					
	0,00788	291,0					
S04 NaCl 1.0	0,01110	660,0	0,01183	1106,7	0,00172	466,1	43
	0,01060	1070,0					
	0,01380	1590,0					
S04 CaCl2 0.1	0,01170	953,0	0,01107	1058,3	0,00085	246,5	50
	0,01010	882,0					
	0,01140	1340,0					
S04 CaCl2 1.0	0,01050	537,0	0,01046	640,7	0,00127	129,6	47
	0,00917	599,0					
	0,01170	786,0					

Dystric Planosol (Soil 04) - 60hPa

sample	γ L [%]	τ y [Pa]	Mw γ L [%]	Mw τ y [Pa]	Stabw γ L [%]	Stabw τ y [Pa]	WC w/w [%]
S04 DW	0,01210	1620,0	0,01280	2006,7	0,00075	363,0	41
	0,01360	2340,0					
	0,01270	2060,0					
S04 NaCl 0.1	0,01320	2290,0	0,01169	2176,7	0,00196	222,8	42
	0,01240	2320,0					
	0,00947	1920,0					
S04 NaCl 1.0	0,01060	789,0	0,01063	859,5	0,00006	99,7	40
	0,01060	930,0					
	0,01070	1730,0					
S04 CaCl2 0.1	0,01170	1380,0	0,01200	1455,0	0,00089	106,1	40
	0,01130	1530,0					
	0,01300	2410,0					
S04 CaCl2 1.0	0,01040	1070,0	0,00966	1033,7	0,00082	187,2	42
	0,00878	831,0					
	0,00979	1200,0					

BRAZIL: Vertisol & Oxisol (S. Angelo, Cruz Alta) saturated

sample	γL [%]	τy [Pa]	Mw γL [%]	Mw τy [Pa]	Stabw γL [%]	Stabw τy [Pa]	WG Gew. [%]
	0,02640	260,0					
Vertisol	0,02830	326,0	0,02630	255,3	0,00205	73,1	44
	0,02420	180,0					
Cruz Alta	0,00600	239,0					
Sandy	0,00710	429,0	0,00682	437,0	0,00072	202,1	32
Oxisol	0,00735	643,0					
Cruz Alta	0,01000	454,0					
Clayey	0,01030	513,0	0,01037	499,3	0,00040	40,3	37
Oxisol	0,01080	531,0					
S. Angelo	0,01270	1100,0					
Cl. Oxis.	0,01190	1030,0	0,01277	1066,7	0,00090	35,1	36
7NT	0,01370	1070,0					
S. Angelo	0,01680	955,0					
Cl. Oxis.	0,01730	1060,0	0,01677	1105,0	0,00055	176,8	41
7FFB	0,01620	1300,0					

BRAZIL: Vertisol & Oxisol (S. Angelo, Cruz Alta) -60 hPa

sample	γL [%]	τy [Pa]	Mw γL [%]	Mw τy [Pa]	Stabw γL [%]	Stabw τy [Pa]	WG w/w [%]
	0,02450	239,0					
Vertisol	0,03020	603,0	0,02835	532,3	0,00366	324,6	42
	0,02620	327,0					
	0,03250	960,0					
Cruz Alta	0,00748	864,0					
Sandy	0,00611	990,0	0,00661	940,7	0,00076	67,3	18
Oxisol	0,00624	968,0					
Cruz Alta	0,01130	876,0					
Clayey	0,00925	1050,0	0,01022	896,7	0,00103	144,1	19
Oxisol	0,01010	764,0					
S. Angelo	0,00995	774,0					
Cl. Oxis.	0,01090	1030,0	0,00917	804,0	0,00223	212,6	22
7NT	0,00665	608,0					
S. Angelo	0,01290	805,0					
Cl. Oxis.	0,01330	1130,0	0,01277	918,7	0,00061	183,2	18
7FFB	0,01210	821,0					

BRAZIL: Oxisol (S. Angelo, Cruz Alta) gesättigt without SOM

sample	γL [%]	τy [Pa]	Mw γL [%]	Mw τy [Pa]	Stabw γL [%]	Stabw τy [Pa]	WG w/w [%]
Cruz Alta Sandy Oxisol	0,00462	207,0	0,00287	51,9	0,00101	5,2	30,6
	0,00283	55,6					
	0,00290	48,2					
Cruz Alta Clayey Oxisol	0,00538	99,0	0,00584	101,3	0,00075	17,7	45,7
	0,00543	84,8					
	0,00670	120,0					
S. Angelo Cl. Oxis. 7FFB	0,00623	138,0	0,00679	149,0	0,00053	11,0	42,6
	0,00685	149,0					
	0,00729	160,0					
S. Angelo Cl. Oxis. 7NT	0,00675	190,0	0,00768	215,3	0,00088	38,8	49,4
	0,00851	260,0					
	0,00778	196,0					

BRAZIL: Oxisol (S. Angelo, Cruz Alta) -60 hPa without SOM

sample	γL [%]	τy [Pa]	Mw γL [%]	Mw τy [Pa]	Stabw γL [%]	Stabw τy [Pa]	WG w/w [%]
	0,00665	*459*					
Cruz Alta Sandy Oxisol	0,00611	342	0,00560	288,3	0,00041	116,5	25,0
	0,00585	226					
	0,00379	126					
Cruz Alta Clayey Oxisol	0,00557	170	0,00610	293,0	0,00070	151,3	39,0
	0,00585	247					
	0,00689	462					
S. Angelo Cl. Oxis. 7FFB	0,00833	439	0,00771	349,7	0,00088	89,5	34,2
	0,00670	260					
	0,00809	350					
S. Angelo Cl. Oxis. 7NT	0,00760	336	0,00856	502,0	0,00127	154,3	43,0
	0,00809	529					
	0,01000	641					

BRAZIL: Oxisol (S. Angelo, Cruz Alta) saturated without Fed

sample	γL [%]	τy [Pa]	Mw γL [%]	Mw τy [Pa]	Stabw γL [%]	Stabw τy [Pa]	WG w/w [%]
Cruz Alta Sandy Oxisol	0,00310 0,00369 0,00206	15,1 9,3 4,4	0,00295	9,6	0,00083	5,3	25,1
Cruz Alta Clayey Oxisol	0,00820 0,02090 0,01330	54,3 44,2 50,6	0,01413	49,7	0,00639	5,1	36,6
S. Angelo Cl. Oxis. 7FFB	0,01560 0,02170 0,01980	34,5 60,1 26,5	0,01903	40,4	0,00312	17,6	25,6
S. Angelo Cl. Oxis. 7NT	0,01390 0,03060 0,03260	20,9 56,8 50,4	0,02570	42,7	0,01027	19,1	43,5

BRAZIL: Oxisol (S. Angelo, Cruz Alta) -60 hPa without Fed

sample	γL [%]	τy [Pa]	Mw γL [%]	Mw τy [Pa]	Stabw γL [%]	Stabw τy [Pa]	WG w/w [%]
Cruz Alta Sandy Oxisol	0,01270 0,01250 0,01940	150,0 96,6 172,0	0,01487	139,5	0,00393	38,8	15,6
Cruz Alta Clayey Oxisol	0,01840 0,01880 0,03610	166,0 121,0 294,0	0,02443	193,7	0,01011	89,8	18,8
S. Angelo Cl. Oxis. 7FFB	0,00657 0,00588 0,00509	108,0 77,5 156,0	0,00585	113,8	0,00074	39,6	22,6
S. Angelo Cl. Oxis. 7NT	0,0232 0,0336 0,0459	170,0 209,0 246,0	0,03423	208,3	0,01136	38,0	17,3

Avdat Loess @ saturated

sample	γL [%]	τy [Pa]	Mw γL [%]	Mw τy [Pa]	Stabw γL [%]	Stabw τy [Pa]	WC w/w [%]
DW	0,000322	0,132	0,000391	0,269	0,00006	0,1	39,7
	0,000446	0,369					
	0,000404	0,305					
NaCl 0.1M	0,000901	0,505	0,000719	0,454	0,00016	0,1	41,5
	0,000589	0,309					
	0,000668	0,547					
NaCl 1.0M	0,001270	0,388	0,000801	0,671	0,00047	0,5	34,1
	0,000331	0,354					
	0,000801	1,270					
CaCl2 0.1M	0,001130	0,621	0,001280	1,627	0,00014	0,9	35,6
	0,001300	2,130					
	0,001410	2,130					
CaCl2 1.0M	0,000963	0,436	0,001079	0,703	0,00038	0,5	35,5
	0,000773	0,403					
	0,001500	1,270					

Avdat Loess @ -60hPa

sample	γL [%]	τy [Pa]	Mw γL [%]	Mw τy [Pa]	Stabw γL [%]	Stabw τy [Pa]	WG w/w [%]
DW	0,008010	58,7	0,009527	69,667	0,00224	19,6	28,6
	0,012100	92,3					
	0,008470	58,0					
NaCl 0.1M	0,006870	41,5	0,007333	37,633	0,00041	5,1	31,2
	0,007640	31,9					
	0,007490	39,5					
NaCl 1.0M	0,005430	32,3	0,007037	40,733	0,00143	16,0	29,4
	0,007510	59,2					
	0,008170	30,7					
CaCl2 0.1M	0,007560	52,9	0,008537	79,533	0,00105	23,1	30,9
	0,008410	94,7					
	0,009640	91,0					
CaCl2 1.0M	0,009270	41,0	0,008180	47,467	0,00095	28,1	29
	0,007590	23,2					
	0,007680	78,2					

Brunisol satur. H2O dest.

sample	γ L [%]	τ y [Pa]	Mw γ L [%]	Mw τ y [Pa]	Stabw γ L [%]	Stabw τ y [Pa]	WG w/w [%]
plot 11 reference	0,00635	132,0	0,00601	110,8	0,00086	23,5	35
	0,00504	85,5					
	0,00665	115,0					
plot 39 CaCO3	0,00755	52,6	0,00768	53,5	0,00014	4,5	40
	0,00767	58,4					
	0,00783	49,5					
plot 6 NH4NO3	0,00681	244,0	0,00604	192,7	0,00067	45,0	36
	0,00576	160,0					
	0,00556	174,0					
plot 17 NaNO3	0,00770	79,3	0,00667	98,3	0,00095	30,9	39
	0,00650	134,0					
	0,00582	81,7					
plot 26 CaO	0,00928	102,0	0,00900	88,4	0,00024	12,4	41
	0,00886	85,5					
	0,00886	77,8					
plot 41 K2SO4	0,00763	43,3	0,00728	35,0	0,00047	9,4	41
	0,00674	24,8					
	0,00747	36,8					
plot 16 Ca(NO3)2	0,00596	112,0	0,00608	110,6	0,00039	35,2	38
	0,00652	145,0					
	0,00577	74,7					

Brunisol - 60hPa

sample	γ L [%]	τ y [Pa]	Mw γ L [%]	Mw τ y [Pa]	Stabw γ L [%]	Stabw τ y [Pa]	WG w/w [%]
plot 11 reference	0,00705	579,0	0,00697	469,0	0,00044	138,1	29
	0,00737	514,0					
	0,00650	314,0					
plot 39 CaCO3	0,01140	501,0	0,01050	344,7	0,00155	154,5	32
	0,00871	192,0					
	0,01140	341,0					
plot 6 NH4NO3	0,00897	476,0	0,00805	470,0	0,00091	78,2	29
	0,00716	545,0					
	0,00801	389,0					
plot 17 NaNO3	0,00735	473,0	0,01005	437,7	0,00075	98,9	30
	0,00877	514,0					
	0,00766	326,0					
plot 26 CaO	0,01100	522,0	0,00813	389,3	0,00092	121,3	31
	0,01000	362,0					
	0,00916	284,0					
plot 41 K2SO4	0,00889	248,0	0,00787	170,7	0,00067	72,2	30
	0,00786	105,0					
	0,00763	159,0					
plot 16 Ca(NO3)2	0,00812	474,0	0,00861	478,0	0,00028	45,1	29
	0,00858	525,0					
	0,00864	435,0					

	highest value
	lowest value